
Synthesis and Characterization of Zirconium-based Metal-Organic Frameworks using a Modulation Approach

Von der Naturwissenschaftlichen Fakultät der
Gottfried Wilhelm Leibniz Universität Hannover
zur Erlangung des Grades

Doktor der Naturwissenschaften
– Dr. rer. nat. –

genehmigte Dissertation von

Dipl.-Chem. Andreas Schaate
geboren am 20.04.1982 in Uelzen

2012

Referent: Prof. Dr. Peter Behrens

Korreferent: Prof. Dr. Jürgen Caro

Tag der Promotion: 20.02.2012

Danksagung

Zuerst möchte ich mich bei Herrn Prof. Dr. Peter Behrens dafür bedanken, dass er mir es ermöglichte meine Doktorarbeit in seinem Arbeitskreis anzufertigen. Die gute Betreuung, die motivierenden Gespräche und die vielen Möglichkeiten wissenschaftlich zu arbeiten und zu präsentieren, haben die Zeit in seinem Arbeitskreis zu einer besonderen in meinem Leben gemacht.

Für die Übernahme des Korreferats danke ich Herrn Prof. Dr. Jürgen Caro. Herrn Prof. Dr. Franz Renz möchte ich dafür danken, als Drittprüfer zur Verfügung zu stehen.

Weite Teile dieser Arbeit wären nicht möglich gewesen ohne die hervorragende Kooperation mit Frau Prof. Dr. Adelheid Godt, ihren Mitarbeitern Pascal Roy und Thomas Preuße sowie mit Herrn Prof. Dr. Michael Wark und seiner Mitarbeiterin Jana Panke. Ich bin sehr dankbar für die konstruktiven Diskussionen bei den Treffen, welche mit dafür verantwortlich sind, dass unser Teilprojekt des SPP 1362 so erfolgreich verläuft.

Bei den experimentellen Arbeiten konnte ich immer auf Unterstützung durch die Mitglieder des Arbeitskreises Behrens vertrauen. Besonders herausstellen möchte ich in diesem Zusammenhang Imke Bremer, Simon Dühren, Britta Hering, Sebastian Lilienthal, Jann Lippke, Georg Platz, Reimar Münnekhoff, Christian Schröder, Dr. Andreas Schneider, Boris Ufer, Florian Waltz, Gesa Wißmann und Philip Zerner und mich bei ihnen für die Hilfe bei der Durchführung und Analyse meiner Experimente bedanken. Für das Korrekturlesen dieser Arbeit möchte ich Imke, Georg und 'Zerner' danken.

Ein großer Dank gebührt Herrn Dr. Michael Wiebcke für die umfangreiche Einführung und die Hilfe bei Fragen in der Welt der Einkristall-Röntgendiffraktometrie.

Die freundschaftliche Atmosphäre in diesem Arbeitskreis führte dazu, dass ich auch immer wieder meine Freizeit mit meinen Kollegen verbrachte. Interessante Gespräche über Wichtiges, Unwichtiges und Banales sowie sportliche Höchstleistungen, regelmäßige Kanutouren auf der Örtze, gemütliche Filmabende und ausgiebige Feiern rundeten so meine Zeit am Institut für Anorganische Chemie ab. Vielen Dank allen Kollegen für diese schöne Zeit.

Ein besonderer Dank geht an meine Mutter Margit, meinen Bruder Marc, meine Großeltern Anneliese und Horst sowie Marion und meinen Onkel Armin, die immer an mich geglaubt haben. Meiner Freundin Sophia danke ich dafür, dass sie während dieser Zeit immer für mich da war, mich aber auch dazu zwang, neben der Uni noch ein Privatleben zu haben.

Abstract

Metal-organic frameworks (MOFs) are a novel class of microporous materials of high interest due to their modular composition of self-assembled metal clusters connected by organic linkers, the resulting high variability and their large specific surface areas, to list only a few reasons. Recently described MOFs which are based on highly charged cations like Zr^{4+} or Ti^{4+} can apparently overcome the often observed limited stability of these materials, which may add more possibilities for research and for applications.

The present thesis shows ways to control the synthesis of the important novel class of Zr-based MOFs in terms of reproducibility and control, specifically with regard to the generation of particles of desired size. In order to approach these goals it was investigated how the addition of so-called modulators (monocarboxylic acids) influences the synthesis of the members of the isorecticular series of UiO-MOFs. It was observed that dependent on the amount of benzoic or acetic acid, the aggregation and size of Zr-bdc-MOF (UiO-66, bdc = terephthalate) particles can be tuned. The syntheses of MOFs with larger linkers like Zr-bpdc- (UiO-67, bpdc = biphenyl-4,4'-dicarboxylate), Zr-tpdc-NH₂- (UiO-68-NH₂, tpdc-NH₂ = 2'-amino-1,1':4,1''-terphenyl-4,4''-dicarboxylate), or Zr-abdc-MOF (abdc = 4,4'-azobenzenedicarboxylate) only succeeded at all when a certain amount of modulator was present in the synthesis. In these cases the modulator approach chiefly ensured the secure access to MOFs, the precursors of which otherwise only precipitated as low-crystallinity materials of low porosity. The thermal stability and the porosity of the products received by this synthesis route were analyzed by thermogravimetric analysis (TGA) and Ar sorption experiments. It was found that the materials can be activated and exhibit high specific surface areas. Furthermore, by using modulated syntheses it was possible to obtain single crystals of Zr-tpdc-NH₂- and Zr-abdc-MOF and to determine for the first time the crystal structure of Zr-MOFs by using single crystal X-ray diffraction (SXRD).

Further results presented here deal with the syntheses of functionalized Zr-MOFs using a variety of long, differently substituted dicarboxylic acids of the type HO₂C[PE-P(R¹,R²)-EP]CO₂H (P = phenylene, E = ethynylene, R¹,R² = side chains at the central phenylene unit). The developed modulation approach was again essential to obtain this novel isostructural series of crystalline materials which were denoted as porous interpenetrated zirconium-organic frameworks (PIZOFs). In the case of three of the eight here described members of the PIZOFs series, it was possible to obtain single crystals and to solve their structure by SXRD. According to their powder X-ray diffraction (PXRD) patterns, all PIZOFs share a common framework structure. It is related to that of UiO-Zr-MOFs, but due to the length of the linkers, PIZOFs are twofold interpenetrated. This interpenetration and the great diversity of functional groups attached to the used linkers are the reason for a structure that is highly adaptable in its properties. The eight PIZOFs here described are porous and show high thermal stabilities, as determined by TGA and PXRD.

Keywords: metal-organic frameworks • Zr-compounds • modulation approach • single crystals • nanoparticles • azo compounds

Inhaltsübersicht

Metall-organische Gerüste (metal-organic frameworks, MOFs) sind eine neuartige Klasse mikroporöser Materialien, die aufgrund ihres modularen Aufbaus aus selbstorganisierten Metallclustern, verbunden durch organische Linker, der daraus resultierenden hohen Variabilität und ihren großen spezifischen Oberflächen, von hohem Interesse sind. Kürzlich beschriebene MOFs, die auf hoch geladenen Kationen wie Zr^{4+} oder Ti^{4+} basieren, scheinen die bei diesen Materialien oft beobachtete Instabilität zu überwinden, was weitere Möglichkeiten für die Forschung und die Anwendung eröffnet.

Die vorliegende Dissertation zeigt Wege zur Kontrolle der Synthese der wichtigen neuartigen Klasse der Zr-basierten MOFs auf, insbesondere hinsichtlich der Reproduzierbarkeit und der Möglichkeit, die Partikel in gewünschter Größe herzustellen. Um diese Ziele zu erreichen, wurde untersucht, wie die Zugabe von sogenannten Modulatoren (Monocarbonsäuren) die Synthese der Vertreter der isoretikulären UiO-MOF-Serie beeinflusst. Es wurde beobachtet, dass, abhängig von der Menge an Benzoe- oder Essigsäure, die Aggregation und Größe von Partikeln des Zr-bdc-MOFs (UiO-66, bdc = Terephthalat) eingestellt werden können. Die Synthesen von MOFs mit längeren Linkern, wie die des Zr-bpdc- (UiO-67, bpdc = Biphenyl-4,4'-dicarboxylat), des Zr-tpdc-NH₂- (UiO-68-NH₂, tpdc-NH₂ = 2'-Amino-1,1':4,1''-terphenyl-4,4''-dicarboxylat) oder des Zr-abdc-MOFs (abdc = 4,4'-Azobenzoldicarboxylat), konnten überhaupt nur mit einer bestimmten Menge an Modulator erfolgreich durchgeführt werden. In diesen Fällen gewährleistete der Modulatoransatz hauptsächlich den Zugang zu diesen MOFs, deren Präkursoren anderenfalls als wenig kristallines Material mit geringer Porosität präzipitierten. Die thermische Stabilität und die Porosität der Produkte, die auf diesem Syntheseweg erhalten wurden, wurde durch thermogravimetische Analyse (TGA) und Ar-Sorptionsexperimente untersucht. Es wurde festgestellt, dass die Materialien aktiviert werden können und große spezifische Oberflächen aufweisen. Darüber hinaus konnten, durch die Verwendung der modulierten Synthese, Einkristalle des Zr-tpdc-NH₂- und des Zr-abdc-MOFs erhalten werden, so dass zum ersten Mal die Kristallstrukturen von Zr-MOFs über Einkristall-Röntgendiffraktometrie (single crystal X-ray diffraction, SXR) bestimmt werden konnten.

Weitere hier präsentierte Ergebnisse befassen sich mit den Synthesen von funktionalisierten Zr-MOFs mit langen, unterschiedlich substituierten Dicarbonsäuren des Typs HO₂C[PE-P(R¹,R²)EP]CO₂H (P = Phenylen, E = Ethinylen, R¹,R² = Seitenketten am zentralen Phenylenring). Abermals war der entwickelte Modulatoransatz erforderlich, um eine neuartige, isoretikuläre Serie poröser Materialien zu erhalten, die als poröse interpenetrierte Zirkonium-organische Gerüste (porous interpenetrated zirconium-organic frameworks, PIZOFs) bezeichnet wurden. Im Falle von drei der acht hier beschriebenen PIZOFs war es möglich, Einkristalle zu erhalten, deren Struktur durch SXR bestimmt wurde. Über Pulver-Röntgendiffraktometrie (powder X-ray diffraction, PXR) wurde festgestellt, dass alle PIZOFs eine gemeinsame Netzwerkstruktur besitzen. Sie ist mit der UiO-Zr-MOF-Struktur verwandt, aufgrund der Länge der Linker aber sind PIZOFs zweifach interpenetriert. Diese Interpenetration und die große Vielfalt an funktionellen Gruppen, die an den verwendeten Linkern angebracht sind, führen zu einer Struktur, die in ihren Eigenschaften vielfältig einstellbar ist. Die acht hier vorgestellten PIZOFs sind porös und zeigen in der TGA und in der PXR eine hohe thermische Stabilität.

Stichwörter: metall-organische Gerüste • Zr-Verbindungen • Modulationsansatz • Einkristalle • Nanopartikel • Azoverbindungen

Erklärung

Hierdurch erkläre ich, dass ich die Dissertation „Synthesis and Characterization of Zirconium-based Metal-Organic Frameworks using a Modulation Approach“ selbstständig verfasst habe und alle benutzten Hilfsmittel sowie eventuell zur Hilfeleistung herangezogene Institutionen vollständig angegeben wurden.

Die Dissertation wurde nicht schon als Diplom- oder ähnliche Prüfungsarbeit verwendet.

Hannover, den 20.02.2012

Dipl.-Chem. Andreas Schaate

Table of contents

1	Introduction	1
2	General Principles	5
2.1	Metal-organic frameworks (MOFs).....	5
2.2	Synthetic strategies.....	11
2.2.1	The concept of isoreticular synthesis	11
2.2.2	Synthesis of single crystals.....	14
2.2.3	Synthesis of nanocrystals	15
2.2.4	Synthesis control via coordination modulation approach.....	17
2.3	Potential applications of MOFs	23
2.3.1	Separation.....	23
2.3.2	Sorption and storage	23
2.3.3	Catalytic application.....	25
2.3.4	Biological applications	26
2.4	Zr-based MOFs.....	29
2.4.1	UiO-66 family.....	29
2.4.2	Porous interpenetrated Zr-organic framework (PIZOFs).....	35
2.5	References	39
3	Modulated Synthesis of Zr-Based Metal–Organic Frameworks: From Nano to Single Crystals	45
4	A novel Zr-based porous coordination polymer containing an azo-linker ..	55
5	Porous interpenetrated zirconium-organic frameworks (PIZOFs), a chemically versatile family of MOFs.....	63
6	Modulated Synthesis of Zr-fumarate MOF	71
7	Conclusions and Outlook	79
8	List of publications	84
8.1	Articles presented in this work.....	84
8.2	Further Articles.....	84
8.3	Oral presentations	85
8.4	Poster presentations	85
9	Curriculum Vitae	87

1 Introduction

The exploration of novel materials to meet requirements that are becoming increasingly specific is one of the major driving forces of today's materials research. In particular porous materials are of high interest due to their unique properties and diverse possible applications. In this sense, the discovery of microporous zeolites^[1] and the preparation of the first synthetic zeolites more than 60 years ago^[2-4] initialized a nowadays prospering field of research. Zeolites show a high potential in applications in important areas like adsorption,^[5,6] separation,^[7,8] and catalysis.^[9,10] These robust materials are composed of corner- or edge-sharing $[\text{SiO}_4]$ and $[\text{AlO}_4]^-$ tetrahedra resulting in frameworks with channels and cavities with diameters in the range of 3-15 Å.^[11] This structural principle ensures a high stability of the compounds but limits the variability with respect to the size of the channels and cavities and the functionalities coating the interior of these voids.

This lack of flexibility and functionality has been overcome with the novel and intriguing class of metal-organic frameworks (MOFs) which were published under this name for the first time in 1995.^[12] MOFs or porous coordination polymers (PCPs) are materials composed of hybrid secondary building units (SBUs) and multifunctional organic molecules, so-called linkers, which is a strong difference to zeolites. Whereas inorganic building units in zeolites consist of metalloids or metals and oxygen ions, MOFs are composed of SBUs of metal ions coordinated by oxo or hydroxo groups and by organic linkers which are connecting the SBUs to each other in a scaffold-like arrangement (Figure 1).^[13]

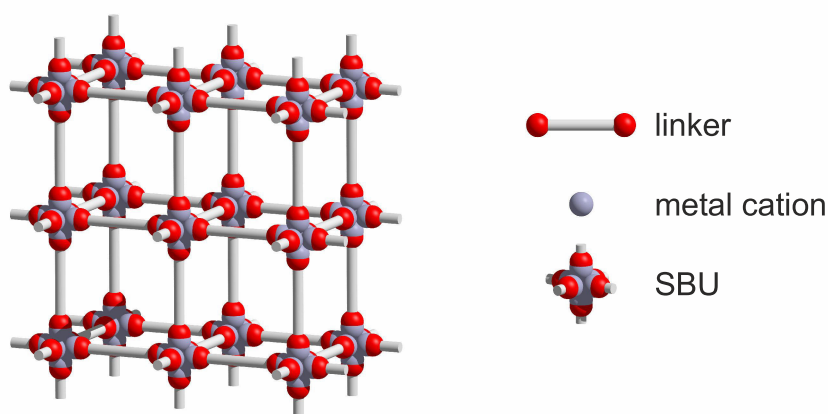


Figure 1. Schematic illustration of the construction principle of MOFs.

In 1999 Yaghi and co-workers published the synthesis and structure of the archetype material MOF-5, which was at this time one of the lowest density materials (0.59 g cm^{-3}) with an exceptionally high surface area ($2900 \text{ m}^2 \text{ g}^{-1}$) for a crystalline compound.^[14] The discovery of this prototypical MOF triggered the tremendous amount of research activity on such porous hybrid materials. Shortly afterwards, in

2002 a series of isorecticular* MOFs was described by the same group,^[15] showing that important properties like pore size and volume, framework functionality, and surface area can be chosen by selecting the appropriate linker. Although these insights suggest a high degree of control over the synthesis of these MOFs it is euphemistically to speak of designing MOFs since the SBU of such materials cannot be freely chosen, because the behavior of the metal centers is often unpredictable.^[16] On the contrary, the organic synthesis, as a powerful instrument to create desired functionalities on linkers located later in a MOF, approaches the concept of design.

Nevertheless, it was possible to find many MOF structures based on divalent metal cations with a huge pool of different linkers and functionalities showing that MOFs indeed could serve as materials with specified properties for applications like adsorption,^[17,18] storage,^[6,19] separation,^[20] catalysis,^[21] sensors,^[22-24] and drug delivery,^[25] to list only a few. A major drawback for applications of MOFs composed of divalent metal cations and carboxylate ligands is that they do not possess an appropriate stability at atmospheric conditions, in particular if they are exposed to moisture.^[26-28]

MOFs based on trivalent metal cations are generally much more stable against moisture.^[26] Although there is a rich variety of structures,^[29-31] including highly porous compounds,^[32,33] the functionality of the used linkers is hitherto poor compared to M^{2+} -based MOFs. Based on the observation of increasing stability from bi- to trivalent transition metals it would be expected that tetravalent cations form MOFs with a similar or even higher stability. Indeed a novel series of recently described Zr-MOFs^[34] and a novel Ti-MOF^[35] meet this expectation.

The focus of this thesis was to combine variability and adaptability (arising from the used linkers) and adequate stability (determined by the metal cations employed) in MOF materials. To achieve the required stability the zirconium-based SBU of the UiO[†] MOF series^[34,36] was chosen because some representatives of this family of MOFs proved to be stable even in aqueous solution.^[37]

As a first step the syntheses of some of these MOFs were evaluated and improved concerning reliability. For this purpose, the coordination modulation approach originally developed by the Kitagawa group^[38,39] was adopted to UiO-MOFs and proved to be a general concept to control the synthesis of these materials. In this approach monocarboxylic acids are considered as modulators and are added to the synthesis to compete with the linkers for the coordination sites of the metal cations (Figure 2). In this way, the nucleation of the MOF is effectively slowed down which gives a certain control of the resulting crystal sizes and is in some cases critical for the success of the synthesis. Especially for linkers with a longer length than that of terephthalic acid it was crucial to add modulators to the synthesis to obtain phase-pure materials. With this concept it was also possible for the first time to yield single crystals of a Zr-MOF and to solve its structure with single crystal X-ray diffraction (SXRD).

The application of the modulation approach to the synthesis of a Zr-MOF with an azo

* Isorecticular means 'having the same network topology'.

† UiO stands for Universitetet i Oslo.

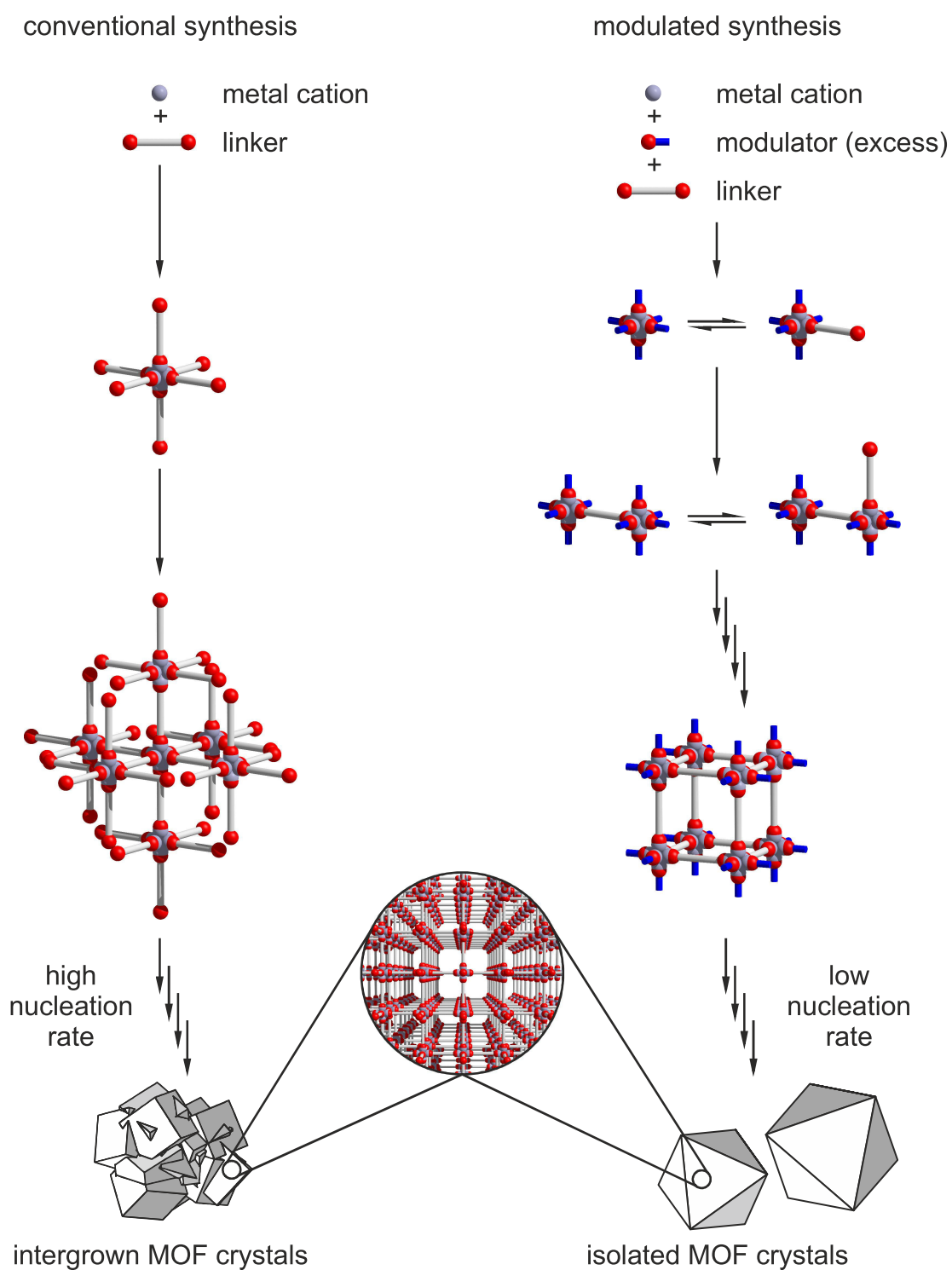


Figure 2. Schematic illustration of the comparison between conventional and modulated synthesis of MOFs.

group-containing linker again yielded single crystals with a structure which is probably isorecticular to the other UiO-MOFs. The kink present in the linker molecule due to the azo group made the determination of the structure somewhat more difficult. Nevertheless, the information gained by SXRD combined with computer-

aided modeling techniques, sorption measurement, and thermogravimetric analysis verified the assignment of this MOF as an UiO-66-analogue compound.

As mentioned above, the design of MOFs is restricted rather by the SBUs which are assembling the framework. As a consequence, highly tunable MOFs can only be prepared if the linker is modified with the desired functional groups post-synthetically^[40] or if the organic synthesis of the linker is highly modular. Post-synthetic modifications have the advantage that functional groups which are not resistant to the synthesis conditions can be introduced into the readily synthesized MOF at milder conditions. On the contrary, it could be difficult to post-synthetically modify a MOF with functionalities that would nearly completely fill its cavities, because of pore blocking effects that would impede a complete modification.

For this purpose, the use of readily synthesized functionalized linkers in combination with a reliably emerging SBU could be a resolution. This route was followed in cooperation with the research group Godt at Bielefeld University within the priority program 1362 (Porous Metal-Organic Frameworks) by the Deutsche Forschungsgemeinschaft. The Godt group uses Pd/Cu-catalyzed C–C cross coupling reactions to yield a variety of differently substituted diacids sharing the same length of the backbone. The synthesis is modular and highly compatible with a large variety of substituents like alkyl, alkoxy, and oligo(ethyleneglycol) chains of different length and post-synthetically modifiable groups like amino, alkyne, and furan.

This variety of linkers together with the developed modulated synthesis led to the constitution of the novel series of porous interpenetrated Zr-organic frameworks (PIZOFs). Again the modulation approach was the key to single crystals which enabled the elucidation of the structure by SXR. Zr-MOFs of UiO- and PIZOF-type share the same SBU leading to a strong structural relationship between them. In contrast to the UiO-MOFs, PIZOFs consist of two interpenetrating frameworks. Despite the expected reduction of the pore system PIZOFs are still highly porous with cavities whose maximal diameter is about 2 nm. Apart from the unexpected interpenetration the most astonishing feature of this family of MOFs is that the same structural backbone is shared by a large variety of PIZOFs, indifferent to the substituents which are attached to the linkers, a fact that underlines the versatility of this new family of MOFs.

2 General Principles

2.1 Metal-organic frameworks (MOFs)

Metal-organic frameworks (MOFs) or porous coordination polymers (PCPs) are crystalline, microporous materials composed of linkers the coordinating groups of which join together metal cations or clusters of metal cations. These clusters are usually denoted as secondary building units (SBUs) or hybrid SBUs since they are composed of inorganic metals and organic linkers.^[13] The linkers have more than one coordinating group which usually consists of oxygen or nitrogen atoms whose free electron pairs are complexing the metals. Usually, rigid aromatic di- or tricarboxylates, N-heterocycles, or imidazole derivatives are used as linkers. An overview with structural formulas of the linkers and commonly used abbreviations can be found in Figure 3.

The idea of extended coordination solids composed of molecular building blocks (the SBUs) and linkers goes back to Robson^[41] and was picked up by Yaghi who was the first using the term MOF on such a compound.^[12] The enhancement of Yaghi to this field of coordination chemistry was the successful introduction of SBUs to obtain porous coordination polymers with large specific surface areas.^[14,42,43] A review concerning transition metal carboxylate clusters which have already served or could

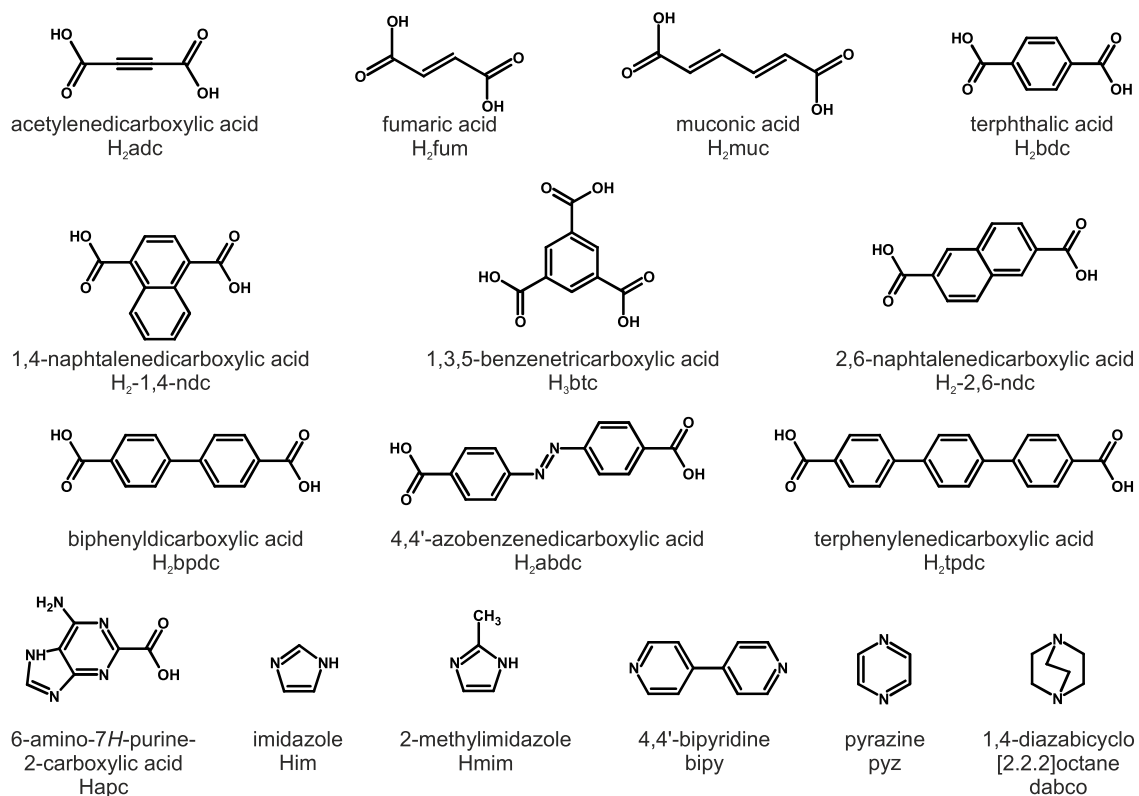


Figure 3. Structural formulas, designations and abbreviations for commonly used linkers in MOF syntheses.

serve as SBUs in MOFs was published in 2009;^[44] a selection of frequently occurring SBUs is presented in Figure 4.

The group of Yaghi concentrates on Zn-based MOFs (often with the basic zinc acetate structure (Figure 4a) as SBU) which were proposed as materials for gas storage^[14] due to their low density and high specific surface area. These MOFs are synthesized under very similar conditions and often isorecticular structures are obtained. The most prominent family of IRMOFs* based on this SBU is described in section 2.2.1, p. 11. The largest Brunauer-Emmett-Teller (BET) surface area which has been reached with a MOF until now is over 6000 m² g⁻¹ in MOF-210.^[18] According to the authors this value should be near the ultimate limit for solid materials. Despite the instability of these Zn-based MOFs towards atmospheric moisture, which was already mentioned in the introduction, such materials might also be interesting for industrial gas storage.^[48]

Another class of MOFs, described by Park *et al.*, which is chemically much more resistant, consists of the zeolitic imidazolate frameworks (ZIFs). The structures are based on the nets of zeolites and are composed of transition metal cations (M: Zn, Co)

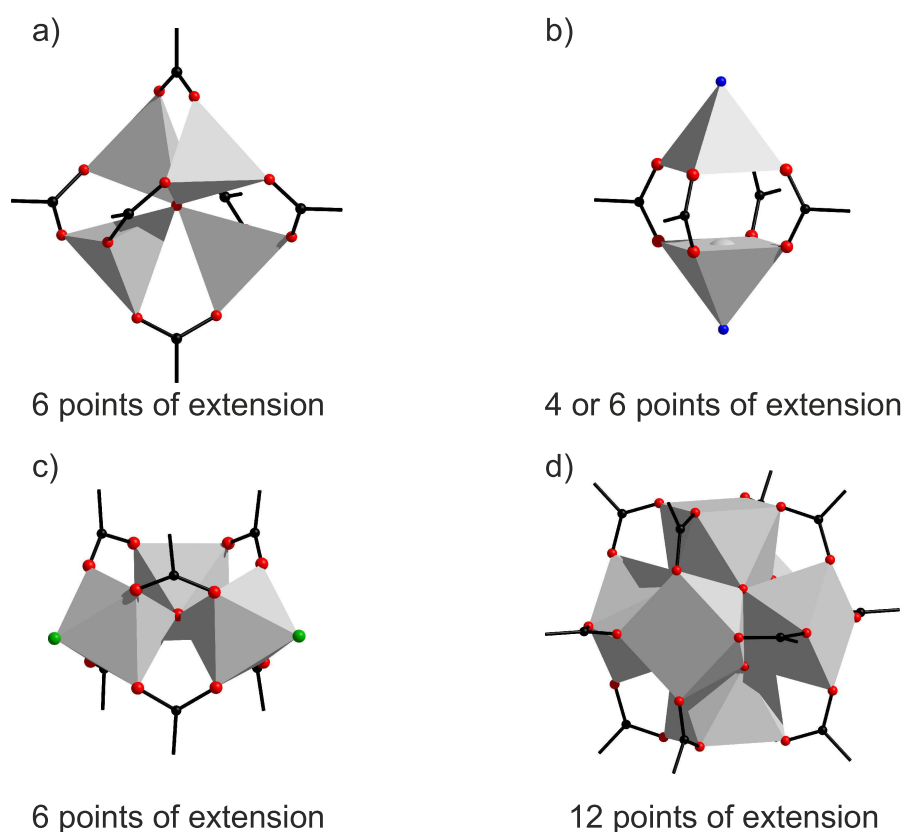


Figure 4. Selection of frequently occurring SBUs in MOFs (black: carbon, blue: nitrogen or oxygen, green: fluorine or oxygen, grey: polyhedra around metal centers, red: oxygen). a) Basic zinc acetate SBU,^[14] b) copper or zinc paddle-wheel SBU,^[45,46] c) trimeric iron or chromium acetate SBU,^[47] d) hexameric zirconium acetate SBU.^[34]

* IRMOF stands for isorecticular metal-organic framework.

tetrahedrally coordinated by imidazolate (im) derivatives.^[49] The bridging angle M–im–M in ZIFs, which approaches the angle of the Si–O–Si bonds in zeolites ($\sim 145^\circ$), is supposed to be the origin of the similarity between the structures of ZIFs and zeolites. Other examples for the persistence of zeolitic topologies in the field of MOFs are the two mesoporous MOFs MIL-100^{*[32]} and MIL-101^[33] described by the Férey group. Both of these compounds are high surface area MOFs (Langmuir surface area: 4000–5900 m² g⁻¹). They are composed of the trimeric chromium acetate SBU (Figure 4c) which occupies the vertices of super tetrahedra with the linker btc³⁻ located on each face (MIL-100, Figure 5a) or bdc²⁻ located on each edge (MIL-101, Figure 5b), respectively. These super tetrahedra can be considered as upper homologues of the [SiO₄] tetrahedra which are the structural motifs of zeolites. The assembly of the corner-sharing super tetrahedra in MIL-100 and MIL-101 reproduces the linkage of [SiO₄] tetrahedra in the Mobile Thirty-Nine (MTN) topology (Figure 5c).^[50]

Kitagawa classified MOFs based on their response upon guest removal in three types of generations.^[51] According to this classification, the pores and channels of a 1st generation material will be only sustained if guest molecules are inside and it collapses irreversibly when they are removed. If guests can be removed reversibly

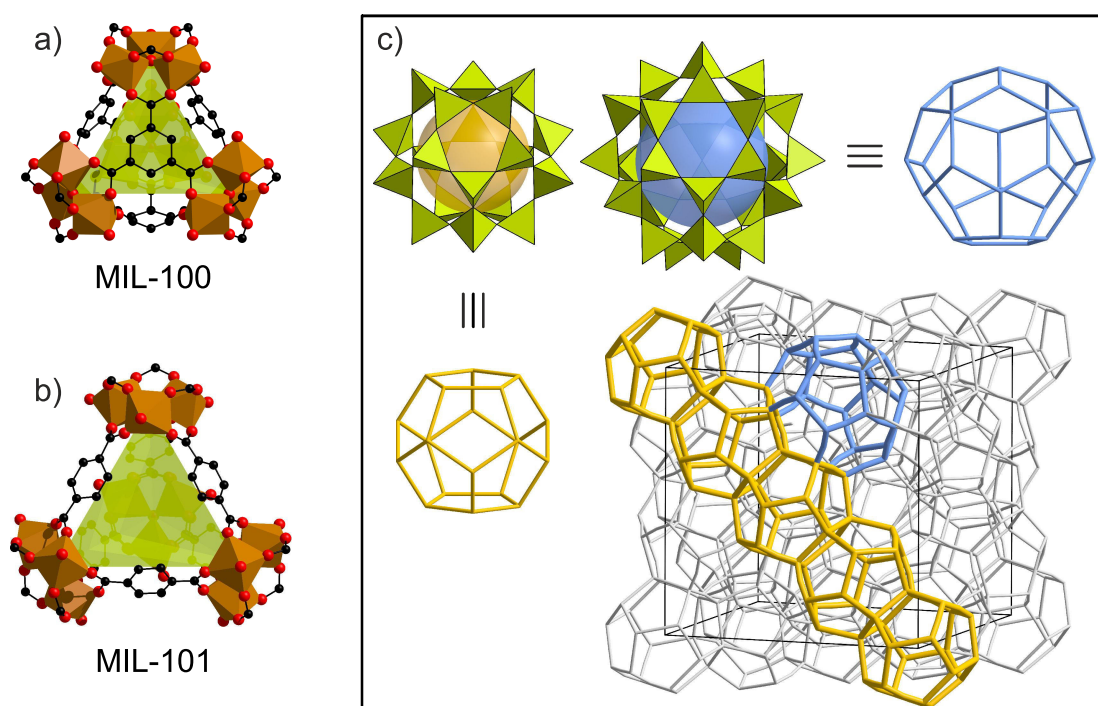


Figure 5. a) Super tetrahedron (green) of MIL-100;^[32] b) super tetrahedron (green) of MIL-101^[33] (black: carbon, red: oxygen or fluorine, brown: polyhedra around Cr); c) relationship between the structure of MIL-100 and MIL-101 and the MTN topology, the green ST enclose large cavities of different dimensions; orange and blue spheres show the accessible pore volume and have a diameter of 25 and 29 Å in MIL-100 or 29 and 34 Å in MIL-101.

* MIL stands for Matériaux de l'Institut Lavoisier.

without degradation of the framework, the compound will be considered to be a member of the 2nd generation. A 3rd generation material shows a response to guest removal or external stimuli (*e.g.* light, electric field, temperature, gas, pressure) and changes its channels and pores reversibly. The previously described MOFs can be considered as 2nd generation materials, because they do not show changes upon guest removal.

Examples of 3rd generation MOFs are the 'breathing' MIL-53 materials^[52,53] and the so-called pillar-layer MOFs which often exhibit similar guest-induced transformations.^[46,54,55] MOFs of MIL-53 type are composed of one-dimensional SBUs linked together in a parallel fashion by bdc^{2-} . This assembly causes the formation of one-dimensional parallel channels throughout the MOF which possess the ability to open and close, *e.g.* if thermally treated^[56] or exposed to gases.^[52] The change of the unit cell parameters in this 'breathing' processes can be up to 5 Å. A prerequisite for the occurrence of the effect is a flexible SBU which is able to change its coordination. These 'breathing' materials are interesting for applications like sensor materials^[57] or as hosts for drug storage and delivery.^[58]

These and the following examples illustrate that, although the pool of possible new structures is far from being exhausted, there is a growing interest in exploring and improving the properties and functionalities of known MOFs. In this context, post-synthetic modification (PSM) should be mentioned as a way to introduce functionalities into a readily synthesized MOF using mild conditions.^[40] The amino group is hitherto the most often post-synthetically modified function of MOFs. Cohen is one of the most active researchers in this young field of research and treated IRMOFs,^[59-61] MILs,^[62] and other MOFs.^[63,64] For example, it was possible to improve the resistance of IRMOFs to water via PSM with alkyl anhydrides (of different chain length) to tune the hydrophobicity of these MOFs.^[65,66] It is also possible to introduce various functionalities into one compound via two-step modifications.^[67,68]

An alternative and interesting approach to yield MOFs with a large variety of different functionalities in one individual crystal is the direct synthesis of multiple functional groups in MOFs. In this approach linkers of the same length (which are able to form the same network topology), with different functionalities attached to them, are used in a one pot synthesis to yield MOF single crystals with a uniform distribution of functionalities in each crystal.^[69] This route offers a new way to novel properties of known materials but major disadvantages of this simple method are the complicated analysis to prove the distribution of functionalities and the lack of control how the functionalities are located to each other in the crystal (which should have a certain impact on the properties).

Kitagawa proposes a more promising approach to improve and control the functionalities in MOFs by taking advantage of the surface chemistry of MOFs, in the majority of cases of so-called pillar-layer MOFs. These MOFs are composed of paddle-wheel SBUs (Figure 4b) coordinated by carboxylates (to form layers) and amines (pillaring these layers). In recent years his group investigated coordinatively immobilized monolayers of light-responsive molecules on the surfaces of MOFs,^[70] the epitaxial

growth of MOF crystals with different pore surface functionality,^[71] and the sequential growth of similar MOFs onto each other to yield core-shell crystals.^[72] These investigations point to the hitherto little regarded surface chemistry of MOFs, which surely will be a topic of the future of these materials.^[73]

2.2 Synthetic strategies

This chapter deals with diverse strategies for the synthesis of MOFs, starting with a section on isorecticular synthesis, describing it as a concept to obtain new hybrid compounds derived from known MOFs. The basic ideas behind this concept, why it is so effective in the field of MOFs and some illustrative examples are presented.

The next two subchapters are about the control of the size of MOF crystals. On the one hand single crystals offer a quick way to gain knowledge about the structure of new compounds and so their synthesis is often an important task for MOF chemists. On the other hand the expertise to synthesize nano crystals of a MOF is invaluable to meet the requirements which are demanded by specific applications like thin film devices or drug delivery.

The last section is devoted to the recently introduced coordination modulation approach which proved to be of great importance to the work presented here. The basic ideas of this method are described and the possible processes occurring during a modulated Zr-MOF synthesis are discussed.

2.2.1 The concept of isorecticular synthesis

The term "isorecticular" was first used for MOFs by Yaghi and co-workers and was defined as "having the same network topology".^[15] It was pointed out that the concept of isorecticular synthesis depends on a close examination of the synthesis parameters to produce the desired SBU which in turn defines the topology of the target compound.^[74] In this way the authors created an isorecticular series of MOFs based on the tetranuclear basic zinc acetate SBU of MOF-5^[14] (Figure 6a,b) combined with 16 different linkers of different length and/or functionality (examples in Figure 6d-f).^[15] The compounds were designated as IRMOF-1* (which was originally termed MOF-5) to IRMOF-16 and showed the same primitive cubic topology (Figure 6c) as MOF-5 with the general composition $[\text{Zn}_4\text{O}(\text{O}_2\text{C-R-CO}_2)_3]$. The synthesis of MOF-5 was optimized to achieve high yields and single crystals and the concept of isorecticular synthesis worked in this case. So it was possible to synthesize single crystals of most of the new compounds and determine their structures from single crystal analyses.

This concept of isorecticular synthesis proved to be very useful and the IRMOF series underlines how important it is to study the synthesis of potentially prototypic MOFs so that new isorecticular compounds with similar linkers can be found.

Nevertheless, it is not always possible to keep nearly identical synthesis conditions especially if the linker does not withstand the temperature of the original synthesis.

This is the case for IRMOF-0, a compound isorecticular to MOF-5. It is composed of the MOF-5 SBU and the very small linker acetylenedicarboxylic acid and forms a two-fold interpenetrated primitive cubic structure. The thermal sensitivity of the linker was bypassed by applying a room temperature synthesis in which the product precipitated upon addition of triethylamine which deprotonates the linker.^[75] Interestingly,

* IRMOF stands for isorecticular metal-organic framework.

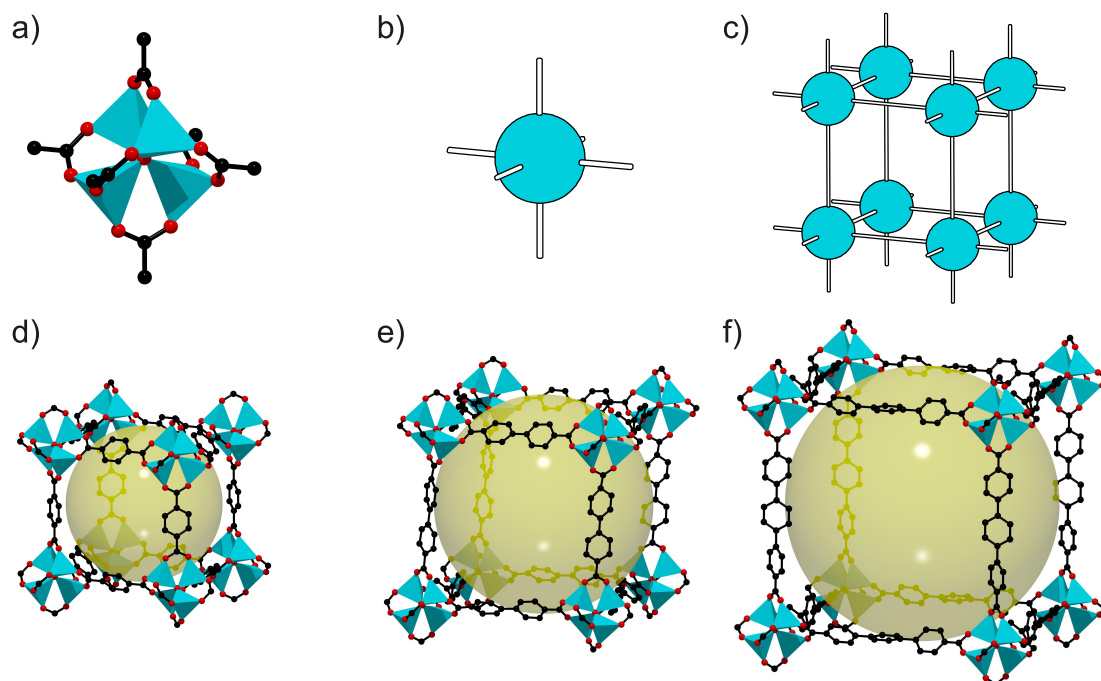


Figure 6. a) Basic zinc acetate SBU of MOF-5 (black: C, red: O, blue: polyhedra around Zn); b) topological representation of the SBU; c) topological representation of the IRMOF series, d) IRMOF-1 with bdc^{2-} ligands; e) IRMOF-10 with bpdc^{2-} ligands; f) IRMOF-16 with tpdc^{2-} ligands. Yellow spheres represent the potential free volume in the structures. Crystal structures produced from cif data given in ref. [15].

the synthesis was conducted again after determining the room temperature synthesis conditions of MOF-5. The structure of IRMOF-0 was solved from PXRD data and the help of the modeling software Cerius² because single crystals suitable for SXRD analysis were not yet obtained with this synthetic route.

Another important isorecticular series was reported as MIL-88.^{*[76]} The parent compound MIL-88A of this series is composed of trinuclear $[\text{M}_3\text{OX}(\text{O}_2\text{C})_6]$ SBUs ($\text{M} = \text{Cr}^{3+}$ or Fe^{3+} and $\text{X} = \text{OH}^-$ or F^-) (Figure 7a,d) which are linked to each other by fum^{2-} dianions ($\text{fum}^{2-} = \text{fumarate}$). The compound forms small hexagonal channels along its c axis (Figure 7b,e) and larger pores of bipyramidal cages which can be seen along the b axis (Figure 7c,f).

The isorecticular higher homologues MIL-88B to -88D can be obtained by replacing fum^{2-} with bdc^{2-} , $2,6\text{-ndc}^{2-}$ or bpdc^{2-} ligands but keeping the original synthesis. Another isorecticular homologue of this series is MIL-89 consisting of the same SBU linked by muconic dicarboxylates. The major change in these structures can be seen in an elongated c -axis, while the a -axis remains nearly unchanged. This elongation can be attributed directly to the longer length of the linker. The authors used two different synthetic routes for Cr-based and Fe-based MIL-88 compounds. For MIL-88(Cr) compounds, traditional hydrothermal, high temperature conditions were

* MIL stand for Matériaux de l'Institut Lavoisier.

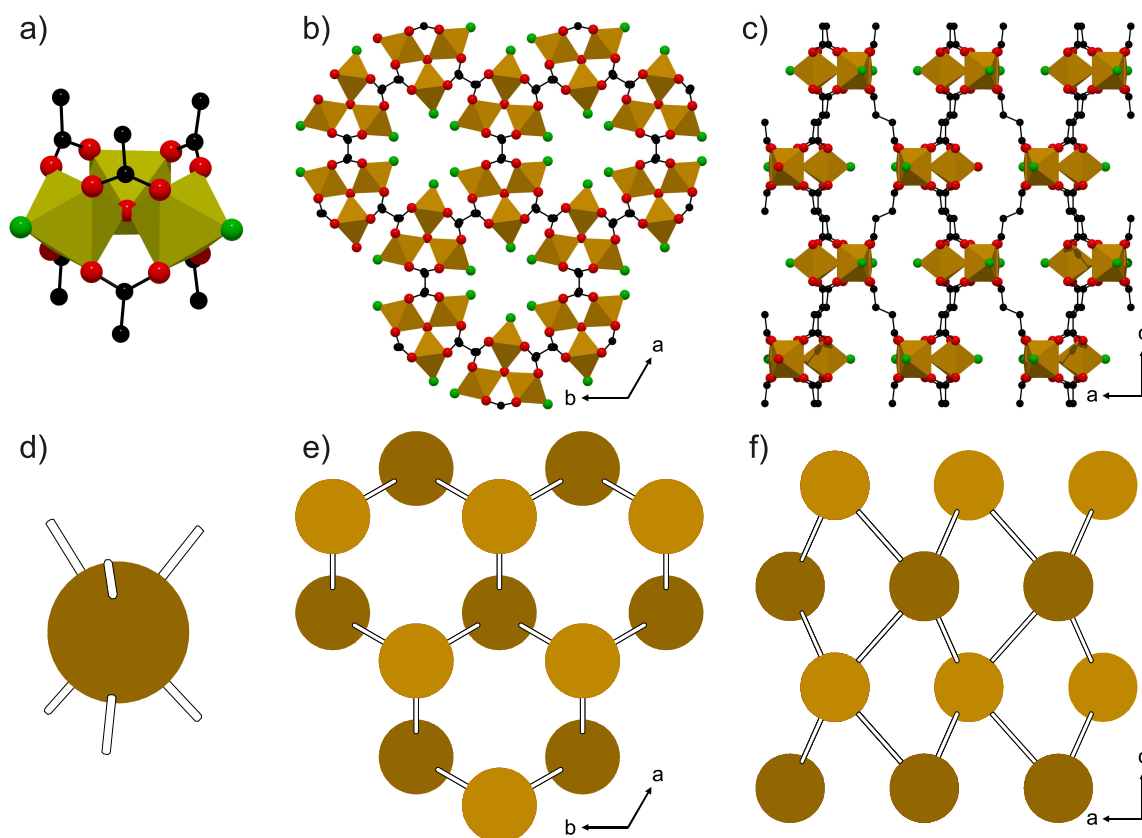


Figure 7. a) Trimeric SBU of composition $[M_3OX(O_2C)_6]$ ($M = Cr^{3+}$ or Fe^{3+} and $X = OH^-$ or F^-) (black: C, red: oxygen, green: OH or F, brown: polyhedral around Fe or Cr); b) view of MIL-88A along the c axis showing small hexagonal channels; c) view of MIL-88A along the b axis showing the larger pores of the compound; topological representation d) of the SBU, e) along the c axis and f) along the b axis. Crystal structures produced from cif data given in ref. [30].

applied, while MIL-88(Fe) compounds were synthesized with a so-called 'chemically controlled SBU'^[30] approach at lower temperatures. This interesting synthetic route will be further described and compared to the coordination modulation approach^[38,39] later (section 2.2.4, p. 17).

MIL-88A was obtained only as powder and so its structure was elucidated from PXRD by a combination of direct methods and modeling software.^[30] This procedure can be very time-consuming. Another method developed by the Férey group is the automated assembly of secondary building units which allows the prediction of the structure of not yet synthesized MOFs.^[77]

It is also possible to take a parent structure and predict isorecticular homologues of this structure with other linkers. This was done in the case of MIL-88B to -88D. In the structure of MIL-88A the fum^{2-} ligands were removed from the model and replaced by the longer linkers. After an energy minimization using the modeling software Cerius² allowing the linker to adopt the correct geometry a pre-model was obtained and applied for further Rietveld refinement.^[78] This example^[76] and others^[79,80] illustrate another advantage of isorecticular synthesis with regard to the elucidation of the

structure of new compounds with modeling techniques, which can speed up the process of discovering their structures.

There are many other examples where isorecticular synthesis allowed for deliberate tuning of the properties of new compounds. For example, the catalytic performances of the chiral MOF (CMOF) series of the Lin group were evaluated with regard to the different sizes of the open channels.^[81]

The UiO-66* to -68 series is a comparatively new family of Zr-based MOFs; it was described in 2008 by the Lillerud group.^[34] Because this family of MOFs represents a central theme of this work it will be discussed in detail in section 2.4.1 (p. 29) and chapter 3 (p. 45). The novel compound Zr-abdc (abdc²⁻ = 4,4'-azobenzenedicarboxylate) is also a new member of this series and is presented in chapter 4 (p. 55). The acquired knowledge of the synthesis of these Zr-based MOFs was also used to create the isorecticular and -structural family of PIZOFs[†] (chapter 5, p. 63).

2.2.2 Synthesis of single crystals

Single crystal X-ray diffraction (SXRD) is still one of the most important and fastest tools to determine the structure of a newly synthesized unknown MOF. In addition to this ubiquitous use for solving crystal structures, single crystals are also important for the study of other properties like loading-dependent transport diffusion coefficients under mixed gas conditions as was done for single crystals of ZIF-8.^[82] These *in-situ* IR microscopy investigations on single crystals helped to explain diffusion phenomena in ZIF-8 membranes.

Another example is the study of the chemical nature of the surface of MOF particles as performed by the Kitagawa group.^[70] In this case the surfaces of single crystals of different MOFs were post-synthetically modified with a fluorescent dye. By modifying only the surface of MOFs, more functionality can be integrated into these materials like controlled gating or sensing properties. The modification was proved by confocal laser scanning microscopy which is only possible if larger crystals are available.

Unfortunately there exists no universal remedy for the synthesis of MOF single crystals but there are a few generalities as well as a large pool of special cases which will be mentioned in the next paragraphs. MOFs are most often synthesized by precipitation from the solution. The use of an appropriate solvent which is able to dissolve both the inorganic and the organic precursor plays a crucial role for a successful synthesis. Elevated temperatures at autogenous pressure and low concentrations of the precursors are often applied for the production of single crystals. The thermal and chemical stability of the organic precursors in solution often defines the limit for the synthesis temperature; however, unfunctionalized linkers like terephthalic acid can withstand temperatures up to 250 °C.^[13]

Increasing one or both of these parameters should decrease the supersaturation of

* UiO stands for Universitetet i Oslo.

† PIZOF stands for porous interpenetrated Zr-organic framework.

the solution and thus lead to a low nucleation rate, so that few nuclei can grow to large crystals. Another approach which also keeps the local concentration of a solution low is the usage of gel diffusion methods. It has to be noted that by now only one paper is known from the beginnings of MOF chemistry which uses this slow growth method.^[83]

The biphasic solvothermal synthesis, albeit diffusion controlled, is a faster approach and was established by Forster *et al.* for MOF syntheses.^[84] They used water as solvent for the metal source and an alcohol (typically 1-pentanol or cyclohexanol) for dissolving the linker. The two phases are not miscible in each other and so the organic phase can be carefully layered on top of the aqueous. This is done in a teflon-lined autoclave, which is placed in an oven and heated under static conditions. It was not observed that even during this treatment the interface between the two phases disappeared. After a reaction time of two days, single crystals of a new compound were isolated, which had previously only been obtained as a powder.

Most often solvothermal methods provide a faster access to single crystals which can be exemplified by the synthesis of ZIF-8. In 2006 the synthesis of this prototypical ZIF were described almost concomitantly by two groups. Huang *et al.* used a liquid-phase diffusion method at room temperature, a procedure which consists of the precursors being dissolved in two liquids, one of which is carefully layered on top of the other. After a time period of seven days crystals began to grow and were finally collected after one month.^[85] Yaghi *et al.* used a solvothermal approach and were able to yield the same structure in a timeframe of 24 h.^[49] In the same paper they described eleven additional ZIFs. The classical solvothermal method was complemented by a high-throughput approach which enabled them to determine adequate synthesis conditions for single crystals of each of the compounds investigated. 25 new ZIF structures followed in 2008 by employing the same approach.^[86] Apart from the fact that the approach is automated (which surely saves a large amount of time) it exemplifies that for determining the reaction conditions for single crystals of unknown compounds a large number of experiments is often needed. Admittedly, for the synthesis of single crystals only favorable but not guaranteeing conditions can be formulated caused by the large number of uncertainties.

2.2.3 Synthesis of nanocrystals

This section describes and discusses different approaches and methods for the preparation of MOF nanocrystals. A rather classical procedure to obtain nanocrystals involves the rapid formation of a large number of crystallization nuclei, so that the precursor material is quickly exhausted and the nuclei can only grow to a certain size. In carboxylate MOF synthesis such conditions can be achieved by addition of an amine which deprotonates the linker and in this way ensures a fast reaction with many nuclei, which can then only grow to nano crystals.^[28]

Microwave supported synthesis of MOFs proved to be a practical method for the preparation of nanocrystals only in some cases, for example for different MIL

materials.^[87,88]

The group of Fischer was the first to introduce so-called 'capping groups'^{*} in the synthesis of MOFs. They investigated the homogeneous nucleation and crystal growth of MOF-5 (see Figure 6d, p. 12) by time-resolved static light-scattering (TLS) in the presence of *p*-perfluoro-methylbenzoic acid (pfmbcH) and reasoned that this capping-group competes with terephthalic acid for the complexation of the Zn cations.^[89] They were able to follow the growth of MOF-5 colloids by TLS and added a certain amount of pfmbcH at different times. After the addition of pfmbcH the MOF-5 particles stopped their growth and the radius of gyration first decreased and then remained constant after a short time. In this context pfmbcH was also denoted as an 'etching ligand'. The nano crystals they yielded were used to deposit them on COOH-terminated self-assembled monolayers (SAMs) on a Au substrate. The approach of the Fischer group will be revisited in the next section.

The synthesis of nanocrystals of MIL-89(Fe) ($[\text{Fe}_3\text{OCl}(\text{O}_2\text{C}-\text{C}_4\text{H}_4-\text{CO}_2)_3]$), a structure isorecticular to MIL-88 (see Figure 7, p. 13), by addition of chemical growth inhibiting agents was studied by the Férey group.^[90] The authors studied the effect of different metal sources and showed that the anionic part has a significant influence on the size of the resulting MOF particles. While the use of iron(III) nitrate and iron(III) chloride resulted in an immediate precipitation of MIL-89 powder, iron acetates as metal source produced a gel-like suspension of MIL-89 particles. In an earlier publication by this group, the use of this precursor for MOF synthesis had also been named 'chemically controlled SBU' approach.^[30] The authors claimed that the monocarboxylic acids already present in the metal precursor acted as inhibitors for crystal growth if the appropriate choice of reaction parameters was made. They further assert that the competition for the complexation of Fe(III) cations between monocarboxylic and dicarboxylic acids gives control over the formation of nanoparticles.^[90]

The 'chemically controlled SBU' approach was later on used by this group to obtain control over the particle size of the Zr-based MOFs UiO-66 and a new Zr-muc MOF ($\text{muc}^{2-} = \text{muconate}$).^[91] The metal source for these MOFs was the isolated complex $[\text{Zr}_6\text{O}_4(\text{OH})_4(\text{ma})_{12}]$ ($\text{ma}^- = \text{methacrylate}$) the structure of which has a strong similarity to that of the SBU found in the resulting MOFs. In the mentioned article it is shown that the particle size is correlated to the synthesis time, as determined by the application of the Scherrer equation to the broadening of the reflections in the PXRDs of samples which were investigated *ex-situ*. In fact this method only judges the mean crystallite size and since there are no SEM images or DLS measurements which are independently proving the particle size, it can be expected that the produced particles consist of nanocrystals which are strongly intergrown. Nevertheless, the authors correlate the control of crystallite size[†] to the mild synthesis conditions that can be applied when only an exchange of the monocarboxylic acids against the linkers, under retention of the cluster core composition, is necessary. To support this view,

^{*} This type of molecule is called modulator in this thesis.

[†] Guillerm *et al.* used the term particle size.^[91]

they refer to *ex-situ* NMR experiments of the Schubert group on similar Zr complexes^[92] and *ex-situ* XANES and EXAFS spectra which show that no significant changes occur from the isolated $[\text{Zr}_6\text{O}_4(\text{OH})_4(\text{OMc})_{12}]$ complex to the Zr-muc MOF.^[91] This is absolutely not surprising because the structures, determined from X-ray based methods, are obviously similar, thus the *ex-situ* analyses are no evidence for the preservation of the SBU during the synthesis.

In another paper the Schubert group postulated a direct exchange of different monocarboxylic acids on the Zr core based on *in-situ* NMR experiments.^[93,94] These findings are a much stronger support for the proposition of a direct exchange of ligands on a Zr complex which is stable in solution. To finally ensure that this mechanism is also true for the 'chemically controlled SBU' approach of the synthesis of Zr-muc MOF and UiO-66, *in-situ* NMR experiments in DMF (the solvent in which the experiments are conducted) should be conducted. Further discussion of the ligand exchangeability on Zr complexes will take place in the next subchapter embedded in the discussion of the coordination modulation approach.

2.2.4 Synthesis control via coordination modulation approach

Various types of modulation of MOF syntheses are conceivable, *e.g.* coordination modulation, protonation/deprotonation modulation^[95] or other reactions with which the modulating agents interacts with the synthesis system. The following section centers on the coordination modulation approach which was firstly described by Fischer and co-workers. While the work of the Fischer group consisted in using only two different modulator concentrations (where the modulator was added to the reaction media at different times),^[89] the Kitagawa group pursued somewhat more systematic approaches. They used the synthesis of the three-dimensional MOF HKUST-1^[45], composed of dimeric copper paddle-wheel SBUs and benzene-1,3,5-tricarboxylate (btc^{3-}), as an example for the coordination modulation approach.^[39] The approach is based on the idea of a competition between linkers and monocarboxylic acids for the coordination of the metal cations. The more monocarboxylic acids (so-called modulators) are present in the synthesis, the more copper cations can be bound into complexes with this modulator. This decreases the supersaturation of the metal precursor and slows down the nucleation of the framework. In the synthesis of HKUST-1, the authors were able to affect the size of the obtained crystals by the concentration of dodecanoic acid as modulator. They postulate that the introduction of modulators influences the formation of nuclei but that the growth rate of the crystals remains the same. Thus they explain the obtained larger crystals with greater size polydispersity at high modulator/metal ratios and the more homogenous size distribution of smaller crystals at low modulator/metal ratios.

As described in parts of this thesis, the coordination modulation method was successfully transferred to the synthesis of Zr-MOFs which contain a more complex SBU than the paddle-wheel SBU of HKUST-1. In the following, the chemistry of isolated complexes, similar in structure to the Zr-SBU, and their interactions with monocarboxylic

acids will be described.

Chojnacki and co-workers described highly symmetric Zr complexes with monocarboxylic acids^[96] which turned out to be very similar to the SBU of Zr-MOFs. They consist of an inner core with the composition $[\text{Zr}_6\text{O}_4(\text{OH})_4]^{12+}$ (Figure 8a). The Zr atoms are arranged as an octahedron the faces of which are capped by alternating $\mu_3\text{-O}^{2-}$ and $\mu_3\text{-OH}^-$ anions. Each Zr atom is coordinated in a square anti-prismatic way (Figure 8b) because the edges of the octahedron are bridged by 12 carboxylates (Figure 8c) of a monocarboxylic acid *e.g.* pivalic acid (Hpv) (Scheme 1a). NMR spectra of this complex reveal that the chemical shifts of the resonance signals are not changed between the complex in solid state and in $[\text{D}_6]$ benzene solution, indicating that the structure does not change in solution.^[96]

If the coordinating monocarboxylic acid has a smaller steric demand like the acids in Scheme 1b-d the structures of the corresponding Zr complexes possess the described $[\text{Zr}_6\text{O}_4(\text{OH})_4]^{12+}$ core but have a somewhat different outer coordination sphere. The behavior of the ligands of such Zr complexes was studied extensively by the Schubert group via single crystal analyses in combination with NMR experiments in solution,

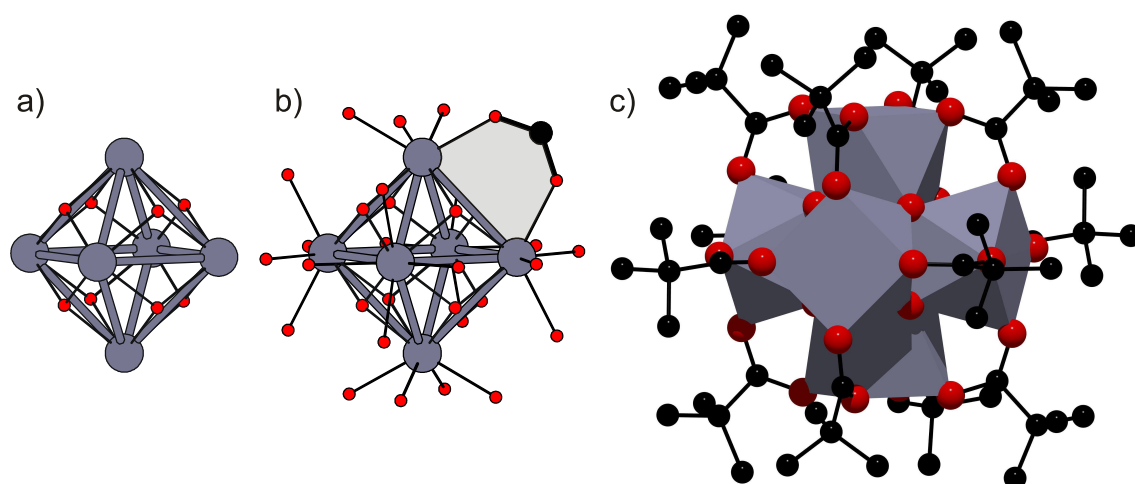
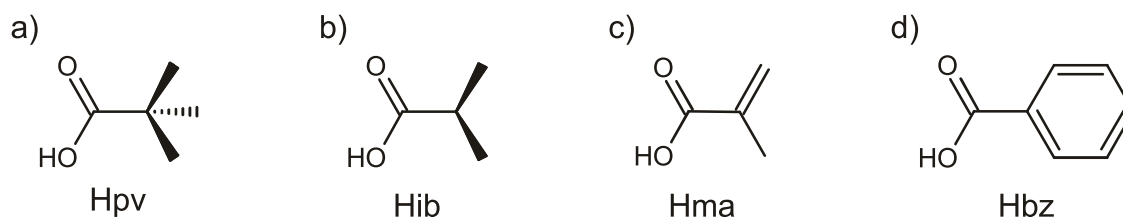


Figure 8. a) $\text{Zr}_6\text{O}_4(\text{OH})_4^{12+}$ core of the hexameric Zr complex; b) outer coordination sphere of the hexameric Zr complex, the grey area indicates the bridging coordination of one carboxylate; c) crystal structure of $[\text{Zr}_6\text{O}_4(\text{OH})_4(\text{pv})_{12}]$ (black: C, red: O, blue: Zr and polyhedral around Zr). The hydrogen atoms are not drawn for clarity. Crystal structure produced from cif data given in ref. [96].



Scheme 1. Examples of ligands used for the formation of hexameric Zr complexes: a) pivalic acid (Hpv); b) isobutyric acid (Hib); c) methacrylic acid (Hma); d) benzoic acid (Hbz).

solid state and by *ab initio* molecular dynamics simulations.^[92-94] Based on these investigations they found several indications, that an exchange of carboxylates under preservation of the $[\text{Zr}_6\text{O}_4(\text{OH})_4]^{12+}$ core is possible in solution. Hereinafter the proposed mechanism of this exchange will be discussed.

The argument starts with the inspection of the crystal structure of $[\text{Zr}_6\text{O}_4(\text{OH})_4(\text{ib})_{12}(\text{H}_2\text{O})]$ (ib^- = isobutyrate).^[93] As mentioned, the inner $[\text{Zr}_6\text{O}_4(\text{OH})_4]^{12+}$ core is very similar to the pivalate complex (Figure 8). However, instead of one coordination mode, the carboxylates show three different modes (Figure 9). There are eight edge-bridging, three chelating and one mono-coordinating carboxylates per molecule. From molecular dynamics simulation it can be stated that the more symmetric $[\text{Zr}_6\text{O}_4(\text{OH})_4(\text{pv})_{12}]$ complex (Figure 8) has a lower energy. The authors explain the occurrence of the lower symmetry and the associated higher energy with extensive hydrogen bonds to the cluster from solvating molecules or with inter-cluster hydrogen bonds in the solid state as well as in solution.^[94] Indeed they can find three different sets of NMR signals for such complexes in solution and correlate them to the three modes of coordination.^[93]

The chelating ligands are surrounding one triangular face of the Zr octahedron (Figure 9b). The monodentate carboxylic acid is situated at the opposite face. Since this 'opening' of the bridging coordination mode on the opposite side of the chelating ligands was found in several complexes, *e.g.* $[\text{Zr}_6\text{O}_4(\text{OH})_4(\text{ma})_{12}(\text{PrOH})]$ and $[\text{Zr}_6\text{O}_4(\text{OH})_4(\text{bz})_{12}(\text{PrOH})]$,^[97] the authors claimed that this position is somewhat activated and that the exchange of carboxylic acids which was proven by NMR experiments could happen in this region of the complexes.^[93]

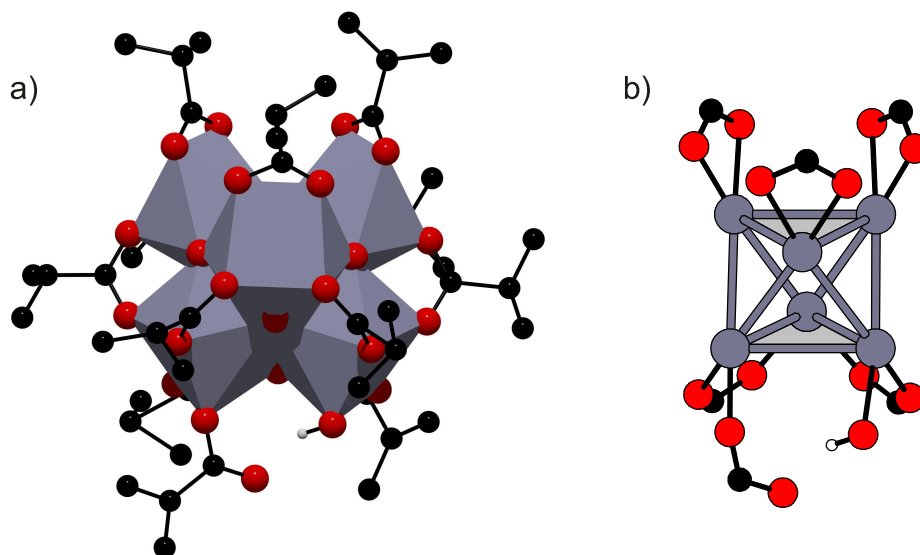
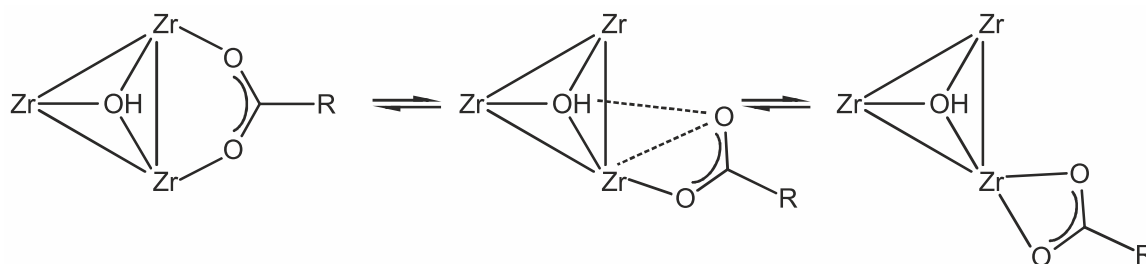


Figure 9. a) The Zr complex in the crystal structure of $\text{Zr}_6\text{O}_4(\text{OH})_4(\text{ib})_{12}(\text{H}_2\text{O})$; b) schematic sketch of the complex: The face of the Zr octahedron surrounded by chelating carboxylic acids (top) and the opposite face with the monodentate carboxylate (bottom) (black: C, red: O, blue: Zr and polyhedral around Zr). The hydrogen atoms and hydrogen-bonded carboxylic acid molecules are not drawn for clarity. Crystal structure produced from cif data given in ref. [93].



Scheme 2. Proposed trajectory for the bridging-chelating rearrangement of carboxylate ligands on the $[\text{Zr}_6\text{O}_4(\text{OH})_4]^{12+}$ core. For the sake of clarity only one triangular face of the octahedron and one carboxylic group are shown. Reproduced and edited slightly from ref. [94].

Ab initio molecular dynamic simulations for a theoretical complex of Zr and formate, analogue to the formerly described versions of the $[\text{Zr}_6\text{O}_4(\text{OH})_4(\text{pv})_{12}]$ complex, indicate the ability of this complex to change between the highly symmetric, more stable version and the 'activated' species. The mechanism of this rearrangement includes the formation of a hydrogen bond to a μ_3 -OH group (a metastable state in the simulation) of the inner $[\text{Zr}_6\text{O}_4(\text{OH})_4]^{12+}$ core (Scheme 2).

On the basis of these hints and assumptions, the rich chemistry of the described Zr complexes seems to be a powerful tool to affect and control to some extent the synthesis of Zr-based MOFs by applying different monocarboxylic acids as modulators. The addition of such molecules to the synthesis of Zr-MOFs seems to be reasonable to gain control of their precipitation in the following way. Starting from zirconium(IV) chloride in DMF, the addition of modulators could lead to the *in-situ* formation of Zr complexes with similar or analogue structures as were described above. These complexes should have the same properties as the prebuilt SBUs used by Férey *et al.* in their 'controlled SBU' approach,^[91] but with the benefit that one reaction step (the synthesis of the isolated complexes) can be skipped.

The addition of more monocarboxylic acids as needed for the formation of the complexes (stoichiometrically more than two equivalents with respect to Zr) ensures that a very large part of Zr cations are bound in these complexes and formation of the network can then only occur via a dynamic exchange of ligands on the Zr complexes, between modulating monocarboxylates and network-forming dicarboxylates. This exchange could probably occur by the mechanism described above. In the synthesis of Zr-MOFs these considerations lead to a scenario where the linkers (which form the MOF) compete with the modulators (which inhibit the formation of the MOF) for the coordination sites of the Zr complexes. If the amount of modulator largely exceeds the amount of linker, a coordinating monocarboxylate molecule should more often be exchanged by other monocarboxylates rather than by linker molecules. The formation of the framework can only proceed when the linkers connect the SBUs and so the excess of modulator should effectively suppress the nucleation of the MOFs. When the number of nuclei is small, they should grow to larger crystals. Another conceivable effect could be that the surfaces of the growing crystals are saturated with modul-

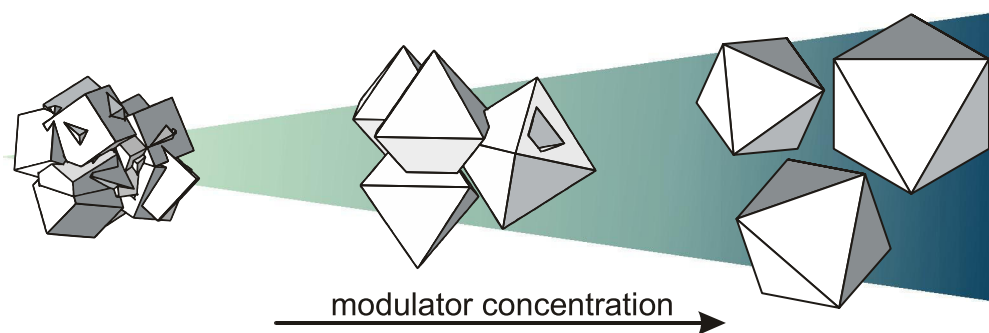


Figure 10. The amount of modulator used during the synthesis of UiO-66 controls the shape, degree of aggregation, and size of the crystals.

tors, a situation that would inhibit the attachment of small crystals to each other and reduce the number of intergrown particles. So the coordination modulation method represents a possibility to control the size of the crystals resulting from a MOF synthesis. This behavior was indeed observed experimentally in this dissertation and by the Kitagawa group^[38,39] and is discussed in more detail in chapter 3 (p. 45). The considerations of this paragraph are summarized in Figure 10.

To date the synthesis of UiO-66 is the prime example for the coordination modulation method on Zr-MOFs. While the products of the syntheses of other Zr-MOFs (especially those with linkers longer than terephthalic acid) tend to have only low crystallinity when no modulating agents are used in their synthesis, the use of modulators increases in these cases primarily the reproducibility of these syntheses. It must be pointed out that the method indeed reliably provides crystalline products but that the size control is much less effective than in the case of UiO-66.

It has to be considered that - although the Zr-MOFs with UiO-topology are isostructural to each other and their synthesis procedures are comparable - the linkers for the individual MOFs have significantly different solubilities in DMF. This is a circumstance that should have a strong influence on the growth of the respective MOF. In the case of a linker with low solubility this should make it difficult to exchange a linker versus a modulator molecule if it is connected to the SBU. The control exerted by the coordination modulation approach on such a synthesis could possibly be reduced.

Despite the fact that meanwhile many observations have been made in our laboratory which cannot be explained by this simple concept, the modulation method practically always increases the quality of the obtained products and provides a secure access to MOFs with many different linkers which would otherwise only produce low-crystallinity materials of low porosity.

2.3 Potential applications of MOFs

MOFs are very versatile compounds concerning their pore and window sizes, surface areas, and functionalities which make them an outstanding class of porous materials. This chapter deals with the currently most promising application fields for MOFs.

2.3.1 Separation

The desired product of a chemical reaction is often included in a mixture of products, by-products and/or starting material. The cost-efficient separation of such a mixture into its components is often a challenge for industrial processes.^[98] Due to their small windows and uniform pores, MOFs could act as molecular sieves and have the potential to contribute to manage such tasks.

The work associated with MOFs on the subject of separation is currently focusing on the separation of gases from gas mixtures. The materials commonly used for this purpose in industry are activated carbon, silica gel, activated alumina, and zeolites.^[20] Among these four examples zeolites are at most comparable to MOFs because of their well-defined pores, similar range of microporosity and high crystallinity. Due to their modular composition the properties of MOFs (window size, pore size, functional groups, adsorption enthalpy) are highly tunable which distinguishes them from zeolites the properties of which can often only be affected by post-treatment modifications and pore size engineering.^[99,100]

Microporous membranes with high selectivity and thermal/hydrothermal stability represent a cost-efficient route for separation processes. Zeolitic imidazolate frameworks (ZIFs) are a subclass of MOFs and ZIF-7 has been used for the preparation of thin film membranes on porous supports which exhibit a high H₂ selectivity.^[101,102] This high selectivity can be attributed to the small window size of ZIF-7 (0.3 nm) which approaches the size of H₂ (0.29 nm) but is below the size of CO₂ (0.33 nm).^[102] Besides the dimensions of the pores which naturally excludes molecules of a certain size from passing through the membrane it is also possible to take advantage of the different adsorption properties of MOFs towards different gases.^[82,103] The attachment of hydroxyl groups to the bdc linker of a paddle-wheel MOF with composition [Zn(bdc-OH)(dabco)_{0.5}] has enabled strong interactions with CO₂ of adsorption enthalpy of 22.5 kJ mol⁻¹. This is a higher value than that of 17.5 kJ mol⁻¹ of the original MOF [Zn(bdc)(dabco)_{0.5}] and shows the potential of such fine-tuned MOFs, for example for the industrial separation of CO₂/CH₄ mixtures.^[103]

2.3.2 Sorption and storage

This section deals with the potential of MOFs to adsorb and store gases (*e.g.* methane or hydrogen), the progress which has been made and the upcoming challenges in this field. The storage and release of biologically active molecules like drugs or specific gases (*e.g.* nitric oxide) are addressed in section 2.3.4 (p. 26).

The porosity of MOFs is nowadays routinely characterized by the adsorption with (comparably) inert gases like N_2 or Ar. This examination method results in characteristic values like the Langmuir^[104] or Brunauer-Emmett-Teller (BET) surface area,^[105] the pore sizes, and the pore volume of the material. The surface areas thus determined are sometimes so outrageously large^[18,33,106] that much experimental and theoretical effort has been spent to verify the applicability of the stubbornly used BET equation to determine surface areas of microporous MOFs.^[107,108] Strictly speaking, this analysis cannot be applied to micropores because it was developed for the determination of specific surface areas of meso- and macroporous materials. That is the reason for the assumption that only a monolayer of gas molecules or atoms is adsorbed in the pressure range of $0.05 < p/p_0 < 0.3$. Microporous materials are already filled with gas in this pressure range. Furthermore, the adsorption of gas by micropores relates rather to a pore-filling mechanism than to a formation of a monolayer on a flat surface. Nevertheless, it was pointed out by Snurr *et al.*^[107] that the BET equation is quite applicable for the characterization of specific surface areas of MOFs. In this investigation sorption isotherms were simulated in crystal structures of MOFs and analyzed with the BET equation like experimental data. The surface areas thus obtained were compared to the theoretical accessible surface area, calculated from a simple Monte Carlo integration technique where a probe molecule is 'rolled' over the framework surface, and to experimental data. It was found that these three values were in good agreement when two consistence criteria^[109] are satisfied: The pressure range selected for the data fitting should have values of $v(p_0 - p)^*$ increasing with p/p_0 and the y intercept of the linear regression must be positive. Although there is no further explanation for the consistence of the obtained values, these investigations justify the application of the BET equation for the evaluation of the surface areas of MOFs.

Due to their microporosity and high surface areas, one of the earliest ideas for applications of MOFs was the adsorption and storage of molecules.^[14,45] Hydrogen is commonly regarded as an alternative energy source to nowadays used fossil fuels. A substantial barrier for its use in vehicular applications is the safe and value-adding storage of it. The use of MOFs for such storage applications are nowadays a frequently encountered research topic. The amount of adsorbed hydrogen is often expressed in wt%, a magnitude which is also dependent on the pressure and the temperature at which the adsorption experiments were conducted. This circumstance makes it difficult to compare the storage capacities of MOFs because often these experimental conditions differ. Anyway, the highest amount of stored hydrogen observed until today was specified to ≈ 16 wt% in NU-100^[106] and MOF-210^[18] at pressures of up to 100 bar and at 77 K. This high value of stored hydrogen should not disguise the fact that the conditions for a safe and cost-efficient use of hydrogen are not complied to. However, to store hydrogen at a lower pressure and higher temperatures, not only a

* v is the volume of gas adsorbed per g of material, p is the pressure of the gas, and p_0 is the saturation pressure.

high surface (for large uptakes) is demanded but also small pores (to enhance adsorbent-adsorbate interactions), two properties which typically go in opposite directions.^[110]

Smaller pores seem to enhance the heat of adsorption which in turn is responsible for a higher uptake of hydrogen at ambient temperature and low pressure. For example, the heat of adsorption of HKUST-1 with bimodal pore sizes of 3.5 and 9 Å in diameter^[111] is 6.1 kJ mol⁻¹,^[112] while the heat of adsorption is significantly enhanced to 9.5 kJ mol⁻¹ in a Mg-based MOF with unimodal pores of 3.5 Å in diameter.^[113] Unfortunately this MOF exhibits a surface area of only 200 m² g⁻¹ which decreases the total uptake. For real world applications, an even higher binding energy of 15-20 kJ mol⁻¹ is desired which could allow for reversible storage at room temperature.

To further increase the heat of adsorption of hydrogen in MOFs, the introduction of exposed and/or charged metal sites appears to be one of the most promising strategies.^[114] For example, the binding energy between Li⁺ cations and H₂ in the gas phase was determined to 27 kJ mol⁻¹.^[115] At the present time the attempts to introduce Li into MOFs have not resulted in a drastic increase of binding energy;^[116] however, MOFs based on metalloligands (see next section) have improved this value to 12.3 kJ mol⁻¹.^[117]

A further advanced development concerns the storage of a gas in MOF-filled canisters where they are already used to enhance the capacity in a given volume or to lower the required pressure to transport an equivalent amount of gas. Some examples include the storage of methane,^[118,119] propane,^[120] and other gases like CO₂.^[121,122]

2.3.3 Catalytic application

When it comes to heterogeneous catalysis, the class of MOFs competes with zeolites, which commercially are one of the most important classes of catalysts.^[9] In terms of chemical and thermal stability MOFs clearly cannot compete with these purely inorganic materials. So it is obvious that any reaction which should be catalyzed by MOFs has to be based on mild conditions, with high value favoring products (fine chemicals, delicate molecules, *etc.*). Correspondingly, the researcher should take advantage of the larger variability MOFs are featuring compared to zeolites.^[123] With this situation in mind, there are a number of different possibilities available, depending on the properties of the respective MOF. Three interesting strategies for the use of MOFs in heterogeneous catalysis are mentioned in this section.

For example, coordinatively unsaturated metal sites (CUS), as they can be generated at the SBUs by removing coordinating water molecules in HKUST-1^[45] or MIL-101,^[33] were surveyed by the group of Kaskel. The experiments showed the ability of these MOFs to serve as Lewis acids to catalyze cyanosilylation reactions.^[124,125]

A linker-based approach is the application of derivatives of homogenous molecular catalysts to build up catalytically active MOFs.^[126] So-called metalloligands (ML) consist of coordinating linking groups (carboxylates, amines, cyanides, *etc.*) and additional metal complexation sites (porphyrins, Schiff bases, azamacrocycles, *etc.*).

The former are used to assemble a MOF. The additional metal of the ligands can be inserted into the linkers before the MOF is synthesized^[127] or by post-synthetic grafting.^[128] Recently, Ma *et al.* have described an isorecticular series of chiral MOFs (CMOFs) composed of BINOL-derived tetracarboxylic acids and copper containing paddle-wheel SBUs. These CMOFs were grafted with $\text{Ti}(\text{O}^i\text{Pr})_4$ and used to catalyze reactions of a wide range of aromatic aldehydes to afford chiral secondary alcohols.^[81] Another strategy to obtain catalytically active MOFs is based on the encapsulation of molecular catalysts^[129] or clusters inside the MOFs.^[130] The latter approach has a certain appeal because the MOF could serve as a template for the formation of metal or metal oxide particles, the size of which would be delimited by the size of the cavities. These nanoparticles would naturally have a very small size distribution due to the uniform pore size of the hosting MOF. The recurring problem of this plan is to prove that the particles are really encapsulated; a difficult matter if the particle size clearly exceeds the size of the cavities as it is frequently the case. For example, Cu particles of 3-4 nm were 'embedded' in MOF-5,^[131] the cavity of which has a maximal diameter of 1.5 nm.^[14] On the contrary, the infiltration of MIL-101 with Keggin-type polyoxometallates and the subsequent tests, showing that the infiltrated MOF shows a fairly good catalytic activity and selectivity,^[132] are positive examples in this context.

2.3.4 Biological applications

Porous materials of different types have a potential use for biological and medical application.^[133-135] MOFs bring some properties with them which could make them in particular suitable for such usage. Due to their wide range of composition, pore size and pore volume they are highly customizable for specific demands. Although this research area is still very young, some recent and promising examples can be cited. Major attention is spent to the delivery of drugs from nanosized MOF particles which act as a kind of nano carrier. In a first step the drug has to be adsorbed by the MOF by soaking in a saturated drug solution. An example for such a procedure was published for the antitumour drug Busulfan. It exhibits a low stability in aqueous solution and should therefore be delivered in a carrier to its place of destination. The loading of Busulfan in MIL-100 was 25 wt% which is a five times higher loading than in the best polymer nano particles.^[136] MIL-100 is constructed of the trimeric iron or chromium SBU already described in chapter 2.1 (Figure 4c, p. 6) linked together by the carboxylates of trimesic acid (benzene-1,3,5-tricarboxylate, btc^{3-}). It has a hierarchical pore system (Figure 5, p. 7) of micro- (≈ 5 to 9 \AA) and mesopores (≈ 25 and 29 \AA) and a high specific surface area of $3900 \text{ m}^2 \text{ g}^{-1}$.^[32] These properties make it possible for this material to host large molecules like the here described drugs. Additionally, the authors have shown in cell culture tests that Busulfan can be successfully released from the MOF in its active form. Other important drugs like Cidofovir, Azidothymidine triphosphate and Doxorubicin showed similarly high loadings in MIL-100 of 16, 21, and 29 wt%. In the release curves of these three drugs no 'burst' effect was noticed but a slow, complete release within three to five days,^[136] which for many applications

is favorable.

The release rates of bioactive molecules can further be adjusted by choosing an appropriate MOF that has the desired interaction with the target molecule. For example, ibuprofen can be adsorbed in MIL-100 or MIL-101. MIL-101 is composed of btc^{2-} and the same trimeric SBU mentioned above for MIL-100. It also has a hierarchical pore system (micropores $\approx 9 \text{ \AA}$, mesopores ≈ 29 and 34 \AA) and is topologically related to MIL-100 (Figure 5, p. 7). However, the pore apertures of the mesopores of this material are larger and the specific surface area of this MOF is higher ($5900 \text{ m}^2 \text{ g}^{-1}$);^[33] consequently, much more ibuprofen can be stored in MIL-101 than in MIL-100. Despite its larger apertures MIL-101 releases the stored ibuprofen within a timeframe of six days while a complete release of ibuprofen from MIL-100 requires only a time of three days. The authors explain this phenomenon with a higher proportion of aromatic rings and a higher number of SBUs (both interacting strongly with ibuprofen) in MIL-101.^[137]

Another possibility of drug delivery is provided if charged MOFs are used for the hosting of drugs where the release of the drug is triggered by the concentration of ions in the solution surrounding the MOF. The framework of the so-called bio-MOF-1 consists of a complex columnar SBU composed of Zn^{2+} cations and 6-amino-7H-purine-2-carboxylates. These columns are connected by bpdc^{2-} to form large parallel channels which are initially occupied by dimethylammonium cations, DMF and water molecules. The dimethylammonium guests can be exchanged by cationic drug molecules, for example procainamide-HCl, an antiarrhythmia drug, which has only a short half-life in vivo. The examination of the release curves in PBS buffer showed that the procainamide is continuously released into the buffer within 20 h with a complete release after 72 h. The comparatively low release of procainamide from bio-MOF-1 in nanopure water ($18.2 \text{ m}\Omega$) proved that the release is triggered by the cations present in the buffer solution.^[138]

Morris *et al.* are making use of coordinatively unsaturated metal sites (CUS) as they occur in M-CPO-27^[139] or HKUST-1^[45] for the adsorption of the biological signaling molecule nitric oxide (NO).^[25] NO is adsorbed inside these MOFs and interacts strongly with the CUS.^[140,141] While the adsorbed NO interacts too strongly with the CUS in HKUST-1 for a significant delivery of the gas (although the results indicate that the small amount of released NO is nevertheless biologically active),^[140] in M-CPO-27 it is released if the MOF is exposed to moisture.^[141] The delivery of NO by MOFs has the advantage that no by-products, which usually cause harmful effects (*e.g.* inflammation), were observable.^[25]

A major drawback for many MOF materials is their often poor chemical stability towards water or atmospheric moisture.^[26-28] For biological and in particular medical applications this chemical instability could be a desirable property to avoid accumulation in the body.^[142] For example, Serre *et al.* have investigated the delivery of bioactive molecules from a MOF constructed of iron-containing SBUs which are linked together by nicotinic acid. Although the MOF was decomposed very quickly under physiological conditions, this example demonstrates the principal usability of bioactive molecules as linkers in biodegradable hybrid materials.^[143]

2.4 Zr-based MOFs

The first subchapter of this section provides the reader with an overview of the prototypical family of the UiO-66-MOFs with regard of the structure and the already explored properties and potential applications. The second subchapter deals with the structure of the novel, isostructural family of the porous interpenetrated Zr-organic frameworks (PIZOFs), which was discovered during this thesis.

2.4.1 UiO-66 family

The topology of a MOF is determined by the SBU which is connected to the linkers. As was mentioned in chapter 2.2.4 (p. 17) the SBU in the here described Zr-MOFs is similar to the isolated cluster $[\text{Zr}_6\text{O}_4(\text{OH})_4(\text{pv})_{12}]^{[96]}$ (p. 18). It is the only SBU that is known up to today for Zr carboxylate MOFs since the Lillerud group has published the isorecticular series UiO-66 to UiO-68.^[34] The structure of the MOF is obtained when the monocarboxylic acids of the isolated complex are replaced by dicarboxylic acids. The coordination number of the SBU is twelve (according to the number of carboxylates that surround it) (Figure 11a and c) and the linkers are arranged in such a way that

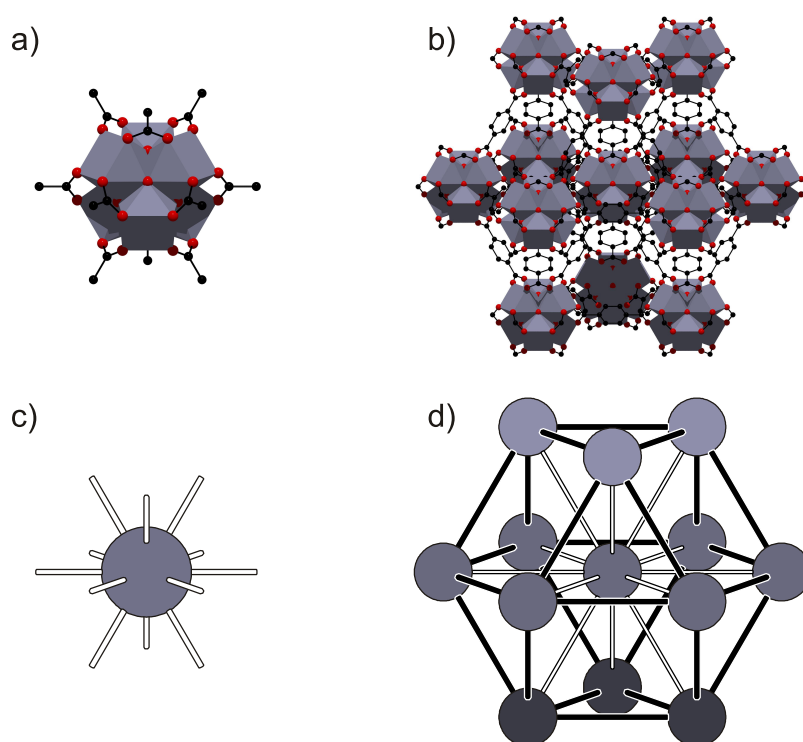


Figure 11. a) Hexameric SBU of composition $[\text{Zr}_6\text{O}_4(\text{OH})_4(\text{O}_2\text{C})_{12}]$ and b) representation of the UiO-66 structure (black: C, red: O, blue: Zr and polyhedral around Zr); c) topological representation of the SBU and d) of the structure of the UiO-66 series; some of the connectors are colored black to indicate the cuboctahedron formed around each SBU (spheres in different shades of blue (corresponding to the different layers in a ccp): SBUs, white rods: linker). Crystal structure produced from crystal data given in ref. [34].

the coordination of the SBU by other SBUs can be described as a cuboctahedron (Figure 11b and d). Thus the topology of the isostructural UiO-66 series corresponds to the cubic close-packed (ccp) structure of metals like copper or gold in which every atom is coordinated by twelve other atoms. Accordingly, the structure of the UiO-66 series can be understood as an extended version of a ccp, stretched by the linkers between the SBUs. If the structure is depicted in a different way, the tetrahedrally and octahedrally shaped cavities can be identified (Figure 12). It becomes clear that the whole structure is accessible via triangular windows the size of which is directly dependent on the length of the linker (Figure 12b).

As can be seen in Figure 12b, the H atoms of the benzene rings are pointing into the octahedral cavities of the structure while the tetrahedral cavities are surrounded by the plain faces of the benzene rings of the linker. If H_2 bpdc was functionalized on the benzene rings, these functionalities would point into the octahedral cavities but would leave the tetrahedral ones free.

To date it was possible for several groups to find Zr-MOFs which crystallize with a topology isorecticular to UiO-66 (Table 1). It is a conspicuous feature of these examples that the linkers, except for those of the UiO-MOF series, is most often a derivative of terephthalic acid or is of shorter length, like muconic acid.

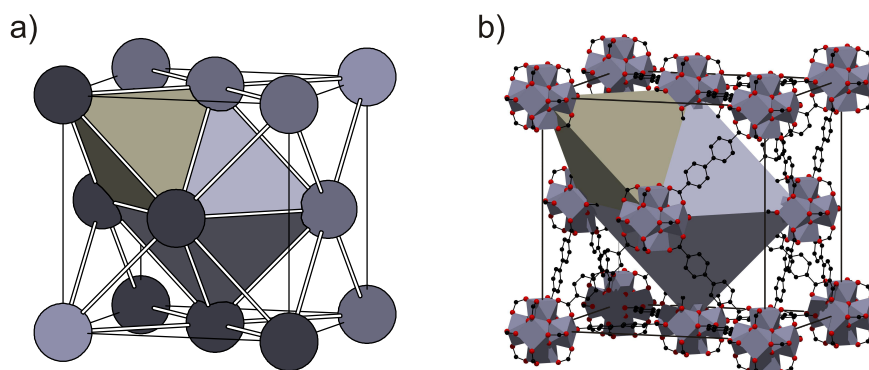
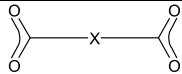
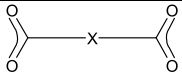
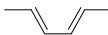
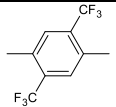
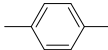
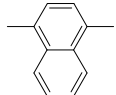
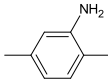
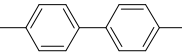
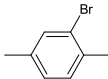
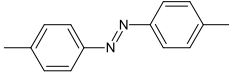
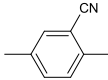
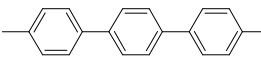
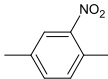
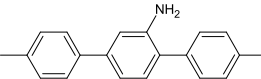


Figure 12. a) Topological representation of the unit cell of the UiO-66 structure, with a tetrahedral (brown) and an octahedral (light blue) void of the structure highlighted (spheres: SBUs, white rods: linkers). The different shades of blue of the spheres correspond to the layers in a ccp. b) crystal structure of UiO-67, the voids are highlighted similar as in a) (black: C, red: O, blue: Zr and polyhedral around Zr).

Apart from the results presented in this thesis there are only two other publications in which the properties of MOFs of the UiO-66 family with longer linkers than terephthalic acid and its derivatives were studied.^[34,147] Presumably this is due to the difficulties experienced so far in producing these MOFs without the aid of a modulator; in ref. [147] acetic acid is used to obtain crystalline products.

The majority of papers in Zr-MOFs deal with UiO-66 analog MOFs, which are composed of linkers which are derivatives of terephthalic acid. Such compounds appear to be relatively easy to access by simply replacing the linker used in the synthesis.

Table 1. Designation of Zr-MOFs (UiO-type), their linkers and the related reference.

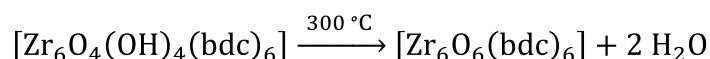
Designation		Ref.	Designation		Ref.
Zr-muc		[91]	Zr-bdc-(CF ₃) ₂		[144]
Zr-bdc (UiO-66)		[34]	Zr-1,4-ndc		[145]
Zr-bdc-NH ₂		[145]	Zr-bpdc (UiO-67)		[34]
Zr-bdc-Br		[145]	Zr-abdc		this work
Zr-bdc-CN ^[a]		[146]	Zr-tpdc (UiO-68)		[34]
Zr-bdc-NO ₂		[145]	Zr-tpdc-NH ₂		this work

[a] This MOF was synthesized via a post-synthetic modification of Zr-bdc-Br.

Thus, first of all the important properties of UiO-66 are described in order to discuss more specific UiO-66 analog MOFs (see Table 1).

UiO-66 is stable in many commonly used solvents such as benzene, acetone, ethanol and DMF,^[36] but it is the high stability in aqueous solution what really distinguishes this compound from other carboxylate MOFs.^[34] Even in an acidic solution of HCl (pH = 1) the MOF maintains its structure, while it loses its crystallinity if immersed in aqueous NaOH (pH = 14).^[36,37]

The Zr-SBU can eliminate two water molecules upon thermal treatment. This dehydroxylation of UiO-66 begins at temperatures of ca. 100 °C and is completed at 300 °C.^[34,36,148]



The reaction can be monitored by IR spectroscopy. At elevated temperatures and reduced pressure the IR band associated with the vibration of isolated hydroxyl groups situated at the SBUs of the starting material disappears from the spectrum. The consequence of this reaction is a lower coordination number of seven for each zirconium cation which leads to a compression of the Zr-SBU (Figure 13).

If this compression would proceed in an ordered fashion, this process should lead to changes in the PXRD due to the lower symmetry of the resulting network. Since the removal of the hydroxyl groups leaves the PXRD patterns almost unaffected, the distortion of the SBUs occurs most likely randomly in the framework. The diagonal splitting of the Zr octahedron was only observed in the analysis of EXAFS data, a method probing the local environment.^[36]

As already mentioned, after dehydroxylation of the SBU the Zr atoms are only seven-fold coordinated by oxygen atoms and potentially possess one open coordination site per Zr atom. These Lewis acid sites can be used for catalytic applications. De Vos *et al.* have studied the ability of UiO-66 and Zr-bdc-NH₂ for the catalysis of organic reactions. They found that especially the combination of acid (the dehydroxylated SBU) and base sites (the amino groups) in Zr-bdc-NH₂ is advantageous for the catalysis of the condensation of heptanal and benzaldehyde to jasminaldehyde.^[148] Besides this catalytic activity they also found a lower temperature of 200 °C for the elimination of all water in Zr-bdc-NH₂. Even if the same Zr₆O₄(OH)₄(O₂C)₁₂ SBU is present in all Zr-MOFs investigated so far, the conditions for the dehydroxylation process seem to be affected by the linkers.

Concomitantly, the respective linker also determines the maximum thermal stability of the entire framework (Table 2). In this context Zr-MOFs with less reactive functionalities have usually a higher thermal stability, for example UiO-66 with no functionalities is thermally stable up to 500 °C^[34] while Zr-bdc-NH₂ decomposes at

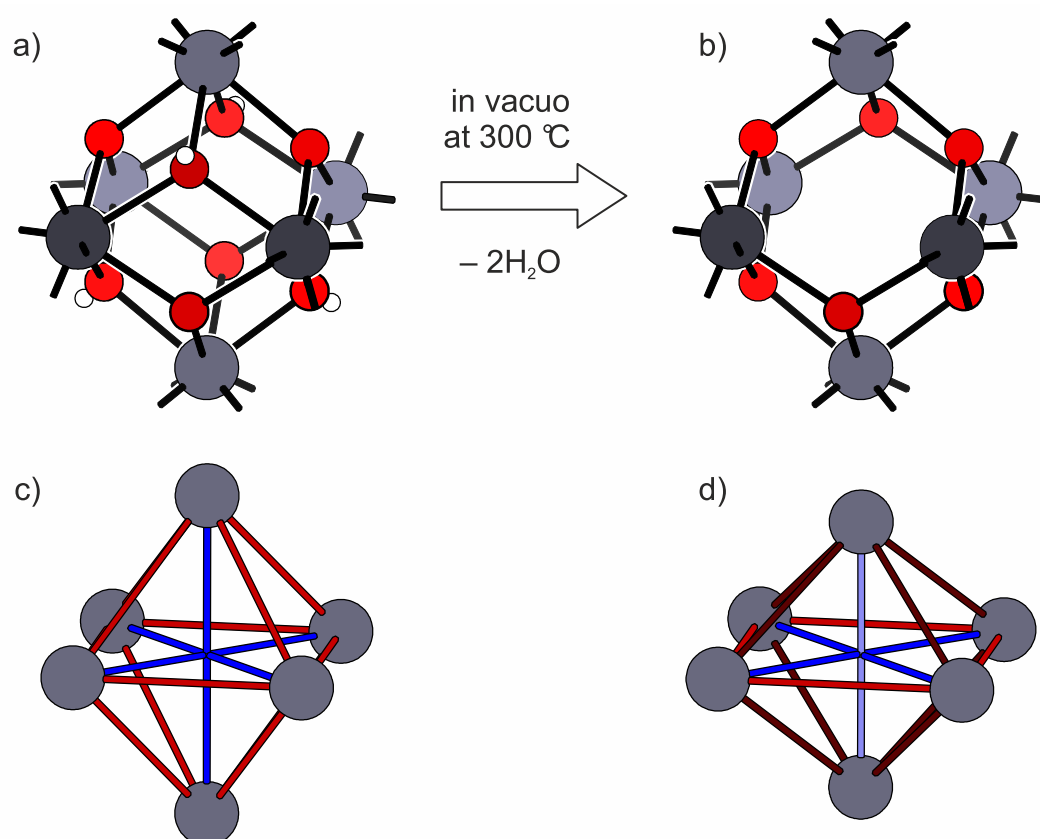


Figure 13: Dehydroxylation process of the SBU in UiO-66 (red: O, white: H, blue: Zr). a) The Zr₆O₄(OH)₄ SBU eliminates two water molecules upon thermal treatment in vacuo, which results in b) a distorted coordination of Zr in a Zr₆O₆ SBU; c) the twelve edges of the Zr₆O₄(OH)₄ octahedron (red) split up into d) four long in-plane edges (red) and eight shorter edges (brown). The diagonals of the octahedron are splitted into two longer in-plane (blue) and one orthogonal short diagonal (grey). The figure was reproduced from ref. [36].

Table 2. Comparison of BET surface areas determined from sorption isotherms of Zr-MOFs isorecticular to UiO-66 and their thermal stability in air.

Designation	specific surface area [m ² g ⁻¹]	Thermal stability [°C]
Zr-muc	705 ^[91]	250 ^[91]
Zr-bdc (UiO-66)	1187 ^[34]	500 ^[34]
Zr-bdc-NH ₂	1112 ^[145]	350 ^[37]
Zr-bdc-Br	851 ^[145]	500 ^[145]
Zr-bdc-CN	661 ^[146]	400 ^[146]
Zr-bdc-NO ₂	756 ^[145]	350 ^[37]
Zr-bdc-(CF ₃) ₂	540 ^[144]	- ^[a]
Zr-1,4-ndc	615 ^[145]	450 ^[145]
Zr-bpdc (UiO-67)	3000 ^[34]	500 ^[34]
Zr-abdc	3000 ^[b]	400 ^[b]
Zr-tpdc (UiO-68)	4170 ^[34]	500 ^[34]

[a] No data provided

[b] Data from this work

350 °C.^[37] Nevertheless, all the Zr compounds are still thermally very robust MOFs. Sorption measurements proved the accessibility of the pores in Zr-MOFs and gave high specific surface areas as determined with the BET equation (Table 2).^[107,108] Although it is possible to calculate pore size distributions from the sorption data, the pore sizes of UiO-66 are often estimated from the crystal structure to diameters* of 1.1 nm and 0.8 nm for the octahedral and tetrahedral cavity, respectively.^[148] The triangular window sizes are estimated from the "largest sphere which may fit the window"^[34] and are given as 6, 8, and 10 Å for UiO-66 to UiO-68, respectively.^[34,148] It seems that this estimation is not consistent because others^[149] give a window diameter of 7 Å for UiO-66. This shows that the opening of a triangular window may not be described in the best way by the diameter of a sphere. Additionally, this is apart from the fact that a certain dynamic of the linkers should be expected,^[150,151] which should consequently lead to different window sizes compared to the ones estimated from the crystal structure with fixed linkers.

Comparing the Zr-MOFs with terephthalic acid derivatives, it is striking that any additional functionality at the framework leads to a decrease in the specific surface area (Table 2). This can be explained by the fact that, although the surface should in principal increase due to the presence of additional organic groups, the molecular mass of the MOF also increases, which in the end leads to a decrease in the specific surface area. Larger specific surface areas can be reached with longer linkers like bpdc²⁻, abdc²⁻, or tpdc²⁻.

The functionalities on the linker can also change the chemical stability of Zr-MOFs. While UiO-66 (and other derivatives) dissolves in NaOH the isorecticular Zr-bdc-NO₂ remains intact.^[37] The reasons for these different stabilities are not yet clarified but the example shows that there are further opportunities to increase the chemical

* For the estimation of pore sizes often the diameter of the biggest sphere which can be placed into the cavity without contacting the framework atoms is indicated.

stability of Zr-MOFs.

Another possibility to tune the properties of MOFs isostructural to UiO-66 is the post-synthetic modification (PSM) of the functional groups on the linker. Simulation methods show that $-\text{SO}_3\text{H}$ and $-\text{CO}_2\text{H}$ functionalized forms of UiO-66 should be suitable for CO_2 capturing from gas mixtures with CH_4 .^[152] As it should be difficult to synthesize such UiO-66 analog MOFs directly if these functional groups are situated on the linker, PSM appears as a capable tool to introduce these functions into a readily synthesized MOF at milder conditions. Since these compounds are usually very resistant to various solvents and insensitive to acidic and slightly alkaline environments, they are particularly suitable for the introduction of a variety of functionalities into this family of MOFs with PSM. Today the most commonly modified organic group of Zr-MOFs is the amino group in Zr-bdc- NH_2 , most likely due to the commercial availability of $\text{H}_2\text{bdc-NH}_2$. It is possible to convert this type of functionality post-synthetically into different amides using anhydrides^[145,153] and to hemiaminal and aziridine products with acetaldehyde.^[154] Cohen *et al.* showed that it is possible to convert the bromide of Zr-bdc-Br into a cyano group with high yields using microwave irradiation for 60 min. Zr-bdc-CN can also be prepared from $\text{H}_2\text{bdc-CN}$, which is not commercially available and has to be synthesized first in four steps. In this case the PSM is particularly effective because it reduces the number of reaction steps from four to two, the required time from ≈ 98 h to ≈ 24 h, and the overall yield increases from 31% to 90%.^[146]

2.4.2 Porous interpenetrated Zr-organic framework (PIZOFs)

After establishing the reliable route of coordination modulation for the synthesis of Zr-MOFs, it has been possible to think about deliberate design of the pore interior of this type of porous material. The design of MOFs with similar topologies and unit cell dimensions is actually the design of the linker molecules which are assembling the framework with the same recurring SBU. The family of porous interpenetrated Zr-organic frameworks (PIZOFs) is the result of the combination of the reliably emerging $\text{Zr}_6\text{O}_4(\text{OH})_4(\text{O}_2\text{C})_{12}$ SBU and very long linkers (Figure 14) whose functional groups are adjustable by their modular synthesis.

These specialized linkers were synthesized by Pascal Roy in the Godt group at the University Bielefeld as a part of the cooperation within the priority program "Porous Metal-Organic Frameworks" (SPP 1362, MOFs). They are prepared from dihalobenzenes, carrying the appropriate functionalities (blue part in Figure 14) coupled with 4-ethynylcarboxylates (yellow part in Figure 14) to yield long rodlike dicarboxylic

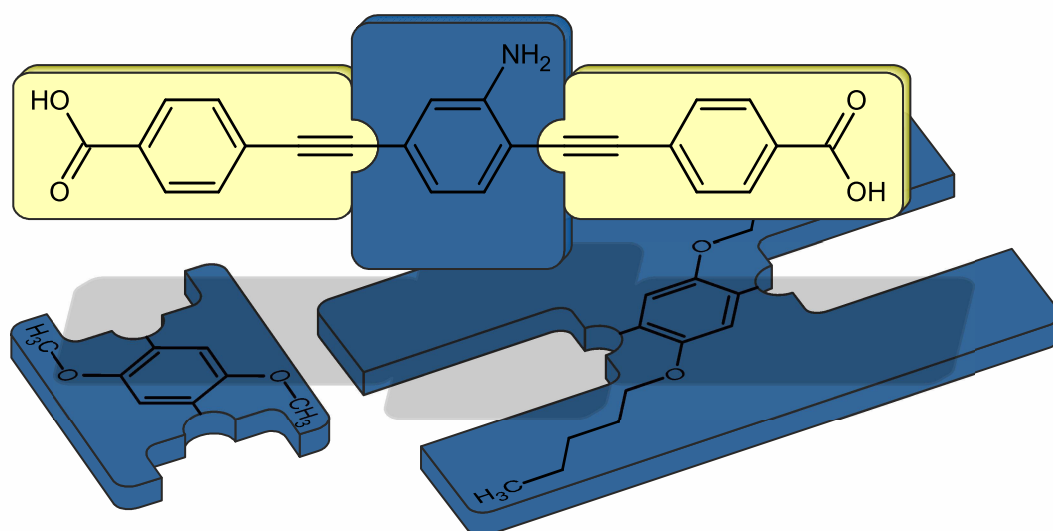


Figure 14. Basic structure of the linkers used for the synthesis of PIZOFs. The yellow parts are kept constant while the blue part is exchangeable by a large pool of functionalized benzene units.

acids of general composition $\text{HO}_2\text{C}[\text{PE-P}(\text{R}^1, \text{R}^2)\text{-EP}]\text{CO}_2\text{H}$ (P = phenylene, E = ethynylene; R^1, R^2 = side chains at the central phenylene unit). This way represents an approved access to a large variety of different diacids which opens the door to a broad spectrum of fine-tuned MOFs.

Due to the fact that PIZOFs and the UiO-66 family share the same type of SBU (cp. section 2.4.1, p. 29) the structures of both are related to each other. Indeed one of the independent frameworks of the PIZOF structure has the same topology as UiO-66 with large windows and pores due to the length of the linkers. The difference between the two structures becomes clear when the tetrahedral cavities are compared. In the UiO-

66 family all these cavities are equivalent to each other (Figure 15a,b). Due to the bending of the long linkers in the PIZOFs their structure exhibits two differing tetrahedral cavities which are arranged alternately (Figure 15c-e).

The linkers are bent either into the centre of the cavity or away from it which leads to convex (Figure 15d) and concave (Figure 15e) pores with different pore sizes. Actually only the larger convex pores exhibit substantial free pore volume, the smaller ones are occupied with linkers and SBUs of another identical framework (Figure 16a) which interpenetrates the first one (Figure 16b,c). The SBUs of the PIZOFs are so to speak wrapped by linkers from the 'other' framework. The interpenetrating framework extends its linkers into the octahedral cavity of the first framework and thereby reduces this cavity into another convex tetrahedral one. Another possibility to describe the PIZOF structure is the comparison with the zinc blende structure (Figure 16d), because the positions of the SBUs are analog to the positions of Zn^{2+} and S^{2-} in this structure. Summarizing so far, the long linkers employed cause very large

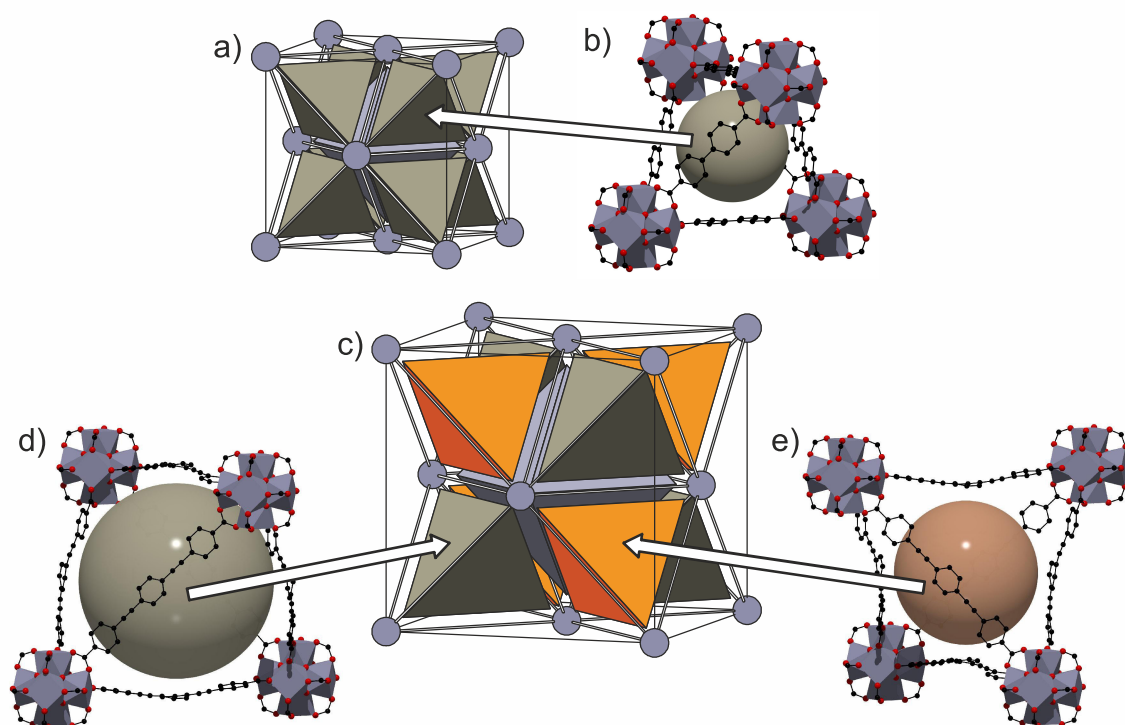


Figure 15. a) Topological representation of UiO-67 showing the equivalent tetrahedral cavities throughout the framework and one octahedral cavity (to a large part occluded by the tetrahedral cavities); b) tetrahedral cavity in UiO-67 (diameter of brown sphere = 10 Å). c) Topological representation of the PIZOF structure showing the alternating tetrahedral cavities of the framework and one octahedral cavity (to a large part occluded by the tetrahedral cavities); d) Convex cavity of the PIZOF structure (diameter of brown sphere = 19 Å); e) concave tetrahedral cavity of the PIZOF structure (diameter of orange sphere = 14 Å). a) and c) blue spheres: SBUs, white rods: linkers, b), d) and e) black: C, red: O, blue: polyhedral around Zr. Brown or orange spheres are representing the potential free volume (excluding van der Waals radii), respectively.

cavities the size of which is sufficient for an interpenetration of two independent frameworks. Compared to the uninterpenetrated UiO family this arrangement causes some special features. Again the benzene rings of the linkers are arranged in such a way that their aromatic H atoms and possible functionalities point into the octahedral cavities while the plain faces of the benzene rings enclose the tetrahedral ones. Each convex tetrahedral cavity is enclosed by an octahedral one of the second framework (Figure 17a,b). The functionalities on the central benzene units of the linkers of the former are then pointing into the convex cavities. In the case that the linkers carry extended functionalities, for example long alkyl chains, these should fill out a large part of the cavities as it is the case for PIZOF-6 (Figure 17c). The highly modular synthesis of the linkers and the tolerance of the PIZOF structure towards many functional groups provides a high degree of control over the interior of the pores of this family of MOFs.

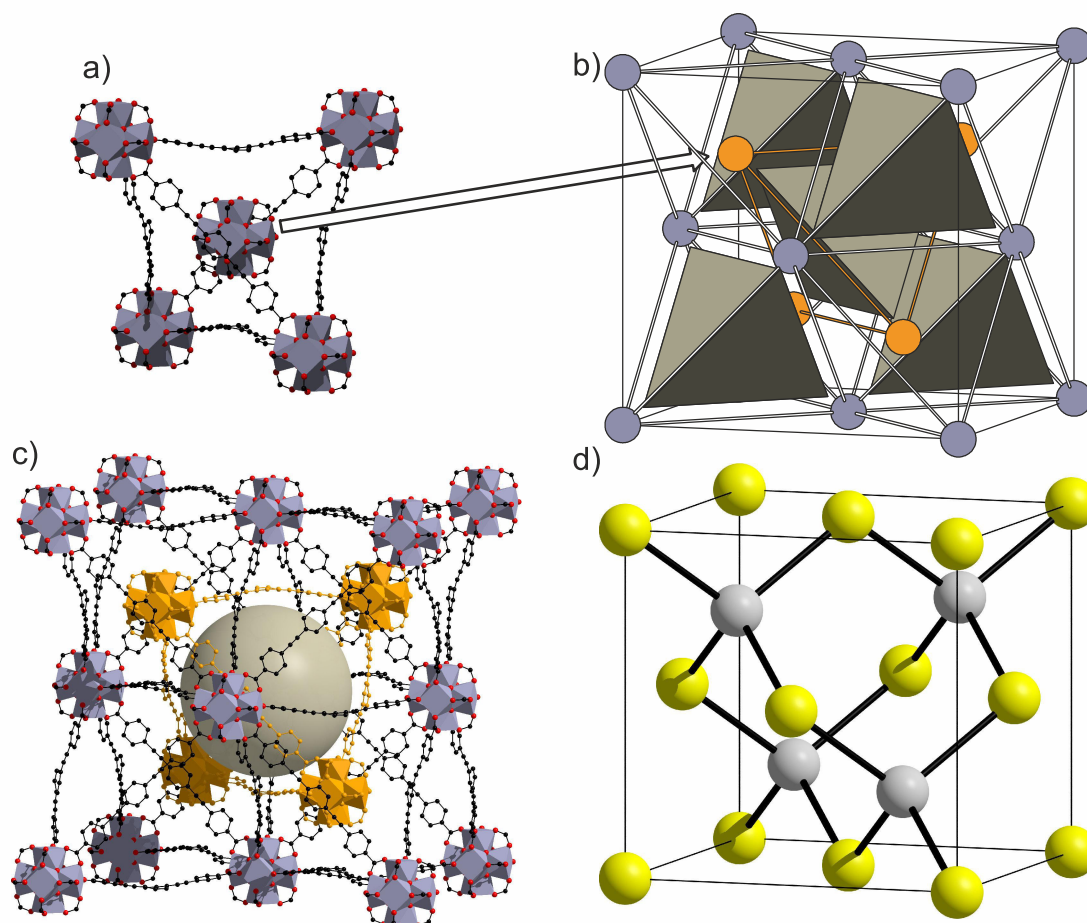


Figure 16. a) Concave tetrahedral cavity of the PIZOF structure with a SBU of the interpenetrating framework in its centre (black: C, red: O, blue: polyhedral around Zr); b) full topological representation of the PIZOF structure, one interpenetrating framework is depicted in orange (blue and orange spheres: SBUs, rods: linkers); c) crystal structure of the PIZOFs corresponding to the topological representation in b); d) crystal structure of zinc blende (grey: Zn, yellow: S).

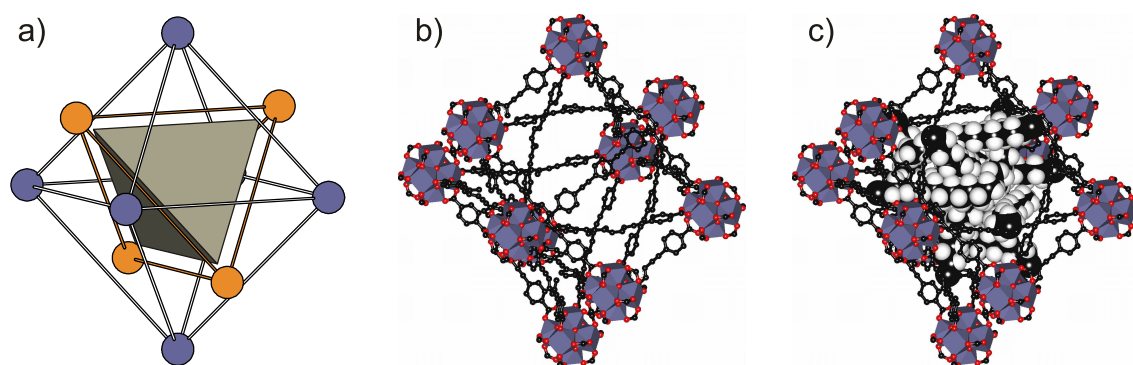


Figure 17. a) Topological representation of the PIZOF structure with a tetrahedral cavity enclosed by an octahedral cavity of the interpenetrating framework (blue and orange spheres: SBUs, white rods: linkers); b) PIZOF structure as determined by SXRD and c) theoretically modeled functionalities within PIZOF-6, filling a large part of the pore volume (black: C, red: O, blue: polyhedral around Zr).

2.5 References

- [1] A. F. Cronstedt, *Akad. Handl. Stockholm* **1756**, 18, 120–123.
- [2] R. M. Barrer, *J. Chem. Soc.* **1948**, 127–132.
- [3] R. M. Barrer, D. W. Riley, *J. Chem. Soc.* **1948**, 133–143.
- [4] R. M. Barrer, *J. Chem. Soc.* **1948**, 2158–2163.
- [5] S. Babel, T. A. Kurniawan, *J. Hazard. Mater.* **2003**, B97, 219–243.
- [6] R. E. Morris, P. S. Wheatley, *Angew. Chem., Int. Ed.* **2008**, 47, 4966–4981.
- [7] T. Bein, *Chem. Mater.* **1996**, 8, 1636–1653.
- [8] J. Caro, M. Noack, P. Kölsch, R. Schäfer, *Microporous Mesoporous Mater.* **2000**, 38, 3–24.
- [9] A. Corma, *Chem. Rev.* **1995**, 95, 559–614.
- [10] A. Corma, *J. Catal.* **2003**, 216, 298–312.
- [11] C. S. Cundy, P. A. Cox, *Chem. Rev.* **2003**, 103, 663–701.
- [12] O. M. Yaghi, G. Li, H. Li, *Nat. Chem.* **1995**, 378, 703–706.
- [13] G. Férey, *Chem. Soc. Rev.* **2008**, 37, 191–214.
- [14] H. Li, M. Eddaoudi, M. O'Keeffe, O. M. Yaghi, *Nature* **1999**, 402, 276–279.
- [15] M. Eddaoudi, J. Kim, N. L. Rosi, D. Vodak, J. Wachter, M. O'Keeffe, O. M. Yaghi, *Science* **2002**, 295, 469–472.
- [16] R. Robson, *Dalton Trans.* **2008**, 5113–5131.
- [17] K. Koh, A. G. Wong-Foy, A. J. Matzger, *J. Am. Chem. Soc.* **2009**, 131, 4184–4185.
- [18] H. Furukawa, N. Ko, Y. B. Go, N. Aratani, S. B. Choi, E. Choi, A. O. Yazaydin, R. Q. Snurr, M. O'Keeffe, J. Kim, O. M. Yaghi, *Science* **2010**, 329, 424–428.
- [19] S. S. Han, J. L. Mendoza-Cortés, W. A. Goddard III, *Chem. Soc. Rev.* **2009**, 38, 1460–1476.
- [20] J.-R. Li, R. J. Kuppler, H.-C. Zhou, *Chem. Soc. Rev.* **2009**, 38, 1477–1504.
- [21] L. Ma, C. Abney, W. Lin, *Chem. Soc. Rev.* **2009**, 38, 1248–1256.
- [22] W. J. Rieter, K. M. L. Taylor, W. Lin, *J. Am. Chem. Soc.* **2007**, 129, 9852–9853.
- [23] A. Kobayashi, H. Hara, S.-i. Noro, M. Kato, *Dalton Trans.* **2010**, 39, 3400–3406.
- [24] G. Lu, J. T. Hupp, *J. Am. Chem. Soc.* **2010**, 132, 7832–7833.
- [25] N. J. Hinks, A. C. McKinlay, B. Xiao, P. S. Wheatley, R. E. Morris, *Microporous Mesoporous Mater.* **2010**, 129, 330–334.
- [26] J. J. Low, A. I. Benin, P. Jakubczak, J. F. Abrahamian, S. A. Faheem, R. R. Willis, *J. Am. Chem. Soc.* **2009**, 131, 15834–15842.
- [27] J. A. Greathouse, M. D. Allendorf, *J. Am. Chem. Soc.* **2006**, 128, 10678–10679.
- [28] L. Huang, H. Wang, J. Chen, Z. Wang, J. Sun, D. Zhao, Y. Yan, *Microporous Mesoporous Mater.* **2003**, 58, 105–114.
- [29] T. Loiseau, L. Lecroq, C. Volkringer, J. Marrot, G. Férey, M. Haouas, F. Taulelle, S. Bourrelly, P. L. Llewellyn, M. Latroche, *J. Am. Chem. Soc.* **2006**, 128, 10223–10230.
- [30] C. Serre, F. Millange, S. Surblé, G. Férey, *Angew. Chem., Int. Ed.* **2004**, 43, 6285–6289.
- [31] T. Ahnfeldt, N. Guillou, D. Gunzelmann, I. Margiolaki, T. Loiseau, G. Férey, J.

- Senker, N. Stock, *Angew. Chem, Int. Ed.* **2009**, *48*, 5163–5166.
- [32] G. Férey, C. Serre, C. Mellot-Draznieks, F. Millange, S. Surblé, J. Dutour, I. Margiolaki, *Angew. Chem., Int. Ed.* **2004**, *43*, 6296–6301.
- [33] G. Férey, C. Mellot-Draznieks, C. Serre, F. Millange, J. Dutour, I. Margiolaki, *Science* **2005**, *309*, 2040–2042.
- [34] J. H. Cavka, S. Jakobsen, U. Olsbye, N. Guillou, C. Lamberti, S. Bordiga, K. P. Lillerud, *J. Am. Chem. Soc.* **2008**, *130*, 13850–13851.
- [35] M. Dan-Hardi, C. Serre, T. Frot, L. Rozes, G. Maurin, C. Sanchez, G. Férey, *J. Am. Chem. Soc.* **2009**, *131*, 10857–10859.
- [36] L. Valenzano, B. Civalieri, S. Chavan, S. Bordiga, M. H. Nilsen, S. Jakobsen, K. P. Lillerud, C. Lamberti, *Chem. Mater.* **2011**, *23*, 1700–1718.
- [37] M. Kandiah, M. H. Nilsen, S. Usseglio, S. Jakobsen, U. Olsbye, M. Tilset, C. Larabi, E. A. Quadrelli, F. Bonino, K. P. Lillerud, *Chem. Mater.* **2010**, *22*, 6632–6640.
- [38] T. Tsuruoka, S. Furukawa, Y. Takashima, K. Yoshida, S. Isoda, S. Kitagawa, *Angew. Chem., Int. Ed.* **2009**, *48*, 4739–4743.
- [39] S. Diring, S. Furukawa, Y. Takashima, T. Tsuruoka, S. Kitagawa, *Chem. Mater.* **2010**, *22*, 4531–4538.
- [40] Z. Wang, S. M. Cohen, *Chem. Soc. Rev.* **2009**, *38*, 1315–1329.
- [41] B. F. Abrahams, B. F. Hoskins, D. M. Michail, R. Robson, *Nature* **1994**, 727–729.
- [42] H. Li, M. Eddaoudi, T. L. Groy, O. M. Yaghi, *J. Am. Chem. Soc.* **1998**, *120*, 8571–8572.
- [43] M. O'Keeffe, M. Eddaoudi, H. Li, T. Reineke, O. M. Yaghi, *J. Solid State Chem.* **2000**, *152*, 3–20.
- [44] D. J. Tranchemontagne, J. L. Mendoza-Cortés, M. O'Keeffe, O. M. Yaghi, *Chem. Soc. Rev.* **2009**, *38*, 1257–1283.
- [45] S. S.-Y. Chui, S. M.-F. Lo, J. P. H. Charmant, A. G. Orpen, I. D. Williams, *Science* **1999**, *283*, 1148–1150.
- [46] D. N. Dybtsev, H. Chun, K. Kim, *Angew. Chem., Int. Ed.* **2004**, *43*, 5033–5036.
- [47] F. Millange, C. Serre, G. Férey, *Chem. Commun.* **2002**, 822–823.
- [48] A. U. Czaja, N. Trukhan, U. Müller, *Chem. Soc. Rev.* **2009**, *38*, 1284–1293.
- [49] K. S. Park, Z. Ni, A. P. Côté, J. Y. Choi, R. Huang, F. J. Uribe-Romo, H. K. Chae, M. O'Keeffe, O. M. Yaghi, *Proc. Natl. Acad. Sci. U. S. A.* **2006**, *103*, 10186–10191.
- [50] C. Baerlocher, L. B. McCusker, "Database of Zeolite Structures", to be found under <http://www.iza-structure.org/databases/>.
- [51] S. Kitagawa, R. Kitaura, S.-i. Noro, *Angew. Chem., Int. Ed.* **2004**, *43*, 2334–2375.
- [52] C. Serre, S. Bourrelly, A. Vimont, N. A. Ramsahye, G. Maurin, P. L. Llewellyn, M. Daturi, Y. Filinchuk, O. Leynaud, P. Barnes, G. Férey, *Adv. Mater.* **2007**, *19*, 2246–2251.
- [53] T. Loiseau, C. Serre, C. Huguenard, G. Fink, F. Taulelle, M. Henry, T. Bataille, G. Férey, *Chem. Eur. J.* **2004**, *10*, 1373–1382.
- [54] R. Matsuda, R. Kitaura, S. Kitagawa, Y. Kubota, T. C. Kobayashi, S. Horike, M. Takata, *J. Am. Chem. Soc.* **2004**, *126*, 14063–14070.
- [55] T. K. Maji, R. Matsuda, S. Kitagawa, *Nat. Mater.* **2007**, *6*, 142–148.

- [56] C. Serre, F. Millange, C. Thouvenot, M. Noguès, G. Marsolier, D. Louër, G. Férey, *J. Am. Chem. Soc.* **2002**, *124*, 13519–13526.
- [57] G. Férey, C. Serre, *Chem. Soc. Rev.* **2009**, *38*, 1380–1399.
- [58] P. Horcajada, C. Serre, G. Maurin, N. A. Ramsahye, F. Balas, M. Vallet-Regí, M. Sebban, F. Taulelle, G. Férey, *J. Am. Chem. Soc.* **2008**, *130*, 6774–6780.
- [59] Z. Wang, S. M. Cohen, *J. Am. Chem. Soc.* **2007**, *129*, 12368–12369.
- [60] E. Dugan, Z. Wang, M. Okamura, A. Medina, S. M. Cohen, *Chem. Commun.* **2008**, 3366–3368.
- [61] Z. Wang, S. M. Cohen, *Angew. Chem., Int. Ed.* **2008**, *47*, 4699–4702.
- [62] C. Volkringer, S. M. Cohen, *Angew. Chem., Int. Ed.* **2010**, *49*, 4644–4648.
- [63] Z. Wang, K. K. Tanabe, S. M. Cohen, *Inorg. Chem.* **2009**, *48*, 296–306.
- [64] K. K. Tanabe, S. M. Cohen, *Inorg. Chem.* **2010**, *49*, 6766–6774.
- [65] K. K. Tanabe, Z. Wang, S. M. Cohen, *J. Am. Chem. Soc.* **2008**, *130*, 8508–8517.
- [66] J. G. Nguyen, S. M. Cohen, *J. Am. Chem. Soc.* **2010**, *132*, 4560–4561.
- [67] M. Savonnet, D. Bazer-Bachi, N. Bats, J. Perez-Pellitero, E. Jeanneau, V. Lécocq, C. Pinel, D. Farrusseng, *J. Am. Chem. Soc.* **2010**, *132*, 4518–4519.
- [68] Z. Wang, S. M. Cohen, *Angew. Chem., Int. Ed.* **2008**, *47*, 4699–4702.
- [69] H. Deng, C. J. Doonan, H. Furukawa, R. B. Ferreira, J. Towne, C. B. Knobler, B. Wang, O. M. Yaghi, *Science* **2010**, *327*, 846–850.
- [70] M. Kondo, S. Furukawa, K. Hirai, S. Kitagawa, *Angew. Chem., Int. Ed.* **2010**, *49*, 5327–5330.
- [71] S. Furukawa, K. Hirai, Y. Takashima, K. Nakagawa, M. Kondo, T. Tsuruoka, O. Sakata, S. Kitagawa, *Chem. Commun.* **2009**, 5097–5099.
- [72] K. Hirai, S. Furukawa, M. Kondo, H. Uehara, O. Sakata, S. Kitagawa, *Angew. Chem., Int. Ed.* **2011**, *50*, 8057–8061.
- [73] D. Zacher, R. Schmid, C. Wöll, R. A. Fischer, *Angew. Chem., Int. Ed.* **2011**, *50*, 176–199.
- [74] O. M. Yaghi, M. O'Keeffe, N. W. Ockwig, H. K. Chae, M. Eddaoudi, J. Kim, *Nature* **2003**, *423*, 705–714.
- [75] D. Tranchemontagne, J. Hunt, O. M. Yaghi, *Tetrahedron* **2008**, *64*, 8553–8557.
- [76] S. Surblé, C. Serre, C. Mellot-Draznieks, F. Millange, G. Férey, *Chem. Commun.* **2006**, 284–286.
- [77] C. Mellot-Draznieks, J. Dutour, G. Férey, *Angew. Chem., Int. Ed.* **2004**, *43*, 6290–6296.
- [78] H. M. Rietveld, *Acta Cryst.* **1967**, *22*, 151–152.
- [79] T. Loiseau, C. Mellot-Draznieks, H. Muguerra, G. Férey, M. Haouas, F. Taulelle, *C. R. Chim.* **2005**, *8*, 765–772.
- [80] S. E. Wenzel, M. Fischer, F. Hoffmann, M. Fröba, *Inorg. Chem.* **2009**, *48*, 6559–6565.
- [81] L. Ma, J. M. Falkowski, C. Abney, W. Lin, *Nat. Chem.* **2010**, *2*, 838–846.
- [82] H. Bux, C. Chmelik, R. Krishna, J. Caro, *J. Membrane Sci.* **2011**, *369*, 284–289.
- [83] O. M. Yaghi, L. Guangming, T. L. Groy, *J. Solid State Chem.* **1995**, *117*, 256–260.
- [84] P. M. Forster, P. M. Thomas, A. K. Cheetham, *Chem. Mater.* **2002**, *14*, 17–20.

- [85] X.-C. Huang, Y.-Y. Lin, J.-P. Zhang, X.-M. Chen, *Angew. Chem., Int. Ed.* **2006**, *45*, 1557–1559.
- [86] R. Banerjee, A. Phan, B. Wang, C. B. Knobler, H. Furukawa, M. O'Keeffe, O. M. Yaghi, *Science* **2008**, *319*, 939–943.
- [87] S. H. Jhung, J.-H. Lee, J. W. Yoon, C. Serre, G. Férey, J.-S. Chang, *Adv. Mater.* **2007**, *19*, 121–124.
- [88] T. Chalati, P. Horcajada, R. Gref, P. Couvreur, C. Serre, *J. Mater. Chem.* **2011**, *21*, 2220–2227.
- [89] S. Hermes, T. Witte, T. Hikov, D. Zacher, S. Bahn Müller, G. Langstein, K. Huber, R. A. Fischer, *J. Am. Chem. Soc.* **2007**, *129*, 5324–5325.
- [90] P. Horcajada, C. Serre, D. Grosso, C. Boissière, S. Perruchas, C. Sanchez, G. Férey, *Adv. Mater.* **2009**, *21*, 1931–1935.
- [91] V. Guillerm, S. Gross, C. Serre, T. Devic, M. Bauer, G. Férey, *Chem. Commun.* **2010**, *46*, 767–769.
- [92] M. Puchberger, F. R. Kogler, M. Jupa, S. Gross, H. Fric, G. Kickelbick, U. Schubert, *Eur. J. Inorg. Chem.* **2006**, 3283–3293.
- [93] F. R. Kogler, M. Jupa, M. Puchberger, U. Schubert, *J. Mater. Chem.* **2004**, *14*, 3133–3138.
- [94] P. Walther, M. Puchberger, F. R. Kogler, K. Schwarz, U. Schubert, *Phys. Chem. Chem. Phys.* **2009**, *11*, 3640–3647.
- [96] P. Piszczek, A. Radtke, A. Grodzicki, A. Wojtczak, J. Chojnacki, *Polyhedron* **2007**, *26*, 679–685.
- [95] J. Cravillon, R. Nayuk, S. Springer, A. Feldhoff, K. Huber, M. Wiebcke, *Chem. Mater.* **2011**, *23*, 2130–2141.
- [97] G. Kickelbick, P. Wiede, U. Schubert, *Inorg. Chim. Acta* **1999**, *284*, 1–7.
- [98] P. Bernardo, E. Drioli, G. Golemme, *Ind. Eng. Chem. Res.* **2009**, *48*, 4638–4663.
- [99] X. Gu, Z. Tang, J. Dong, *Microporous Mesoporous Mater.* **2008**, *111*, 441–448.
- [100] M. Hong, J. L. Falconer, R. D. Noble, *Ind. Eng. Chem. Res.* **2005**, *44*, 4035–4041.
- [101] Y. Li, F. Liang, H. Bux, W. Yang, J. Caro, *J. Membrane Sci.* **2010**, *354*, 48–54.
- [102] Y.-S. Li, F.-Y. Liang, H. Bux, A. Feldhoff, W.-S. Yang, J. Caro, *Angew. Chem., Int. Ed.* **2010**, *49*, 548–551.
- [103] Z. Chen, S. Xiang, H. D. Arman, P. Li, D. Zhao, B. Chen, *Eur. J. Inorg. Chem.* **2011**, 2227–2231.
- [104] I. Langmuir, *J. Am. Chem. Soc.* **1916**, *38*, 2221–2295.
- [105] S. Brunauer, P. H. Emmett, E. Teller, *J. Am. Chem. Soc.* **1938**, *60*, 309–3019.
- [106] O. K. Farha, A. Özgür Yazaydın, I. Eryazici, C. D. Malliakas, B. G. Hauser, M. G. Kanatzidis, S. T. Nguyen, R. Q. Snurr, J. T. Hupp, *Nat. Chem.* **2010**, *2*, 944–948.
- [107] K. S. Walton, R. Q. Snurr, *J. Am. Chem. Soc.* **2007**, *129*, 8552–8556.
- [108] Y.-S. Bae, A. O. Yazaydın, R. Q. Snurr, *Langmuir* **2010**, *26*, 5475–5483.
- [109] J. Rouquerol, P. L. Llewellyn, F. Rouquerol, *Stud. Surf. Sci. Catal.* **2007**, *160*, 49–56.
- [110] M. Hirscher, B. Panella, *Scr. Mater.* **2007**, *56*, 809–812.
- [111] A. Vishnyakov, P. I. Ravikovitch, A. V. Neimark, M. Bülow, Q. M. Wang, *Nano Lett.* **2003**, *3*, 713–718.

- [112] P. Krawiec, M. Kramer, M. Sabo, R. Kunschke, H. Fröde, S. Kaskel, *Adv. Eng. Mater.* **2006**, *8*, 293–296.
- [113] M. Dincă, J. R. Long, *J. Am. Chem. Soc.* **2005**, *127*, 9376–9377.
- [114] L. J. Murray, M. Dincă, J. R. Long, *Chem. Soc. Rev.* **2009**, *38*, 1294–1314.
- [115] C. H. Wu, *J. Chem. Phys.* **1979**, *71*, 783–787.
- [116] M. Dincă, J. R. Long, *Angew. Chem., Int. Ed.* **2008**, *47*, 6766–6779.
- [117] B. Chen, X. Zhao, A. Putkham, K. Hong, E. B. Lobkovsky, E. J. Hurtado, A. J. Fletcher, K. M. Thomas, *J. Am. Chem. Soc.* **2008**, *130*, 6411–6423.
- [118] K. Seki, W. Mori, *J. Phys. Chem. B* **2002**, *106*, 1380–1385.
- [119] W. Zhou, *The Chemical Record* **2010**, *10*, 200–204.
- [120] U. Mueller, M. Schubert, F. Teich, H. Puetter, K. Schierle-Arndt, J. Pastré, *J. Mater. Chem.* **2006**, *16*, 626.
- [121] B. Chen, S. Ma, E. J. Hurtado, E. B. Lobkovsky, H.-C. Zhou, *Inorg. Chem.* **2007**, *46*, 8490–8492.
- [122] S. Ma, H.-C. Zhou, *Chem. Commun.* **2010**, *46*, 44–53.
- [123] J. Lee, O. K. Farha, J. Roberts, K. A. Scheidt, S. T. Nguyen, J. T. Hupp, *Chem. Soc. Rev.* **2009**, *38*, 1450–1459.
- [124] K. Schlichte, T. Kratzke, S. Kaskel, *Microporous Mesoporous Mater.* **2004**, *73*, 81–88.
- [125] A. Henschel, K. Gedrich, R. Kraehnert, S. Kaskel, *Chem. Commun.* **2008**, 4192–4194.
- [126] S. Kitagawa, S.-i. Noro, T. Nakamura, *Chem. Commun.* **2006**, 701–707.
- [127] S.-i. Noro, S. Kitagawa, M. Yamashita, T. Wada, *Chem. Commun.* **2002**, 222–223.
- [128] C.-D. Wu, A. Hu, L. Zhang, W. Lin, *J. Am. Chem. Soc.* **2005**, *127*, 8940–8941.
- [129] M. H. Alkordi, Y. Liu, R. W. Larsen, J. F. Eubank, M. Eddaoudi, *J. Am. Chem. Soc.* **2008**, *130*, 12639–12641.
- [130] F. Schröder, D. Esken, M. Cokoja, M. W. E. van den Berg, O. I. Lebedev, G. van Tendeloo, B. Walaszek, G. Buntkowsky, H.-H. Limbach, B. Chaudret, R. A. Fischer, *J. Am. Chem. Soc.* **2008**, *130*, 6119–6130.
- [131] S. Hermes, M.-K. Schröter, R. Schmid, L. Khodeir, M. Muhler, A. Tissler, R. W. Fischer, R. A. Fischer, *Angew. Chem., Int. Ed.* **2005**, *44*, 6237–6241.
- [132] N. V. Maksimchuk, M. N. Timofeeva, M. S. Melgunov, A. N. Shmakov, Y. A. Chesalov, D. N. Dybtsev, V. P. Fedin, O. A. Kholdeeva, *J. Catal.* **2008**, *257*, 315–323.
- [133] K. Rezwan, Q. Z. Chen, J. J. Blaker, A. R. Boccaccini, *Biomaterials* **2006**, *27*, 3413–3431.
- [134] S. Giri, B. G. Trewyn, M. P. Stellmaker, V. S.-Y. Lin, *Angew. Chem., Int. Ed.* **2005**, *44*, 5038–5044.
- [135] N. Ehlert, M. Badar, A. Christel, S. J. Lohmeier, T. Luessenhop, M. Stieve, T. Lenarz, P. P. Mueller, P. Behrens, *J. Mater. Chem.* **2010**, *21*, 752–760.
- [136] P. Horcajada, T. Chalati, C. Serre, B. Gillet, C. Sebrie, T. Baati, J. F. Eubank, D. Heurtaux, P. Clayette, C. Kreuz, J.-S. Chang, Y. K. Hwang, V. Marsaud, P.-N. Bories, L. Cynober, S. Gil, G. Férey, P. Couvreur, R. Gref, *Nat. Mater.* **2009**, *9*, 172–178.

- [137] P. Horcajada, C. Serre, M. Vallet-Regí, M. Sebban, F. Taulelle, G. Férey, *Angew. Chem., Int. Ed.* **2006**, *45*, 5974–5978.
- [138] J. An, S. J. Geib, N. L. Rosi, *J. Am. Chem. Soc.* **2009**, *131*, 8376–8377.
- [139] P. D. C. Dietzel, Y. Morita, R. Blom, H. Fjellvåg, *Angew. Chem., Int. Ed.* **2005**, *44*, 6354–6358.
- [140] B. Xiao, P. S. Wheatley, X. Zhao, A. J. Fletcher, S. Fox, A. G. Rossi, I. L. Megson, S. Bordiga, L. Regli, K. M. Thomas, R. E. Morris, *J. Am. Chem. Soc.* **2007**, *129*, 1203–1209.
- [141] A. C. McKinlay, B. Xiao, D. S. Wragg, P. S. Wheatley, I. L. Megson, R. E. Morris, *J. Am. Chem. Soc.* **2008**, *130*, 10440–10444.
- [142] A. C. McKinlay, R. E. Morris, P. Horcajada, G. Férey, R. Gref, P. Couvreur, C. Serre, *Angew. Chem., Int. Ed.* **2010**, *49*, 6260–6266.
- [143] S. R. Miller, D. Heurtaux, T. Baati, P. Horcajada, J.-M. Grenèche, C. Serre, *Chem. Commun.* **2010**, *46*, 4526–4528.
- [144] C. Zlotea, D. Phanon, M. Mazaj, D. Heurtaux, V. Guillerm, C. Serre, P. Horcajada, T. Devic, E. Magnier, F. Cuevas, G. Férey, P. L. Llewellyn, M. Latroche, *Dalton Trans.* **2011**, *40*, 4879–4881.
- [145] S. J. Garibay, S. M. Cohen, *Chem. Commun.* **2010**, *46*, 7700–7702.
- [146] M. Kim, S. J. Garibay, S. M. Cohen, *Inorg. Chem.* **2011**, *50*, 729–731.
- [147] C. Wang, Z. Xie, K. E. deKrafft, W. Lin, *J. Am. Chem. Soc.* **2011**, *133*, 13445–13454.
- [148] F. Vermoortele, R. Ameloot, A. Vimont, C. Serre, D. de Vos, *Chem. Commun.* **2011**, *47*, 1521–1523.
- [149] P. S. Bárcia, D. Guimarães, P. A. Mendes, J. A. Silva, V. Guillerm, H. Chevreau, C. Serre, A. E. Rodrigues, *Microporous Mesoporous Mater.* **2011**, *139*, 67–73.
- [150] S. Amirjalayer, M. Tafipolsky, R. Schmid, *Angew. Chem., Int. Ed.* **2007**, *46*, 463–466.
- [151] N. Lock, Y. Wu, M. Christensen, L. J. Cameron, V. K. Peterson, A. J. Bridgeman, C. J. Kepert, B. B. Iversen, *J. Phys. Chem. C* **2010**, *114*, 16181–16186.
- [152] Q. Yang, A. D. Wiersum, P. L. Llewellyn, V. Guillerm, C. Serre, G. Maurin, *Chem. Commun.* **2011**, *47*, 9603–9605.
- [153] M. Kandiah, S. Usseglio, S. Svelle, U. Olsbye, K. P. Lillerud, M. Tilset, *J. Mater. Chem.* **2010**, *20*, 9848–9851.
- [154] W. Morris, C. J. Doonan, O. M. Yaghi, *Inorg. Chem.* **2011**, *50*, 6853–6855.

3 Modulated Synthesis of Zr-Based Metal–Organic Frameworks: From Nano to Single Crystals

Preface

This work has been published as a full paper in "Chemistry – A European Journal" and focuses on the effect of modulators on the synthesis of a series of isorecticular Zr-MOFs. The driving force of this investigation was the lack of reproducibility in the syntheses of such novel and important MOFs with linkers of longer length than H_2bdc . The idea to introduce monocarboxylic acids to modulate such syntheses was adopted from the work of the Kitagawa group and firstly investigated by Jann Lippke and the author in the synthesis of Zr- bdc during the bachelor thesis of Lippke. Thereafter the author pursued the modulation approach to the synthesis of Zr- $bpdc$ and Zr- $tpdc-NH_2$. The linker $H_2tpdc-NH_2$ is not commercially available and was synthesized as part of the collaboration within the priority program "Porous Metal–Organic Frameworks" (SPP 1362, MOFs) by Pascal Roy in the Godt group at the Bielefeld University.

As a result of the modulating agents the crystal sizes and the morphology of Zr- bdc was controllable in the 100 nm region and below. The application of the modulation approach to syntheses with longer linkers like H_2bdpc and $H_2tpdc-NH_2$ led further to a significant increase of the reproducibility of the synthesis of these Zr-MOFs. In the case of Zr- $tpdc-NH_2$ the modulated synthesis produced the first single crystals of a Zr-based MOF and so its structure was determined by evaluation of the SXRD data.

The concentration of water proved to be essential for the synthesis of Zr- $bdc-NH_2$ and Zr- $tpdc-NH_2$ and its effect on the crystallite sizes of Zr- bdc and Zr- $bdc-NH_2$ was also studied.

The author conducted or supervised all experiments concerning the synthesis of MOFs and analyzed the products by PXRD, SXRD, and TGA/DTA. The determination of the structure of Zr- $tpdc-NH_2$ was done together with Dr. Michael Wiebcke. DLS measurements were carried out together with Jann Lippke. The SEM investigations were carried out together with Florian Waltz and Ar sorption isotherms were measured together with Felix Brieler, Sven Jare Lohmeier, and Georg Platz. NMR investigations were carried out by Pascal Roy at the Bielefeld University.

Modulated Synthesis of Zr-Based Metal–Organic Frameworks: From Nano to Single Crystals

Andreas Schaate,^[a] Pascal Roy,^[b] Adelheid Godt,^[b] Jann Lippke,^[a] Florian Waltz,^[a] Michael Wiebcke,^[a] and Peter Behrens*^[a]

Abstract: We present an investigation on the influence of benzoic acid, acetic acid, and water on the syntheses of the Zr-based metal–organic frameworks Zr–bdc (UiO-66), Zr–bdc–NH₂ (UiO-66–NH₂), Zr–bpdc (UiO-67), and Zr–tpdc–NH₂ (UiO-68–NH₂) (H₂bdc: terephthalic acid, H₂bpdc: biphenyl-4,4'-dicarboxylic acid, H₂tpdc: terphenyl-4,4''-dicarboxylic acid). By varying the amount of benzoic or acetic acid, the synthesis of Zr–bdc can be modulated. With increasing concentration of the modulator, the products change from intergrown to individual crystals, the

size of which can be tuned. Addition of benzoic acid also affects the size and morphology of Zr–bpdc and, additionally, makes the synthesis of Zr–bpdc highly reproducible. The control of crystal and particle size is proven by powder XRD, SEM and dynamic light scattering (DLS) measurements. Thermogravimetric analysis (TGA) and Ar

sorption experiments show that the materials from modulated syntheses can be activated and that they exhibit high specific surface areas. Water proved to be essential for the formation of well-ordered Zr–bdc–NH₂, Zr–tpdc–NH₂, a material with a structure analogous to that of Zr–bdc and Zr–bpdc, but with the longer, functionalized linker 2'-amino-1,1':4',1''-terphenyl-4,4''-dicarboxylic acid, was obtained as single crystals. This allowed the first single-crystal structural analysis of a Zr-based metal–organic framework.

Keywords: metal–organic frameworks • microporous materials • modulation approach • nanoparticles • zirconium

Introduction

The combination of linker molecules with metal–oxo clusters as nodes to metal–organic frameworks (MOFs) or porous coordination polymers (PCPs) with permanent porosity is currently a field of high activity. MOFs have been established as a new class of porous crystalline materials with the aim to use them for gas sorption,^[1,2] separation,^[3,4] chemical sensing devices,^[5] and catalysis.^[6] New MOF structures are published frequently, but systematic investigations of the synthetic procedures and their parameters are rarely reported.^[7] The parameters that are changed in such studies are usually the concentrations or molar ratios of the starting materials, the type of metal sources, or solvents, as well as pH.

The addition of ligands with only one coordination site, which compete with linkers for coordination to the metal cations, the so-called modulator approach,^[8,9] was recently introduced by using acetic acid as a modulator in the synthesis of [Cu₂(ndc)₂(dabco)] (ndc²⁻ = 1,4-naphthalene dicarboxylate, dabco = diazabicyclo[2.2.2]octane).^[9] The examined material features Cu-based paddle-wheel secondary building units (SBUs) that are connected by ndc²⁻ linkers within the layers, which are in turn pillared by dabco units. The authors proposed a coordination modulation process in which acetic acid acts as a regulator for the reaction rate and the crystal morphology. In this case, the competing reagents were the ndc²⁻ linker and acetate. It was reported that the addition of the modulator limited the growth of the layers, but did not affect the growth of the crystals along the pillaring direction. This type of control of the morphology of porous crystalline materials is of great interest, for example, for the assembly of thin layers for sensing applications.^[10]

Recently, the syntheses of an isorecticular series of robust and porous Zr MOFs were reported.^[11] These materials contain a highly stable SBU, which leads to a strong resistance towards water, benzene, ethanol, and other chemicals. The SBU is constructed of six zirconium cations, which form an octahedron. Each Zr is coordinated in a square-antiprismatic geometry by bridging μ_3 -O, μ_3 -OH, and carboxylate groups. Such a Zr–oxo–hydroxo cluster, saturated by monocarboxylate ligands on its periphery, was previously discovered as an isolated molecule.^[12] The MOF materials containing this building unit have been designated as UiO-66 to

[a] A. Schaate, J. Lippke, F. Waltz, Dr. M. Wiebcke, Prof. Dr. P. Behrens
Institute of Inorganic Chemistry
Leibniz University Hannover, Callinstr. 9
30167 Hannover (Germany)
Fax: (+49) 511-762-3006
also at the ZFM
Center for Solid-State Chemistry and New Materials
Leibniz University Hannover (Germany)
E-mail: peter.behrens@acb.uni-hannover.de

[b] P. Roy, Prof. Dr. A. Godt
Department of Chemistry, Bielefeld University
Universitätsstr. 25, 33615 Bielefeld (Germany)

Supporting information for this article is available on the WWW under <http://dx.doi.org/10.1002/chem.201003211>.

UiO-68, depending on the dicarboxylic acid they contain as linkers (UiO-66: bdc^{2-} linkers, H_2bdc : terephthalic acid; UiO-67: bpdc^{2-} linkers, H_2bpdc : biphenyl-4,4'-dicarboxylic acid; UiO-68: tpdc^{2-} linkers, H_2tpdc : terphenyl-4,4'-dicarboxylic acid). Each Zr–oxo–hydroxo SBU is connected to twelve other SBUs by the dicarboxylate linkers. The structures of these isorecticular Zr MOFs can therefore be described as an expanded cubic close-packed (ccp) structure. The high affinity of zirconium towards oxygen ligands and the compact structure of this SBU explain the high chemical and thermal stability of these MOFs. Thermogravimetric measurements of UiO-66 and UiO-67 showed that the Zr MOFs were stable up to 450 °C in air.

The original synthesis of these materials starts from a solution of ZrCl_4 and the corresponding organic linker in DMF.^[11] The mixture was added to a vessel, which was capped, sealed, and heated to 120 °C in a preheated oven for 24 h. Precipitation of the product started fairly quickly on a timescale of hours. It consisted of microsized aggregates of intergrown crystals. For the Zr–bdc material, this synthesis is reproducible and gives highly crystalline materials. In our hands, however, the described synthesis for the Zr–bpdc MOF often led to poorly crystalline materials with broad reflections in the powder XRD patterns, and our attempts to synthesize a Zr–tpdc MOF failed. Recently, Guillermin et al. published a prebuilt SBU approach for the synthesis of UiO-66 and also reported a new compound consisting of the same SBU and the muconic acid dianion as a linker.^[13] They used the known zirconium methacrylate oxocluster $[\text{Zr}_6\text{O}_4(\text{OH})_4(\text{OMc})_{12}]^{14}$ ($\text{OMc}^- = \text{methacrylate}$) as a precursor for the SBUs in the synthesis. According to the authors, during the synthesis, the methacrylate ligands were exchanged with the linkers to build up the desired framework. By this approach, the mentioned materials can be synthesized from 25–150 °C.

Herein, we show how the syntheses of isorecticular Zr MOFs can be modulated by the addition of acetic and benzoic acid as ligands competing with the linkers. By using this approach, it is possible to synthesize these materials as octahedral crystals in different well-defined sizes, depending on the ratio of modulator added to the synthesis. This approach also led to the production of the first single crystals of a Zr-based MOF, and consequently, the results of the first single-crystal structural analysis of such a compound are reported.

Results and Discussion

Modulated synthesis of Zr–bdc MOF: Zr–bdc MOF (UiO-66) was synthesized under similar reaction conditions and within the range of reactant concentrations described by Cavka et al.^[11] It was found that benzoic acid influenced this MOF synthesis and that the crystallite size of the Zr–bdc MOF could be regulated by the ratio of benzoic acid to zirconium(IV) chloride. This can be stated on the basis of the widths of the reflections in the powder XRD patterns (Figure 1 a). The addition of up to three equivalents of benzoic

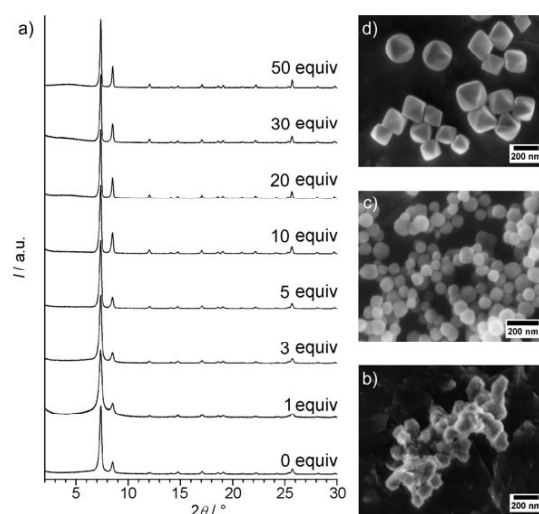


Figure 1. a) Powder XRD patterns of Zr–bdc MOFs prepared with different amounts of benzoic acid (given as equivalents with respect to ZrCl_4) as the modulator. SEM images of Zr–bdc MOFs synthesized in the presence of b) 0, c) 10, and d) 30 equivalents of benzoic acid are also given.

acid resulted in a broadening of the reflections, and thus, in smaller crystals. Broadened reflections and smaller crystals than those of the material synthesized from ZrCl_4 were also found by Guillermin et al.,^[13] who used the $\text{Zr}_6\text{O}_4(\text{OH})_4(\text{OMc})_{12}$ cluster as a precursor; this precursor compound already contained two equivalents of a monocarboxylic acid, in this case methacrylic acid, which could act as a modulating agent. In the work presented herein, upon further increasing the amount of the modulator benzoic acid, the widths became smaller, which indicated the formation of larger crystals (Table 1). The SEM pictures of the Zr–bdc MOF samples show a development from intergrown aggregates of very small crystals to individual and octahedrally shaped nanocrystals of increasing size (Figure 1 b–d).

To further investigate the influence of benzoic acid on the formation of Zr–bdc MOFs, we performed DLS experiments on the products, which were dispersed in water and

Table 1. Size determination of Zr–bdc MOFs from syntheses carried out in the presence of benzoic acid as the modulator.

Benzoic acid ^[a] [equiv]	$d_{\text{DLS,water}}^{[b]}$ [nm]	$d_{\text{DLS,EtOH}}^{[b]}$ [nm]	$d_{\text{XRD}}^{[b]}$ [nm]
0	122–615 (220)	220–712 (295)	85
1	105–396 (255)	190–459 (220)	39
3	142–459 (164)	148–308 (198)	67
5	105–396 (164)	105–396 (142)	95
10	79–255 (105)	91–255 (122)	120
20	122–342 (164)	95–265 (128)	– ^[c]
30	164–458 (190)	164–531 (164)	– ^[c]

[a] The equivalents of benzoic acid added are given with respect to ZrCl_4 . [b] Data for particle sizes from dynamic light scattering (DLS) measurements (the maximum of the distribution is given in parentheses) in water ($d_{\text{DLS,water}}$) and in ethanol ($d_{\text{DLS,EtOH}}$), and crystallite sizes from the evaluation of powder XRD patterns using Scherrer's equation (d_{XRD}). [c] Crystallite sizes were out of scope for determination by Scherrer's equation.

ethanol (Table 1). Owing to the aggregation of the nanoparticles at low modulator concentrations, the particle sizes derived from DLS were larger than the crystallite sizes obtained from powder XRD line broadening. The differences became smaller with increasing amounts of modulator, and when 10 equivalents of benzoic acid were employed, the crystal size calculated with Scherrer's equation corresponded well to the particle sizes observed by SEM and DLS.

A reason for the growth of larger crystals with an increasing number of equivalents of the modulator benzoic acid is probably the in situ formation of complexes between zirconium cations and benzoic acid. Molecular zirconium complexes with different monocarboxylic acids (HO_2CR , $\text{R} = t\text{Bu}$, $\text{C}(\text{CH}_3)_2\text{Et}$) and structures similar to the SBU in Zr MOFs have been described.^[12] Such complexes could form as intermediates during the modulated synthesis with benzoic acid. The framework construction would then proceed through an exchange between benzoic acid and linker molecules at the coordination sites of the zirconium ion. If this applies, an increasing number of equivalents of monocarboxylic acid would decrease the possibility that a dicarboxylic acid is connected to the SBU. Therefore, the formation of framework nuclei is disfavored and fewer nuclei grow to larger crystals. Although the growth rate of the crystals is also affected by the exchange equilibrium between mono- and dicarboxylic acids, the timescale for growth is much larger than the rate associated with nucleation.

For the sake of clarity in the coming discussion, the materials are named in the following way: Zr–linker (equivalents of added modulator, as-synthesized) refers to a material that was prepared from ZrCl_4 and the linker in the presence of the given equivalents of benzoic acid and which was washed once with DMF and ethanol (standard washing procedure). Zr–linker (equivalents of added modulator, washed) refers to a material that was prepared in the same way, but was additionally washed extensively with DMF and THF.

In addition to controlling the nucleation of the Zr–bdc MOFs, the benzoic acid probably acted as a guest of the MOF. This was suggested by ^1H NMR spectroscopic investigations (Figure S1 in the Supporting Information): although a sample of Zr–bdc (30 equiv, as-synthesized) had been washed with DMF and THF until no more benzoic acid was detectable with ^1H NMR spectroscopy in suspensions of the obtained Zr–bdc (30 equiv, washed) in $[\text{D}_6]\text{DMSO}$, the material still contained benzoic acid, as found by ^1H NMR spectroscopy after dissolving it in a warm 1:6 mixture of D_2SO_4 and $[\text{D}_6]\text{DMSO}$ (Figure S1 in the Supporting Information). The ratio of 8:10 of benzoic acid and terephthalic acid was much larger than the estimated ratio of about 1:10 for the case in which benzoate ligands were present as surface ligands to complete the coordination shells of surface zirconium atoms. The benzoic acid molecules still present in the Zr–bdc (30 equiv, washed) sample after extensive washing thus appear to be entrapped.

In agreement with the entrapment of benzoic acid, the thermogravimetric analyses (TGA) data of Zr–bdc (0 equiv, as-synthesized) and Zr–bdc (30 equiv, washed) differ slightly,

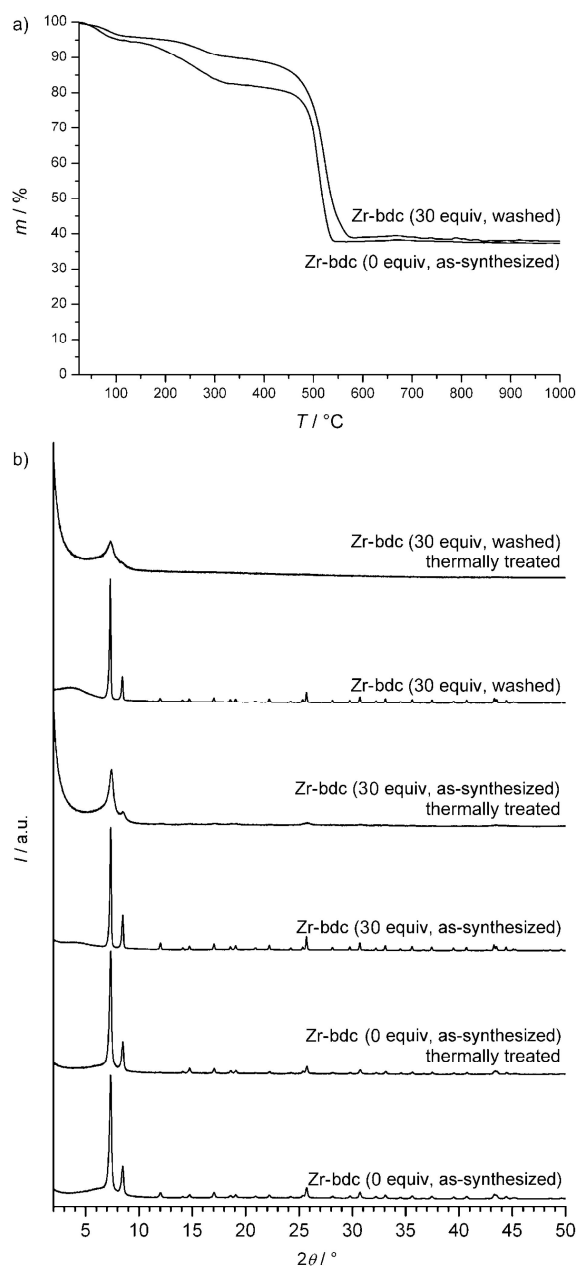


Figure 2. a) TGA (in a flow of air) for Zr–bdc MOFs synthesized in the absence and in the presence of benzoic acid (30 equiv with respect to ZrCl_4); Zr–bdc MOFs produced in the presence of benzoic acid were investigated in the as-synthesized state (Zr–bdc (30 equiv, as-synthesized)) and after extensive washing (Zr–bdc (30 equiv, washed)). b) Powder XRD patterns of Zr–bdc (0 equiv, as-synthesized), Zr–bdc (30 equiv, as-synthesized), and Zr–bdc (30 equiv, washed) MOFs before and after thermal treatment at 300 °C in air.

but significantly (Figure 2a, Table 2). Both curves show two steps, which are assigned to the loss of guest molecules during heating to 300 °C and to the decomposition of the linkers above 450 °C. The residue was identified to be monoclinic ZrO_2 . The experimentally determined mass loss of

Table 2. Comparison between measured and calculated TGA mass loss values [%], in a flow of air, for Zr–bdc MOFs synthesized in the absence of benzoic acid or presence of benzoic acid (30 equiv with respect to ZrCl₄).

Step	Calculated	As-synthesized (0 equiv)		Washed (30 equiv)	
		Measured	Guest free ^[a]	Measured	Guest free ^[a]
guests	–	16.1	–	9.1	–
linker	55.6	46.6	55.5	51.8	57.0
residue	44.4	37.3	44.5	39.0	43.0

[a] Mass loss after correction for the removal of guest molecules.

Zr–bdc (0 equiv, as-synthesized) matches perfectly with this assignment (Table 2). The differences between the experimentally determined mass loss of Zr–bdc (30 equiv, washed) and the calculated data are taken as an indication that even at 300 °C some benzoic acid molecules are trapped inside the MOF. The entrapped benzoic acid molecules are most probably the reason for the thermal instability of the crystals of Zr–bdc (30 equiv, as-synthesized) and Zr–bdc (30 equiv, washed). Upon heating to 300 °C in a flow of air, Zr–bdc (30 equiv, as-synthesized) and Zr–bdc (30 equiv, washed) both lose their crystallinity. The nanosized aggregates of Zr–bdc (0 equiv, as-synthesized), however, remain crystalline (Figure 2b). The fact that entrapped benzoic acid molecules cannot be removed through washing and release upon heating is only possible with destruction of the framework is not surprising because the windows in the Zr–bdc MOF are too small for molecules to pass through.

Occluded modulator molecules can, however, easily be removed when, instead of benzoic acid, acetic acid is chosen as the modulating agent. Our experiments show that acetic acid can act as a modulator in the same way as benzoic acid. The modulation properties of acetic and benzoic acid are similar, as seen from the powder XRD patterns (Figure S2 in the Supporting Information) of the obtained products, the crystal sizes determined from the line widths of the powder XRD reflections, and from the particle sizes determined with DLS (Table S1 in the Supporting Information). The addition of up to five equivalents of acetic acid causes a decrease of the crystallite size. SEM images of these samples again show aggregated and intergrown crystals. With higher amounts of acetic acid, the crystal size increases and larger and more isolated MOF particles can be seen. In remarkable contrast to Zr–bdc obtained in the presence of benzoic acid, the framework of Zr–bdc obtained in the presence of acetic acid is stable up to 300 °C. The smaller acetic acid molecules can thus be removed from the pores of the Zr–bdc MOF, either by the standard washing procedure or during thermal treatment, if they had been entrapped at all.

A comparison of the BET surface areas (determined from Ar sorption isotherms, see Figure S3 in the Supporting Information) of the different Zr–bdc materials, which were activated at 300 °C, is given in Table 3. The Zr–bdc (0 equiv) (which contains no guest molecules that cannot be removed) has a BET surface area of 700 m²g^{−1}. The Zr–bdc MOF synthesized in the presence of 30 equivalents of acetic acid, which is stable during thermal treatment, exhibits a larger

Table 3. Comparison of BET surface areas determined from Ar sorption isotherms of Zr MOFs synthesized under different conditions and after heating them to 300 °C.

	Specific surface area [m ² g ^{−1}]	
	Zr–bdc MOF	Zr–bpdc MOF
no modulator	700	270
benzoic acid (30 equiv)	600	3000
acetic acid (30 equiv)	1400	2400
ref. [11]	1187 ^[a]	3000 ^[a]

[a] Langmuir surface area.

surface area of 1400 m²g^{−1}; a value that is significantly higher than the surface area of 1187 m²g^{−1} reported for UiO-66.^[11] The disordered material that resulted from heating microcrystals of Zr–bdc (30 equiv, as-synthesized) exhibits a reduced specific surface area of 600 m²g^{−1}.

Modulated synthesis of Zr–bpdc MOF: We found that the published synthetic procedure for UiO-67 (Zr–bpdc MOF) was difficult to reproduce and often led to products that show only very broad reflections in the powder XRD at around 2θ = 6, 12, and 18° (see Figure 3a, 0 equiv). With in-

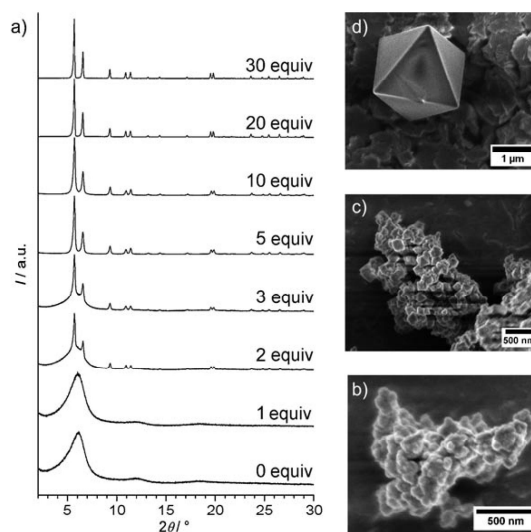


Figure 3. a) Powder XRD patterns of Zr–bpdc MOFs prepared with different amounts of benzoic acid as the modulator. The equivalents are given with respect to ZrCl₄. SEM images of Zr–bpdc samples synthesized in the presence of b) 0, c) 3 and d) 30 equivalents of benzoic acid.

creasing length of the linker, the ccp structure of the UiO materials seems to be disfavored and another phase, possibly with a layered structure (the regular intervals between the reflections could correspond to a 00l series of such a material), is formed.

When using one equivalent of benzoic acid, once again only the unidentified phase was formed. At modulator additions corresponding to two and three equivalents, the characteristic powder XRD pattern of the Zr–bpdc MOF begins to emerge, but with broadened reflections and superimposed

onto a background caused by the unidentified phase. The appearance of this phase precludes the preparation of well-defined nanoparticles of the Zr–bpdc MOF at low equivalents of modulator, in contrast to the case with Zr–bdc in which, under such conditions, crystals with a size of around 100 nm were produced.

The use of larger amounts of modulator enhances the crystallinity of the Zr–bpdc MOF considerably. This can be seen in the sequence of powder XRD patterns shown in Figure 3a. When five or more equivalents of benzoic acid are used in the synthesis, the obtained material can be designated as crystalline. With the addition of more benzoic acid, the size of the crystals increases, as reasoned from the decreasing widths of the reflections and the particles become less aggregated, as revealed by SEM images (Figure 3b–d). Upon the addition of 30 equivalents of benzoic acid, individual microcrystals with edge lengths around 2 μm were obtained. The addition of five and more equivalents of benzoic acid not only gives access to well-defined particles, but also makes the procedure highly reproducible.

The crystals from all syntheses with more than five equivalents of benzoic acid were already too large for a size determination with Scherrer's equation. The particle sizes obtained through DLS measurements in ethanol (Table 4) fit

Table 4. Particle size determination of Zr–bpdc MOFs obtained in the presence of benzoic acid as the modulator. The equivalents are given with respect to ZrCl_4 . Data from DLS measurements (the maximum of the distribution is given in parentheses) are recorded in ethanol ($d_{\text{DLS,EtOH}}$).

Benzoic acid [equiv]	$d_{\text{DLS,EtOH}}$ [nm]	Benzoic acid [equiv]	$d_{\text{DLS,EtOH}}$ [nm]
0	356–995 (641)	5	229–478 (308)
1	356–859 (553)	10	356–742 (478)
2	356–859 (553)	20	— ^[a]
3	308–641 (413)	30	— ^[a]

[a] No stable suspension was obtained.

well to those seen in the SEM images (Figure 3b–d). DLS measurements in water were not possible, because Zr–bpdc is instable in water. When stirred in water at room temperature for 24 h, crystallinity is lost (see the powder XRD in Figure S4 in the Supporting Information). Interestingly, the smaller analogue, UiO-66, is stable under these conditions.^[11]

As found for Zr–bdc, the TGA curve for Zr–bpdc (30 equiv, as-synthesized) (Figure 4) reveals two steps that are attributed to guest removal up to 300 °C and linker decomposition above 450 °C. This assignment is supported by the excellent agreement between experimentally determined and calculated mass losses (Table 5). The residue is monoclinic ZrO_2 . A two-step TGA curve was also recorded for Zr–bpdc (0 equiv, as-synthesized), that is, the unidentified phase, with the difference that a considerably larger amount of guest molecules is released (Table 5) and the mass decreases constantly between 300 and 450 °C, whereas the TGA curve of Zr–bpdc (30 equiv, as-synthesized) shows a

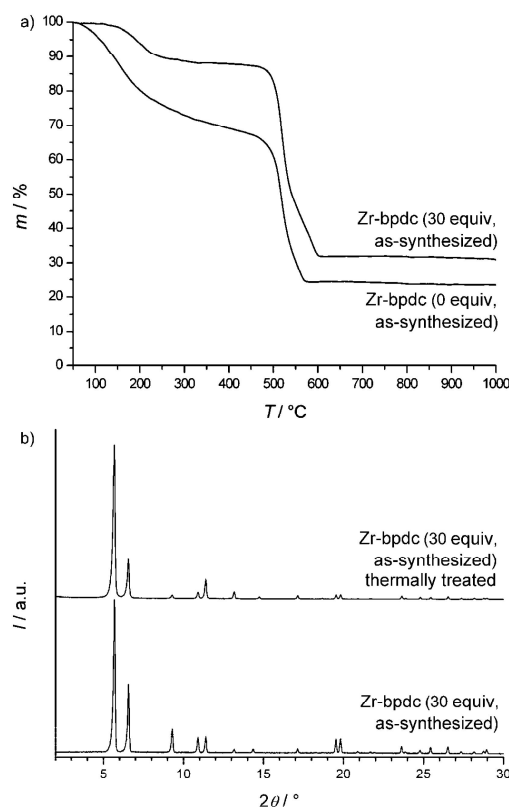


Figure 4. a) TGA (in a flow of air) of Zr–bpdc MOFs synthesized with and without benzoic acid (30 equiv). The equivalents are given with respect to ZrCl_4 . b) Powder XRD patterns of Zr–bpdc MOFs synthesized in the presence of benzoic acid (30 equiv) before and after thermal treatment at 300 °C in air.

Table 5. Comparison between measured and calculated values TGA mass losses [%] in a flow of air for Zr–bpdc MOFs synthesized in the absence or presence of benzoic acid (30 equiv with respect to ZrCl_4).

Step	Calculated	As-synthesized (0 equiv)		As-synthesized (30 equiv)	
		Measured	Guest free ^[a]	Measured	Guest free ^[a]
guests	–	27.1	–	11.3	–
linker	65.1	49.3	67.6	57.4	64.7
residue	34.9	23.6	32.4	31.3	35.3

[a] Mass loss after correction for the removal of guest molecules.

plateau in this range. The experimentally determined mass losses differ distinctly from those calculated for UiO-67, which is not unexpected because of the different structure of Zr–bpdc (0 equiv, as-synthesized) compared with UiO-67.

In striking difference to Zr–bdc (30 equiv, as-synthesized), the framework of analogously prepared Zr–bpdc (30 equiv, as-synthesized) is stable at least up to 300 °C in a flow of air, as proven by XRD measurements (Figure 4b). This suggests that either the benzoic acid was easily removed during the standard washing procedure or that it left the pores during heating without destruction of the framework. The windows of the Zr–bpdc framework should be large enough to allow

benzoic acid to pass through. Indeed, with a ratio of 4:1 between the linker H₂bpdc and the modulator benzoic acid in Zr–bpdc (30 equiv, as-synthesized), the content of modulator in the as-synthesized sample was significantly lower than in the corresponding Zr–bdc (30 equiv, as-synthesized). Heating a sample of Zr–bpdc (30 equiv, as-synthesized) up to 300 °C in air increased the ratio to 10:1. An even larger ratio of 50:1 between H₂bpdc and benzoic acid, that is, a much smaller modulator content, was found when Zr–bpdc (30 equiv, as-synthesized) had been extensively washed with DMF and THF (Figure S5 in the Supporting Information). The residual benzoic acid was thought to reside on the outer surface of the microcrystals. In all cases, the ratio was determined by ¹H NMR spectroscopy after dissolving the sample in a warm 1:6 mixture of D₂SO₄ and [D₆]DMSO.

The BET surface areas determined from Ar sorption isotherms of Zr–bpdc samples (Figure S6 in the Supporting Information) are summarized in Table 3. The Zr–bpdc (0 equiv, as-synthesized) material of unidentified structure exhibits only a low surface area of 270 m²g⁻¹. Zr–bpdc (30 equiv, as-synthesized) exhibit very high surface areas of 2400 and 3000 m²g⁻¹ when acetic and benzoic acid, respectively, were used as the modulators. These values are in the same range as the published Langmuir surface area of 3000 m²g⁻¹ for UiO-67.^[11]

To exclude the possibility that the effects observed were simply due to a variation of the pH caused by the addition of benzoic acid, we conducted the Zr–bpdc MOF synthesis in the presence of hydrochloric acid instead of benzoic acid. Being aware that the concomitant addition of water could also affect the synthesis (see below), we also added the corresponding amount of water to a reaction modulated with benzoic acid. The powder XRD patterns show that the addition of the inorganic acid had no positive effect on crystallization because the material obtained showed the same broad reflections as a sample of Zr–bpdc (0 equiv) (Figure S7 in the Supporting Information). On the contrary, the modulated synthesis in the presence of water gave a crystalline Zr–bpdc MOF.

Influence of water on the synthesis of Zr–bdc and Zr–bdc–NH₂ MOFs: Further investigations showed that water played a crucial role in the synthesis of Zr-based MOFs. This was not unexpected because the SBU also contains OH⁻ ions in addition to O²⁻ ions. We first examined the effect of the addition of water (up to 150 equiv) on the synthesis of Zr–bdc MOFs. With increasing water content, the solution turned turbid more quickly, which indicated a higher aggregation rate, and the size of the crystallites, as determined by Scherrer's equation, decreased (Table 6). The obtained materials are nanosized crystallites and therefore exhibit very broad reflections in the powder XRD patterns (Figure S8 in the Supporting Information). SEM images show particles that are intergrown and cannot be dispersed by ultrasound (Figure S9 in the Supporting Information).

Surprisingly, water addition was essential to obtain well-ordered materials of Zr–bdc–NH₂; a MOF isorecticular to

Table 6. Crystallite sizes of Zr–bdc and Zr–bdc–NH₂ MOFs from syntheses carried out with varying equivalents of H₂O (given as equivalents with respect to ZrCl₄); *d*_{XRD} was derived by the evaluation of powder XRD patterns using Scherrer's equation.

H ₂ O [equiv]	<i>d</i> _{XRD} [nm]		H ₂ O [equiv]	<i>d</i> _{XRD} [nm]	
	Zr–bdc MOF	Zr–bdc–NH ₂ MOF		Zr–bdc MOF	Zr–bdc–NH ₂ MOF
0	85	–	20	71	80
4	83	115	50	46	54
8	81	90	100	23	21
12	78	85	150	14	16
16	74	82			

the UiO-66 MOF, but with an amino group at the linking terephthalic acid. Without the addition of water, the powder XRD pattern of the product exhibits only broad reflections, whereas the addition of as little as four equivalents of water is sufficient to produce UiO-66–NH₂^[15] (Figure S10 in the Supporting Information). The similarity of the powder XRD patterns of the unidentified disordered phases obtained in the syntheses of Zr–bdc–NH₂ without the addition of water and Zr–bpdc (0 equiv, as-synthesized) suggest that also in the case of Zr–bdc–NH₂ a layered phase might be the product. In agreement with the smaller linker, H₂bdc–NH₂, in comparison with H₂bpdc, the reflections were found at larger 2θ values (ca. 8, 16, and 24°).

We tried to modify the particle size of the Zr–bdc–NH₂ MOFs by adding different amounts of benzoic acid as modulators to synthesis solutions possessing a water content of four equivalents. However, the synthesis of this material was nearly unaffected by modulating agents, as concluded from the constant crystallite size of around 100 nm, no matter whether or not 30 equivalents of benzoic acid, or any amount in between these limits, were added (Figure S11 and Table S2 in the Supporting Information).

Modulation of the synthesis of Zr–tpdc–NH₂ MOF and single-crystal diffraction study: The modulated synthesis approach also gave access to large single crystals (Figure 5b) of a Zr MOF with tpdc²⁻–NH₂ as the linker (Figure 5a), which is a longer linker with three benzene rings. The SBUs and their connectivity are the same as in the UiO materials (Figure 5c).

We selected the amino-functionalized *p*-terphenyl dicarboxylic acid because of the possibility for postsynthetic modification of the framework by making use of the amino function.^[15–18] Another advantage of the amino group is that the solubility of H₂tpdc–NH₂ is much better than that of H₂tpdc. The extremely low solubility of the latter in DMF and other solvents is probably the reason for unsuccessful attempts to synthesize UiO-68. Due to the fact that H₂tpdc–NH₂ is not commercially available, we restricted our experiments with this linker to obtain a phase-pure product and did not scan the whole range of possible modulator concentrations. By adding benzoic acid (30 equiv) and H₂O (3 equiv) to the reaction mixture, we were able to obtain a phase-pure sample containing crystals with a size sufficient

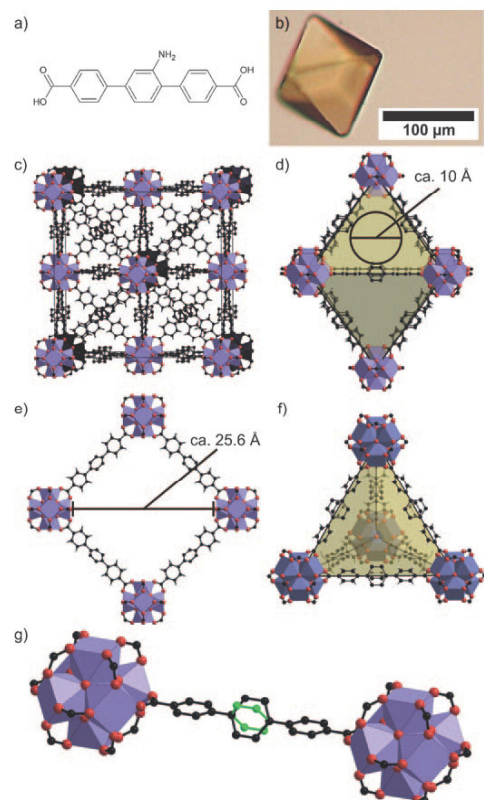


Figure 5. a) Structure of the linker 2'-amino-1,1':4,1''-terphenyl-4,4''-dicarboxylic acid ($H_2tpdc-NH_2$); b) image of an octahedral single crystal of the $Zr-tpdc-NH_2$ MOF. Crystal structure of the $Zr-tpdc-NH_2$ MOF (color code: blue: coordination polyhedra around zirconium, black and green: carbon, red: oxygen); c) unit cell of the framework; d) "octahedral" cavity with calculated effective window size; e) free cavity diameter calculated as the effective distance between two "trans-standing" SBUs of the "octahedral" cavity; f) "tetrahedral" cavity; g) positional disorder of the central benzene ring of the linker. Hydrogen atoms are omitted for clarity.

for single-crystal experiments (Figure 6). To the best of our knowledge, this is the first Zr-based MOF for which the structure was solved from single-crystal data.

The $Zr-tpdc-NH_2$ MOF crystallizes in the space group $Fm\bar{3}m$. The crystal structure shows the same ccp linking topology as UiO-66 and UiO-67^[11] (Figure 5c). There are two different-shaped cavities in the structure, corresponding to the tetra- and octahedral voids of ccp packing. The large octahedral pores of this framework are accessible through triangular windows with a size of about 10 Å, estimated from the largest sphere that may pass through the window (Figure 5d). The distance between the oxygen atoms of the SBUs in the larger, octahedrally shaped pores is 25.6 Å (Figure 5e). Figure 5f shows a picture of the "tetrahedral" void.

Single-crystal data were measured at 173 K. Even at this temperature, the carbon atoms of the benzene rings have large anisotropic displacement parameters perpendicular to their bonds. The amino group of the central ring is clearly too large to allow a planar alignment of all three benzene

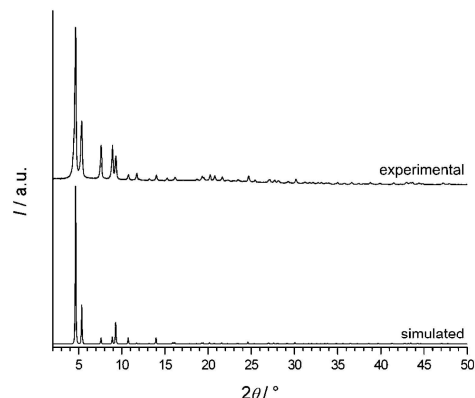


Figure 6. Comparison between simulated and experimental powder XRD patterns of the $Zr-tpdc-NH_2$ MOF.

units and so the central ring exhibits positional disorder (Figure 5g). The refinement gave a torsion angle between the two outer benzene rings and the central ring of $\pm 47.9^\circ$. There is residual electron density in the pores that cannot be reasonably assigned to the amino groups of the linker or to guest molecules. Most likely the guest species are too strongly disordered in the large pores of the material; an amino group on a linker is eightfold disordered for symmetry reasons. The residual electron density was removed by using the Platon routine Squeeze.^[19]

The introduction of an amino group into the UiO materials can, as described above, also be achieved by using 2-aminoterephthalic acid. However, the pores of the resulting UiO-66- NH_2 appear to be too narrow for postsynthetic modifications with larger molecules.^[15] The new $Zr-tpdc-NH_2$ compound opens up the possibility to carry out modifications at the synthesized framework with larger reactants due to its larger pores and cavities.

Conclusion

The size and morphology of Zr-based MOFs can be regulated by adding acetic or benzoic acid to the synthesis. These acids act as modulators, probably by controlling the nucleation rate of the MOFs. Without modulation, the Zr MOFs precipitate as micro-sized aggregates of nanocrystals or the synthesis leads to products that exhibit a disordered phase with a low specific surface area. In the case of $Zr-bdc$ MOF, crystallite and particle sizes can be adjusted in the nanometer range by varying the amount of the modulating agent. Water present in the system also plays a role, especially in the case of UiO-66- NH_2 . The syntheses of Zr MOFs with longer linkers, H_2bpdC and $H_2tpdc-NH_2$, are considerably improved by modulation and show high reproducibility. In the case of the $H_2tpdc-NH_2$ Zr MOF, the first single-crystal structural analysis of a Zr MOF could be carried out. The crystal structure resulting from single-crystal X-ray structural analysis confirms the general structural topology of the

UiO series.^[11] In addition, it allows the precise measurement of structural features, for instance, pore diameters, and the detection of disorder phenomena within the linking molecules.

Our work, and that of Kitagawa et al.,^[8,9] shows that the modulation approach is key to slowing down fast-reacting systems to obtain highly crystalline products or even single crystals. Our current work is focused on using this type of reaction control to obtain Zr MOFs with more specialized linkers.

Experimental Section

H₂tpdc-NH₂: The linker H₂tpdc-NH₂ was synthesized by Suzuki–Miyaura cross-coupling of 2,5-dibromoaniline with 4-(methoxycarbonyl)phenylboronic acid, followed by saponification of the diester.

Dimethyl 2'-amino-1,1':4,1''-terphenyl-4,4''-dicarboxylate: The reaction was carried out under an argon atmosphere by using Schlenk techniques. A suspension of 2,5-dibromoaniline (1.03 g, 4.11 mmol), 4-(methoxycarbonyl)phenylboronic acid (2.22 g, 12.2 mmol), and potassium fluoride (2.36 g, 40.6 mmol) in THF (dried over Na/benzophenone; 20 mL) was degassed through three freeze–pump–thaw cycles. [Pd₂(dba)₃] (270 mg, 0.294 mmol; dba = dibenzylideneacetone) and PrBu₃ in toluene (1.0 mol/L; 820 µL, 0.820 mmol) were added and the reaction mixture was stirred at 50 °C for 17 h. A voluminous precipitate formed. After cooling to room temperature, the reaction mixture was poured into water (25 mL) and the aqueous phase was extracted with CH₂Cl₂. The combined organic phases were concentrated in vacuo. The solid residue was dissolved in CH₂Cl₂, silica gel (4.5 g) was added, and the solvent was removed under reduced pressure to obtain a freely flowing powder, which was transferred onto the top of a silica gel column. Elution with CH₂Cl₂/Et₂O (50:1, volume ratio; R_f = 0.35) gave dimethyl-2'-amino-1,1':4,1''-terphenyl-4,4''-dicarboxylate as a slightly yellow solid containing a trace of a structurally unknown byproduct (1.35 g, 91%). ¹H NMR (250 MHz, CDCl₃; Figure S12 in the Supporting Information): δ = 8.13 and 8.10 (2AA' parts of 2AA'XX' spin systems, 2H each; H3, H5, H3'', H5''), 7.66 and 7.58 (2XX' parts of 2AA'XX' spin systems, 2H each; H2, H6, H2'', H6''), 7.22 (d, ³J = 7.9 Hz, 1H; H6'), 7.09 (dd, ³J = 7.9, ⁴J = 1.7 Hz, 1H; H5'), 7.02 (d, ⁴J = 1.7 Hz, 1H; H3'), 3.95 and 3.94 (s, 3H each; CH₃), 3.88 ppm (br s, 2H; NH₂); ¹³C NMR (63 MHz, CDCl₃; the signal assignment is in agreement with the DEPT-135 spectrum): δ = 167.0 and 166.8 (CO₂Me), 145.3, 143.9, and 141.0 (C1, C1', C4', C1''), 130.9, 130.2, and 130.1 (CH), 129.10 and 129.06 (C4, C4'') 129.00 and 127.0 (CH), 126.3 (C2'), 117.8 (C5'), 114.5 (C3'), 52.2 and 52.1 ppm (CH₃); HRMS (EI): *m/z*: calcd for C₂₂H₁₉NO₄: 361.13141; found: 361.13120.

H₂tpdc-NH₂: A suspension of dimethyl-2'-amino-1,1':4,1''-terphenyl-4,4''-dicarboxylate (2.51 g, 6.95 mmol) in THF (500 mL) was heated to 40 °C. KOH in methanol (5.5 mol L⁻¹; 250 mL, 1.38 mol) was added and the reaction mixture was stirred at 40 °C for 20.5 h. The suspension was allowed to cool to room temperature and was filtered. The isolated colorless solid was suspended in THF (200 mL) and trifluoroacetic acid (25 mL, 0.34 mol) was added. After the suspension had been stirred for 1.5 h at room temperature, water (500 mL) was added and the yellow solid was isolated and dried in vacuo to give H₂tpdc-NH₂ containing 4.7 mol % of THF was obtained as a yellow powder (2.07 g, 90%). M.p. 349 °C (dec); ¹H NMR (250 MHz, [D₆]DMSO; Figure S13 in the Supporting Information): δ = 12.82 (br s, 2H; OH), 8.03 (2AA' parts of 2AA'XX' spin systems, 4H; H3, H5, H3'', H5''), 7.74 and 7.61 (2XX' parts of 2AA'XX' spin systems, 2H each; H2, H2''), 7.17 (d, ⁴J = 1.9 Hz, 1H; H3'), 7.16 (d, ³J = 7.7 Hz, 1H; H6'), 7.02 (dd, ³J = 7.9, ⁴J = 1.6 Hz, 1H; H5'), 4.9 ppm (v br s, 2H; NH₂); ¹³C NMR (63 MHz, [D₆]DMSO; the signal assignment is in agreement with the DEPT-135 spectrum): δ = 167.12 and 167.10 (CO₂H), 145.5, 144.5, 143.7, and 139.5 (C1, C1', C4', C1''), 130.8, 129.9, and 129.8 (CH), 129.5 and 129.1 (C4, C4''), 128.7 and 126.5 (CH), 124.7 (C2'), 115.6

(C5'), 113.9 ppm (C3'); elemental analysis calcd (%) for C₂₀H₁₅NO₄ (333.342): C 72.06, H 4.54, N 4.20; found: C 72.01, H 4.60, N 4.12.

Preparation of Zr–bdc, Zr–bdc–NH₂, Zr–bpdcm, and Zr–tpdc–NH₂ MOFs: All syntheses of the Zr-based metal-organic frameworks were performed in 100 mL teflon capped glass flasks. ZrCl₄ (0.080 g, 0.343 mmol for Zr–bdc and Zr–bdc–NH₂; 0.120 g, 0.514 mmol for Zr–bpdcm and Zr–tpdc–NH₂) and different equivalents of modulator (benzoic or acetic acid) were dissolved in DMF (20 mL; 750 equiv for Zr–bdc and Zr–bdc–NH₂, 500 equiv for Zr–bpdcm and for Zr–tpdc–NH₂) by using ultrasound for about 1 min. The linker was added to the clear solution in an equimolar ratio with regard to ZrCl₄ (0.057 g, 0.343 mmol for Zr–bdc; 0.062 g, 0.343 mmol for Zr–bdc–NH₂; 0.125 g, 0.514 mmol for Zr–bpdcm; 0.172 g, 0.514 mmol for Zr–tpdc–NH₂) and dissolved or, in the case of H₂bpdcm, dispersed by ultrasound for about 3 min. When preparing Zr–bdc–NH₂ MOF and Zr–tpdc–NH₂ MOF, water (0.025 mL, 1.372 mmol and 0.028 mL, 1.243 mmol, respectively) was added to the solution. The tightly capped flasks were kept in an oven at 120 °C under static conditions. After 24 h, the solutions were cooled to room temperature and the precipitates were isolated by centrifugation. The solids were suspended in DMF (10 mL). After standing at room temperature for 2–6 h, the suspensions were centrifuged and the solvent was decanted off. The obtained particles were washed with ethanol (10 mL) in the same way as described for washing with DMF. Finally, the solids were dried under reduced pressure. This standard washing procedure yielded the materials denoted with “as-synthesized”.

Washing of MOFs: As-synthesized MOF powders (60–150 mg) were suspended in DMF (1–2 mL). After 6–14 h of standing at room temperature, the suspension was centrifuged and the solvent was decanted off. This treatment was repeated three times. Afterwards the same procedure was pursued with THF (15×). The solids were dried at room temperature under reduced pressure. They are designated as “washed”. Powder XRD patterns of the washed MOFs are identical to those of as-synthesized MOFs.

Characterization: NMR spectra were recorded on a Bruker ARX 250 (250 MHz) and a Bruker DRX 500 (500 MHz) at 30 °C. Powder X-ray diffraction was carried out by using a Stoe Stadi P diffractometer operated with Ge(111)-monochromatized Cu_{Kα1} radiation (λ = 1.54060 Å) in transmission mode. For particle size determination by Scherrer's equation,^[20] a silicon standard was used to determine the experimental broadening. DLS measurements were performed on a Zetasizer Nano ZS from Malvern Instruments. The solid materials were redispersed in water or ethanol by sonification with a Sonorex Digitec ultrasonic bath at 640 W for 5 min and transferred to a polystyrene cuvette through a syringe. Field-emission (FE)-SEM images were taken on a JEOL JESM-6700F microscope with a semi in-lens detector (working distance 3 mm; acceleration voltage 2 kV). Samples were prepared by dispersing in ethanol, dropping onto a carbon block, and drying under reduced pressure. TGA measurements were performed on a Netzsch STA 429 thermoanalyzer. For this purpose, the samples were filled into alumina crucibles and heated under a flow of air at a rate of 5 °C min⁻¹ up to 1000 °C. Ar sorption isotherms were measured on a Quantachrome Autosorb-1 instrument. At first, each sample was heated to 300 °C in air for 1 h to remove all guests. The samples were further outgassed in vacuum at 150 °C for 24 h prior to the sorption measurement.

X-ray single-crystal diffraction for the Zr–tpdc–NH₂ MOF was carried out on a Bruker KAPPA APEX II CCD diffractometer equipped with a graphite crystal monochromator situated in the incident beam for data collection at 173 K. The determination of unit cell parameters and data collections were performed with Cu_{Kα} radiation (λ = 1.54178 Å) and unit cell dimensions were obtained with least-squares refinements. The program SAINT was used for integration of the diffraction profiles. The structure was solved by direct methods using the SHELXS program of the SHELXTL package and refined with SHELXL.^[21] The final refinement was performed by full-matrix least-squares methods with anisotropic thermal parameters for non-hydrogen atoms on F². The hydrogen atoms were added theoretically, riding on the concerned atoms. Crystal data: C₁₂₀H₄₈O₃₂Zr₆, M_r = 2548.90; cubic; space group Fm $\bar{3}$ m; a = 32.7767(5), V = 35212.4(9) Å³; Z = 4; ρ_{calcd} = 0.481 g cm⁻³; T = 173 K; col-

lected/unique = 23 687/1604; $R1 = 0.0436$, $wR2 = 0.1107$ (for $I > 2\sigma(I)$); $R1 = 0.0505$, $wR2 = 0.1147$ (for all data) and $\text{GooF} = 1.019$.

CCDC-777468 contains the supplementary crystallographic data for this paper. These data can be obtained free of charge from The Cambridge Crystallographic Data Centre via www.ccdc.cam.ac.uk/data_request/cif.

Acknowledgements

This work was performed within the DFG priority program 1362 (Porous Metal-organic Frameworks). We would like to thank Birgit Beisse and Olga Kufelt for thermogravimetric analysis and Felix Brieler, Sven Jare Lohmeier, and Georg Platz for sorption measurements.

- [1] R. Banerjee, A. Phan, B. Wang, C. Knobler, H. Furukawa, M. O’Keeffe, O. M. Yaghi, *Science* **2008**, *319*, 939–943.
- [2] B. Chen, S. Ma, F. Zapata, F. R. Fronczek, E. B. Lobkovsky, H. Zhou, *Inorg. Chem.* **2007**, *46*, 1233–1236.
- [3] H. Bux, F. Liang, Y. Li, J. Cravillon, M. Wiebcke, J. Caro, *J. Am. Chem. Soc.* **2009**, *131*, 16000–16001.
- [4] M. Dinca, J. R. Long, *J. Am. Chem. Soc.* **2005**, *127*, 9376–9377.
- [5] C. A. Bauer, T. V. Timofeeva, T. B. Settersten, B. D. Patterson, V. H. Liu, B. A. Simmons, M. D. Allendorf, *J. Am. Chem. Soc.* **2007**, *129*, 7136–7144.
- [6] K. Schlichte, T. Kratzke, S. Kaskel, *Microporous Mesoporous Mater.* **2004**, *73*, 81–88.
- [7] E. Biemmi, S. Christian, N. Stock, T. Bein, *Microporous Mesoporous Mater.* **2009**, *117*, 111–117.
- [8] S. Diring, S. Furukawa, Y. Takashima, T. Tsuruoka, S. Kitagawa, *Chem. Mater.* **2010**, *22*, 4531.
- [9] T. Tsuruoka, S. Furukawa, Y. Takashima, K. Yoshida, S. Isoda, S. Kitagawa, *Angew. Chem.* **2009**, *121*, 4833–4837; *Angew. Chem. Int. Ed.* **2009**, *48*, 4739–4743.
- [10] E. Biemmi, A. Darga, N. Stock, T. Bein, *Microporous Mesoporous Mater.* **2008**, *114*, 380–386.
- [11] J. H. Cavka, S. Jakobsen, U. Olsbye, N. Guillou, C. Lamberti, S. Bordiga, K. P. Lillerud, *J. Am. Chem. Soc.* **2008**, *130*, 13850–13851.
- [12] P. Piszczek, A. Radtke, A. Grodzicki, A. Wojtczak, J. Chojnacki, *Polyhedron* **2007**, *26*, 679–685.
- [13] V. Guillerm, S. Gross, C. Serre, T. Devic, M. Bauer, G. Férey, *Chem. Commun.* **2010**, *46*, 767–769.
- [14] G. Kickelbick and U. Schubert, *Chem. Ber.* **1997**, *130*, 473–477.
- [15] a) S. J. Garibay, S. M. Cohen, *Chem. Commun.* **2010**, *46*, 7700–7702; b) M. Kandiah, S. Usseglio, S. Svelle, U. Olsbye, K. P. Lillerud, M. Tilset, *J. Mater. Chem.* **2010**, *20*, 9848–9851.
- [16] K. T. Tanabe, Z. Wang, S. M. Cohen, *J. Am. Chem. Soc.* **2008**, *130*, 8508–8517.
- [17] Z. Wang, K. T. Tanabe, S. M. Cohen, *Inorg. Chem.* **2009**, *48*, 296–306.
- [18] J. S. Costa, P. Gamez, C. A. Black, O. Roubeau, S. J. Teat, J. Reedijk, *Eur. J. Inorg. Chem.* **2008**, 1551–1554.
- [19] A. L. Spek, *J. Appl. Crystallogr.* **2003**, *36*, 7–13.
- [20] B. D. Cullity, S. R. Stock in *Elements of X-Ray Diffraction: International Edition*, 3rd ed., Pearson/Prentice Hall, Upper Saddle River, **2001**, pp. 388–390.
- [21] SHEXLXTL, Version 5.1, G. M. Sheldrick, Program for Solution and Refinement of Crystal Structures, University of Göttingen (Germany), **1997**.

Received: November 8, 2010
Published online: May 5, 2011

4 A novel Zr-based porous coordination polymer containing an azo-linker

Preface

This work has been published as a full paper for the "European Journal of Inorganic Chemistry" and focuses on the use of the azo linker H₂abdc for the formation of Zr-MOFs. The linker was synthesized and analyzed by Simon Dühren, Georg Platz, and the author of this thesis. As has already been described in chapter 3 (p. 45), crystalline Zr-MOFs with linkers longer than H₂bdc are difficult to obtain. Therefore, again the modulation approach was successfully applied to control the reaction. It was not possible to control the size of particles, as it was the case for the Zr-bdc-MOF, but to increase the reproducibility of the synthesis and in some batches to obtain single crystals. These were used for SXRD experiments which were conducted and analyzed by the author of this thesis. The kink in this linker made it difficult to solve the structure of this Zr-MOF completely, but at least the pattern simulated on the basis of the partial structure, showing a face-centered cubic arrangement of the SBUs, fits the experimental PXRD pattern well. This indicates that the topology of the structure is similar to that of UiO-Zr-MOFs.

The use of a Soxhlet extraction with ethanol to purify the new compound enhanced its thermal stability and was performed prior to Ar sorption experiments. As expected, these showed that the Zr-abdc-MOF has a similar surface area as the Zr-bpdc-MOF (UiO-67).

The author conducted all experiments (some of which were carried out by Simon Dühren during his laboratory course under the supervision of the author) concerning the synthesis of MOFs and analyzed the products by PXRD, SXRD, and TGA/DTA. The partial structure was determined by the author; Sebastian Lilienthal of the Behrens group used it to model a structure with ordered linkers, the PXRD of which show less similarity to the experimental PXRD. The Ar sorption isotherms were measured by Georg Platz and evaluated by the author and him.

FULL PAPER

DOI: 10.1002/ejic.201101151

A Novel Zr-Based Porous Coordination Polymer Containing Azobenzenedicarboxylate as a Linker

Andreas Schaate,^[a] Simon Dühren,^[a] Georg Platz,^[a] Sebastian Lilienthal,^[a]
Andreas M. Schneider,^[a] and Peter Behrens*^[a]

Keywords: Adsorption / Azo compounds / Coordination polymers / Metal–organic frameworks / Zirconium

A novel porous coordination polymer (PCP), Zr-abdc, composed of Zr-based secondary building units (SBUs), $[\text{Zr}_6\text{O}_4(\text{OH})_4]^{12+}$, and 4,4'-azobenzenedicarboxylate (abdc^{2-}) linkers, has been synthesized by a modulated synthetic approach. In accord with the twelve-fold connecting SBU, Zr-abdc has a topology similar to the PCP series UiO-66–UiO-68, which is proposed from single-crystal XRD and powder (P)XRD experiments. The linkers are strongly disordered, which made it impossible to determine the exact structure.

The compound was further characterized by thermogravimetric analysis, scanning electron microscopy and Ar sorption measurements. Soxhlet extraction with ethanol instead of simple washing was helpful to remove guest molecules present in the pores after the synthesis. PXRD patterns measured at elevated temperatures show that a material stable up to 400 °C in air was obtained. After activation, it showed a specific surface area of $3000 \text{ m}^2 \text{ g}^{-1}$ and a pore volume of $1.41 \text{ cm}^3 \text{ g}^{-1}$.

Introduction

Hybrid porous materials that consist of metal-containing nodes linked together by organic molecules are commonly known as metal–organic frameworks (MOFs) or porous coordination polymers (PCPs).^[1] Aside from the rich opportunities organic chemistry offers to design linker molecules, the concept of isorecticular chemistry is one of the most appealing characteristics of this class of materials. The idea is that the of pore size and functionality of PCPs can be systematically tuned by changing the length or functionality of the linker but retaining the metal-containing nodes or secondary building units (SBUs) and therefore the topology of the initial structure.^[2] This idea was introduced with the isorecticular MOF series^[3] and has been proven to be a fruitful concept by several examples.^[4,5a,6,7]

In particular, PCPs based on zirconium-containing SBUs show a huge potential for many applications due to their high thermal stability and resistance towards atmospheric moisture, which can be attributed to the highly charged, oxophilic Zr^{4+} cations, the resulting strong Zr–O bonds and the high coordination number of each Zr ion.^[5,7,8] Lillerud and co-workers introduced the isorecticular series UiO-66–UiO-68.^[5] These compounds are constructed from the $\text{Zr}_6\text{O}_4(\text{OH})_4(\text{O}_2\text{C})_{12}$ SBU and linear dicarboxylate linkers

of different lengths. The SBU can be described as a Zr octahedron whose faces are capped by μ_3 -OH and μ_3 -O anions, which build the inner sphere of the complex, and twelve carboxylates, which complete the outer coordination sphere of the Zr cations. This high coordination number of an SBU is very unusual for PCPs and leads to a topology similar to cubic close-packing. The most prominent member of this series is UiO-66, which contains terephthalic acid (H_2bdc) as a linker. It has been shown that bdc^{2-} can be replaced by a range of different linear dicarboxylates of the same length or shorter, equipped with different functionalities.^[9a,9b,10,11]

In our hands, the syntheses of Zr-based PCPs with longer, linear linkers such as biphenyldicarboxylate (bpdc^{2-}) were difficult to reproduce due to the formation of byproducts of low crystallinity.^[8] We therefore applied the modulator approach^[12] to the synthesis of Zr-based PCPs.^[8] In this approach, monocarboxylic acids are added to the reaction mixture as modulators. We have proposed that a competition between the linker and modulator occurs for the complexation of Zr^{4+} cations in the reaction mixture, which reduces the rate of nucleation of the coordination polymers and enables the formation of products with higher crystallinity. By using the modulator approach, it was possible to crystallize Zr–bpdc PCP and a new Zr–tpdc– NH_2 ($\text{H}_2\text{tpdc-NH}_2 = 2'$ -amino-1,1':4',1''-terphenyl-4,4''-dicarboxylic acid) PCP and to tune crystal sizes from nanocrystals up to single crystals suitable for single-crystal (S)XRD experiments.^[8] Using even longer linkers, we have discovered a new series of porous interpenetrated zirconium–organic frameworks (PIZOFs) with this approach.^[7] The structure of the PIZOFs can be derived from a twofold interpenetrated UiO topology, which is porous. These materials

[a] Institut für Anorganische Chemie and ZFM – Center for Solid State Chemistry and New Materials, Leibniz University Hannover, Callinstrasse 9, 30167 Hannover, Germany
Fax: +49-511-762-3006
E-mail: peter.behrens@acb.uni-hannover.de
Supporting information for this article is available on the WWW under <http://dx.doi.org/10.1002/ejic.201101151>.

form one and the same structure with a large variety of dicarboxylic acids of the same length but with widely differing organic functionalities.^[7]

We set out to use 4,4'-azobenzenedicarboxylic acid (H_2abdc) in the synthesis of Zr-based PCPs. We failed to synthesize UiO-68, the member of the UiO series with the largest pore size, due to the fact that the unfunctionalized terphenylenedicarboxylic acid (H_2tpdc) linker was completely insoluble in *N,N*-dimethylformamide (DMF); only with the amino-substituted derivative $H_2tpdc-NH_2$, which has sufficient solubility, we were able to obtain a functionalized UiO-68- NH_2 analogue.^[8] The H_2abdc molecule is longer than bpd_2^- , the linker in UiO-67. A Zr- $abdc$ PCP would be interesting as it should exhibit large window sizes and a high specific surface area. Unlike most of the other linkers that have been used in the synthesis of PCPs with the UiO-66–UiO-68 topology (which are linear), H_2abdc has a kink in its structure. The favourable synthetic accessibility of functionalized derivatives of H_2abdc , which start from 4-nitrobenzoic acid derivatives,^[13] should allow the insertion of different organic functionalities on the linker, and, possibly, to the corresponding PCPs. H_2abdc and other linkers that contain azobenzene groups have already been used for the preparation of several hybrid materials, most of which are nonporous^[14] and a few of which exhibit microporosity.^[15]

Like other azobenzene derivatives, H_2abdc possesses the possibility of *cis/trans* isomerization of the azo group.^[16] Recently, it was pointed out by Stock and co-workers that the successful isomerization of the azo group within a PCP can only be accomplished if it is not integrated into the backbone of the framework but present as a side chain. They provide an example of a porous interpenetrated pillared layer structure where the azo group is covalently attached to the linker and proved its *cis/trans* isomerization in the framework by UV/Vis experiments.^[17]

Our main focus is to combine a linker with staggered coordination sites with the Zr SBU known from the UiO-66–UiO-68 PCPs and study the influence of its geometry on the resulting product. Such a linker with staggered coordination sites is also present in Zr-based PCPs with fumarate (fum) linkers, the synthesis and characterization of which we have recently described.^[18]

Results and Discussion

For the synthesis of Zr- $abdc$, $ZrCl_4$, benzoic acid and H_2abdc were dissolved in DMF in a tightly-capped flask and heated in a preheated oven to 120 °C for 24 h. Benzoic acid was added to obtain crystalline materials. Without any modulating agent, powder XRD patterns only show broad reflections, which indicate a partially ordered product of low crystallinity (Figure S1). After this time, the reaction mixture was allowed to cool to room temperature, and the resulting red powders or crystals were isolated by centrifugation and washed with DMF and ethanol. Products that were washed by this standard procedure are denoted as

Zr- $abdc$ (as-synt.). Some of the products were purified by Soxhlet extraction with ethanol and are denoted as Zr- $abdc$ (Sox.).

Optical microscopy and scanning electron microscopy (SEM) images of the typical products of such syntheses are shown in Figure 1. These products show an orange-red colour similar to the free linker (the corresponding UV/Vis spectra are discussed below). Crystals with micrometer dimensions were mostly produced. In the SEM, these micrometer-sized crystals exhibited octahedral morphology but showed rough, irregular surfaces (Figure 1a). In a batch that was prepared with 30 equiv. of benzoic acid as modulator, larger crystals were produced (Figure 1b), which were suitable for the measurement of SXRD data (see below).

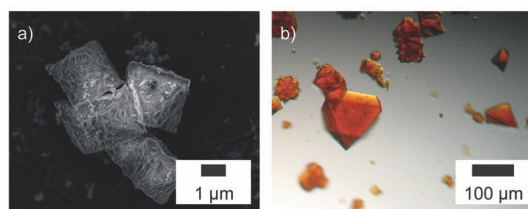


Figure 1. (a) SEM image of Zr- $abdc$ synthesized with 10 equiv. benzoic acid as modulator; (b) image of single crystals of Zr- $abdc$ suitable for SXRD synthesized with 30 equiv. benzoic acid (with respect to $ZrCl_4$) as modulator.

We have used the modulation approach for Zr-based PCPs with a large variety of linkers.^[7,8,18] In most cases, we obtained PCPs only when a modulator was added in the synthesis; an exception is simple UiO-66 with the bdc_2^- linker (bdc : benzenedicarboxylate). For this and other compounds, such as the Zr-fum PCP, we were able to show that an increasing modulator concentration in the reaction mixture led to increasing sizes of the product particles.^[8,18] This, however, was not the case for UiO-67 with the bpd_2^- linker. Although it was possible to obtain highly crystalline, individual particles of micrometer dimension by using benzoic acid as a modulator, it was not possible to regulate the size of the crystallites by varying the amount of the modulator.^[8] The case of the Zr- $abdc$ PCP presented here is similar. After examination of the SEM images and the line widths in PXRD patterns carried out on products from several experiments with varying modulator concentrations, we can say that the concentration of modulator does not control the size of the product particles.

The possibility of size control by modulation may be linked to the solubility of the linker. Whereas H_2bdc and H_2fum are highly soluble in DMF, the solubility of $H_2bpd_2^-$ and H_2abdc is much lower. In a typical Zr PCP synthetic system, various equilibria decide the outcome of a reaction, which possibly involves the formation of highly stable $[Zr_6O_4(OH)_4]^{12+}$ SBUs to which either carboxylate groups from the modulator or linker molecules coordinate. When the linker and the modulator both have a high solubility, they will effectively participate in these equilibria, so that the concentration of the modulator can influence the final result. When the solubility of the linker is small, however,

FULL PAPER

it should also have a strong tendency to stay coordinated to the growing crystallites. Then, the modulator molecules cannot exert any influence on the size of these particles.

PXRD patterns, such as that in Figure 2a, show a general similarity to the patterns of other compounds with the UiO-66 topology with regard to the sequence of the reflections and their approximate intensity distribution. The reflections can be indexed within a face-centred cubic cell, and the lattice constant was refined to $a = 29.4227(4)$ Å. A comparison with cell parameters of other PCPs with UiO-66 topology shows that the size of the unit cell lies between that of Zr-bpdc and of Zr-tpdc-NH₂, as expected (Table 1).

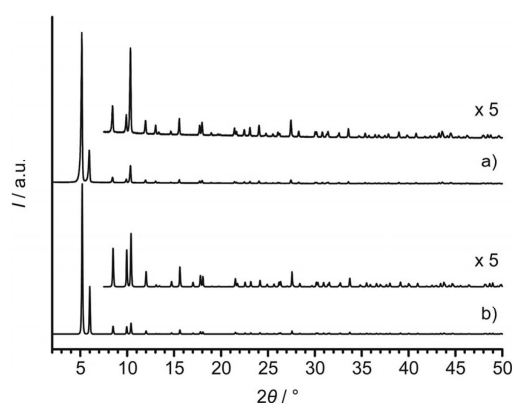


Figure 2. (a) Experimental PXRD pattern of Zr-abdc; (b) theoretical PXRD pattern simulated on the basis of the partial structure derived from SXR data, i.e. a face-centred cubic arrangement of SBUs.

Table 1. Cell parameters a and V [Å³] of different Zr-based PCPs in the space group $Fm\bar{3}m$. Data were obtained from SXR or refined from PXRD patterns.

PCP	$a/\text{Å}$	$V/\text{Å}^3$	Method	Ref.
Zr-bdc	20.7551(5)	8870.3(2)	PXRD	[5a]
Zr-muconic dicarboxylate	20.9550(23)	9201.6(30)	PXRD	[11]
Zr-bpdc	26.8499(15)	19356.6(18)	PXRD	[8]
Zr-abdc	29.4227(4)	25471.1(10)	SXR	this work
Zr-tpdc-NH ₂	32.7767(5)	35212.4(9)	SXR	[8]

Although we successfully synthesized single crystals of Zr-abdc and carried out SXR experiments on them, it was not possible to determine their exact structure from these measurements. In all these experiments we found the space group $Fm\bar{3}m$ [$a = 29.4433(4)$ Å in good agreement with PXRD results]. In the analysis of the data, the atoms of the SBUs (Figure 3b) were readily found (atomic positions are given in Table S1). As expected, and similar to the arrangement found in UiO-66, their centres lie at the lattice points of a face-centred cubic lattice (Figure 3c and d). However, all attempts to further refine the structure gave unsatisfactory results. A possible reason for this is the staggered shape of the linker (Figure 3a).

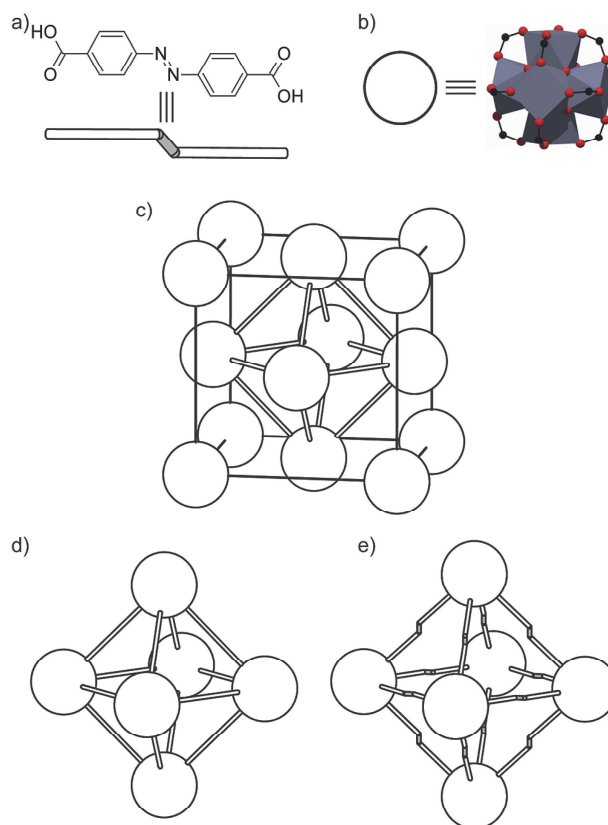


Figure 3. (a) Structural formula and schematic representation of H₂abdc; (b) SBU of Zr-abdc (blue: coordination polyhedral around zirconium; black: carbon; red: oxygen); (c) schematic representation of cubic close-packed spheres, which shows the arrangement of the SBUs in a PCP with UiO-66 topology (the octahedral cavity is emphasized by connections between the SBUs); (d) schematic representation of an octahedral cavity of a PCP with UiO-66 topology and with linear linkers in space group $Fm\bar{3}m$; (e) schematic representation of an octahedral cavity of Zr-abdc with an ordered arrangement of the linkers that possess staggered shapes; the specific order pattern shown here would result in a lowering of the symmetry to space group $I4/m$.

Based on the high symmetry of the space group, it was not possible to locate the atoms of the linker. Either their positions are highly disordered so that the effective electron density at certain atomic positions is too small to be detected or the linkers with their specific nonlinear shape are ordered, which breaks the high symmetry of $Fm\bar{3}m$. With regard to the former case, we can state that a comparison of the experimental PXRD data with a simulated PXRD pattern based on the partial structure derived from the SXR data shows a very good agreement (Figure 2). For the latter case we tried to derive ordered arrangements of the linkers, one of which is shown in Figure 3e. This ordering of the linkers with their staggered structure resulted in a structure with a space group of lower symmetry ($I4/m$; $a = 20.6533$ Å, $c = 29.7535$ Å, atomic positions in Table S2), which allows the representation of the positions of the atoms of the linkers in a coherent fashion, i.e. without the need for disorder models (Figure 3e). We are aware that

lowering the symmetry during such a procedure strongly depends on the forcefield used for the modelling. The deviations between the simulated PXRD pattern of such a structure and an experimental PXRD pattern of Zr-abdc showed that a structure in which the linkers are ordered in this way cannot be justified (Figure S2). Altogether these are strong indications that the structure of the new Zr-abdc PCP has an analogous topology to the UiO-66–UiO-68 Zr-based PCPs, however, with disordered linkers. Accordingly, the new compound should have the empirical formula $Zr_6O_4(OH)_4(abdc)_6$.

To further substantiate this composition, we performed thermogravimetric analysis (TGA) on the obtained Zr-abdc materials. TGA of Zr-abdc (as-synt.) in a flow of air (Figure 4) revealed that the mass loss of the material occurs in two steps. The mass loss that occurred up to 300 °C is assigned to guest molecules that are released from the cavities. Above 400 °C, the curve shows a strong drop, which may tentatively be assigned to the combustion of the linker molecules. The final product is monoclinic ZrO_2 , as identified by PXRD. As the guest contents of PCPs can differ depending on the drying procedure and guest-exchange history, the measured mass losses were corrected for the removal of guest molecules and were compared to the theo-

retical mass losses calculated from the empirical formula of Zr-abdc (Table 2). The comparison shows a discrepancy of about 4% between the corrected and calculated mass losses for Zr-abdc (as-synt.), i.e. the mass loss of the step tentatively ascribed to the linker decomposition is too high. We assumed that the as-synthesized compound still contained guest molecules that can only leave when the framework is destroyed (which, in turn, lowers the decomposition temperature of the compound, see the discussion below).

Table 2. Comparison of measured and calculated TGA mass loss data [%] obtained in a flow of air for Zr-abdc (as-synt.) and Zr-abdc (Sox.).

Step	Calculated	Zr-abdc (as-synt.)		Zr-abdc (Sox.)	
		Measured	Guest-free ^[a]	Measured	Guest-free ^[a]
Guests	–	19.7	–	9.8	–
Linker	67.7	57.5	71.6	61.1	67.7
Residue	32.3	22.8	28.4	29.2	32.3

[a] Mass loss after correction for removal of guest molecules.

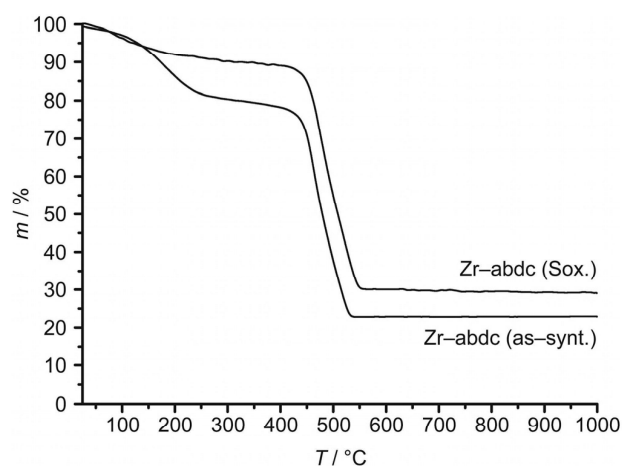


Figure 4. TGA in air of Zr-abdc (as-synt.) and Zr-abdc (Sox.).

We previously found^[8] that the activation of PCP materials obtained from modulated syntheses can be difficult due to the partial occlusion of modulator molecules in the cavities of the porous materials. When the activation of the material is carried out simply by heating, trapped modulator molecules can destroy the PCP, which happens in Zr-bdc prepared with benzoic acid as the modulator.^[8] The reason for this is the small window size of this PCP, which cannot let the modulator molecules pass through. With larger windows, as in Zr-bpdc, this problem disappears, because enclosed benzoic acid molecules can leave the material without hindrance. Zr-abdc should have larger windows than Zr-bpdc judging from the lattice dimensions. However, the thermal activation of Zr-abdc in the as-synthesized state appears to be difficult, which can be judged from variable-temperature PXRD patterns (Figure 5a). Zr-abdc (as-synt.) appears stable up to about 280 °C. Beyond this, the reflections of the material are broadened but do not completely disappear until 440 °C. This is an indication of partial degradation of the material above 280 °C. The reason for this could be that not all of the guest molecules were removed from Zr-abdc (as-synt.) by the standard washing procedure with DMF and ethanol. Higher than 280 °C, these remain-

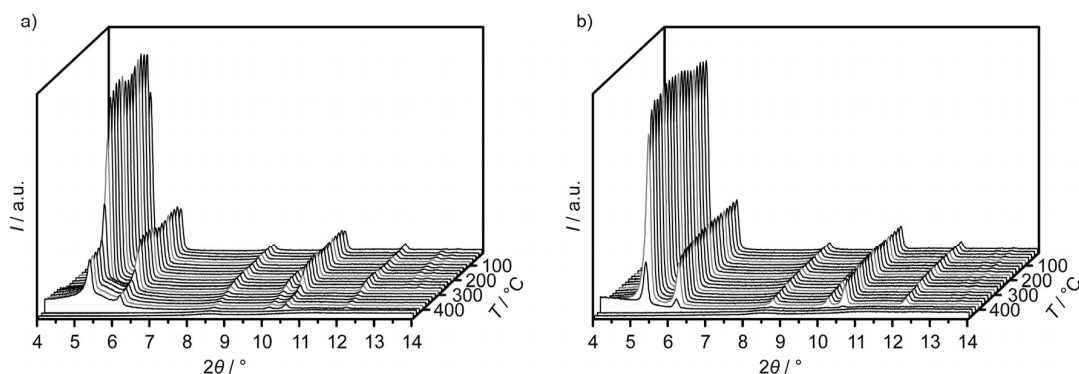


Figure 5. Variable-temperature PXRD patterns of (a) Zr-abdc (as-synt.) and (b) Zr-abdc (Sox.).

FULL PAPER

ing guests could then destroy the framework as they leave the material and would be responsible for the increased mass loss in the TGA step that was assigned to the degradation of the linker.

We therefore chose to apply a more efficient washing procedure to remove guest molecules from Zr-abdc (as-synt.), which consisted of a Soxhlet extraction with ethanol for 24 h. The TGA of Zr-abdc (Sox.) again proceeded in two steps (Figure 4). The first step of Zr-abdc (Sox.) is assigned to the loss of guests up to 300 °C, which is considerably smaller than that of Zr-abdc (as-synt.). This shows that extraction with ethanol reduced the guest content effectively. We also found that Soxhlet extraction saves time compared to other guest removal or exchange procedures that have been applied to purify Zr PCPs.^[9a] The second step that corresponds to the oxidation of the linkers again starts at ca. 400 °C. For Zr-abdc (Sox.), the corrected mass loss is in perfect accordance with the calculated mass loss of Zr-abdc (Table 2). Variable-temperature PXRD patterns of Zr-abdc (Sox.) (Figure 5b) show that the material withstands the conditions of the Soxhlet extraction. The intensities and line widths of the reflections do not change significantly up to about 400 °C, which shows that the Soxhlet extraction has led to higher thermal stability of Zr-abdc. Although Zr-abdc is stable to ambient air and moisture in the as-synthesized and the Soxhlet-extracted state, it is not stable in aqueous solution, which can be judged from a PXRD pattern measured on a sample after immersion in water for 24 h (Figure S3).

The UV/Vis spectra of H₂abdc and Zr-abdc (Figure S4) are similar. Both can be attributed to azobenzene chromophores with a *trans* configuration. Under irradiation at 355 nm, the *trans* isomer of free H₂abdc, in an aqueous solution at pH = 11, can be switched to the *cis* isomer, which results in a drastic change in the absorption properties of H₂abdc.^[16] The *cis* isomer can relax back to the *trans* form by a thermally activated process or by irradiation at 430 nm. As our syntheses were carried out at elevated temperatures, it is not surprising that the azo group is present in its *trans* form in H₂abdc. Carrying out the crystallization of the Zr-abdc PCP under irradiation with UV light did not result in abdc linkers with *cis* configuration due to thermal relaxation at the high synthetic temperature. Attempts to induce *cis/trans* isomerization of the abdc linkers incorporated into the Zr-abdc PCP by using UV light were unsuccessful, because such isomerizations are impossible when the azobenzene chromophore is restrained in a rigid framework. As Stock and co-workers have explained,^[17] isomerization reactions of azobenzene moieties in PCPs can only occur when the switching unit is present as a side chain to the linker (or as part of an unrestrained guest molecule).

Ar sorption experiments were carried out on Zr-abdc (Sox.) to prove the microporosity of the purified product. The Ar sorption curve shows a typical type-I isotherm with a steep increase of the curve at low P/P_0 values (Figure 6a). The specific surface area is 3000 m² g⁻¹, which was determined by applying the Brunauer–Emmett–Teller equation to the data. As expected, this value is similar to the specific

surface area of Zr-bpdc.^[8] The pore size distribution, evaluated by nonlocal (NL) DFT fitting of the data (Figure S5), shows a maximum at 13 Å (Figure 6b). From the modelled Zr-abdc structure, the largest spheres that would fit into the voids that correspond to the octahedral and tetrahedral sites of a cubic close-packing have diameters of 15 and 11 Å, respectively. The pore size distribution gives a reasonable average of these pore sizes, and the total pore volume is 1.41 cm³ g⁻¹.

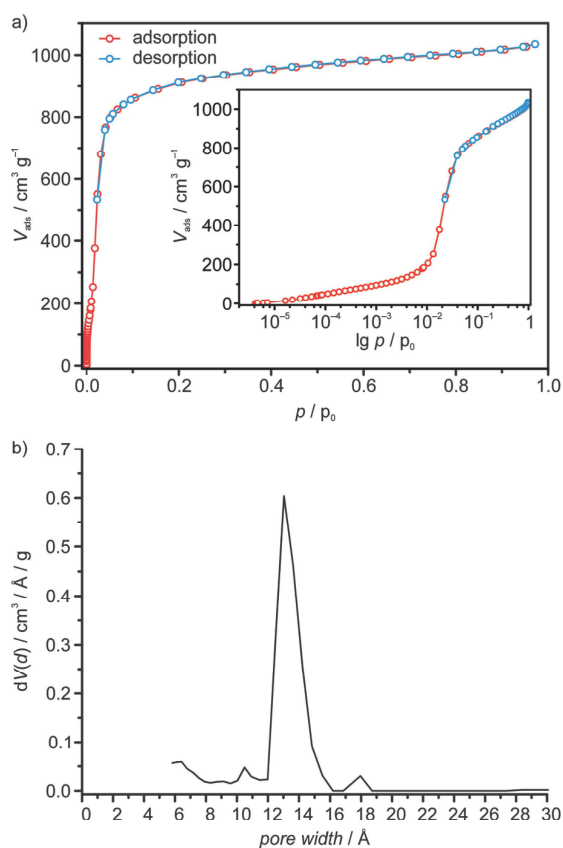


Figure 6. (a) Argon gas sorption isotherms of Zr-abdc (Sox.) (activated at 120 °C prior to sorption experiment) at -186.15 °C as linear scale plot; inset: logarithmic scale plot; red: adsorption, blue: desorption. (b) Pore size distribution of Zr-abdc (Sox.) calculated from the data given in Figure 6a.

Conclusions

We have presented the synthesis and characterization of a new Zr PCP with abdc dianions as linkers. The new compound was obtained from a synthesis modulated with benzoic acid. Evaluation of powder and single-crystal XRD data suggests that the Zr-abdc PCP has the same topology as the PCPs from the UiO-66–UiO-68 series, but the staggered structure of the linker seems to lead to high disorder and makes it impossible to determine the exact structure from SXRD experiments. TGA data and the results from sorption measurements support the proposal of the structure. For activation, it is crucial to purify Zr-abdc exten-

sively prior to thermal activation. For this purpose, Soxhlet extraction with ethanol proved to be a helpful and convenient tool, which also increased the thermal stability of the compound. As the synthesis of H₂abdc derivatives is modular with regard to the introduction of different organic functionalities, this compound could be the first of an isostructural series of Zr-based azo-PCPs with tuneable properties.

Experimental Section

General: All chemicals and solvents were purchased from commercial sources and were used without further purification. PXRD was carried out with a Stoe Stadi P diffractometer operated with Ge(111)-monochromatized Cu-K_α radiation ($\lambda = 1.54060 \text{ \AA}$) in transmission mode. Field-emission (FE) SEM images were recorded with a JEOL JESM-6700F with a semi-in-lens detector (working distance 3 mm; acceleration voltage 2 kV). Samples were prepared by dispersing in ethanol, dropping onto a carbon block and drying under reduced pressure. TGA measurements were performed with a Netzsch STA 429 thermoanalyzer. For this purpose, alumina crucibles were filled with the samples and heated under a flow of air at a rate of 5 °C/min up to 1000 °C. UV/Vis measurements of powder samples were carried out with a Varian Cary 4000 UV/Vis spectrometer in diffuse reflectance with Teflon powder as the white standard. Ar sorption isotherms were measured with a Quantachrome Autosorb-1 instrument. The sample was purified by Soxhlet extraction and activated in vacuo at 120 °C for 54 h prior to the sorption measurement. The specific surface area was determined by applying the Brunauer–Emmett–Teller equation to the P/P_0 range from 0.04 to 0.08. The measured data were fitted with the calculation model Ar at 87 K zeolites/silica (cylinder pores, NLDFT ads.) of the AS 1 Win software from Quantachrome to obtain the pore size distribution and the total pore volume. SXR D studies were carried out with a Bruker KAPPA APEX II CCD diffractometer equipped with a graphite crystal monochromator situated in the incident beam, which produces Cu-K_α radiation ($\lambda = 1.54178 \text{ \AA}$). Data collection was carried out at -100 °C. The SAINT program was used for integration of the diffraction profiles,^[19] and adsorption corrections were applied by using the SADABS routine.^[20] The structure was solved by direct methods and refined by full-matrix least squares on F^2 with anisotropic displacement using the SHELXTL software package.^[21] The modelling of Zr-abdc to a structure that shows the kink in abdc²⁻ was done as follows: the partial structure obtained from SXR D experiments (which contained the atoms of the SBUs) was used as a starting point. The space group was set to $P1$ and the disordered linkers were substituted by complete abdc²⁻ molecules. The constructed model was submitted to a full energy minimization, which included optimization of the unit cell dimensions and metric, with parameters from the Universal Force Field as implemented in Materials Studio 5.5. The geometry optimization converged to result in a plausible tetragonal structure with the space group $I4m$, No. 87 ($a = b = 20.6533$, $c = 29.7535 \text{ \AA}$, $\alpha = \beta = \gamma = 90^\circ$, $V = 12692 \text{ \AA}^3$).

Preparation of 4,4-Azobenzenedicarboxylic Acid (H₂abdc): H₂abdc was prepared according to a literature procedure.^[22]

Preparation of Zr-abdc: All reactions were performed in 100 mL Teflon-capped glass flasks. In a typical synthesis, zirconium(IV) chloride (0.120 g, 0.51 mmol) and different amounts of benzoic acid (e.g. 1.884 g, 15.43 mmol) were dissolved in DMF (20 mL) by using ultrasound for ca. 1 min. To the clear solution, H₂abdc

(0.139 g, 0.51 mmol) was added and dispersed by ultrasound for ca. 5 min. Water (0.037 mL, 2.06 mmol) was added to the suspension, and the flask was tightly capped. The orange suspension was kept in an oven at 120 °C under static conditions. After 30 min, the linker was completely dissolved, and the solution was bright red. After 24 h, the solution was cooled to room temperature, and the precipitate was isolated by centrifugation. The solid was suspended in DMF (20 mL). After standing at room temperature for 2–6 h, the suspension was centrifuged, and the solvent was decanted. The particles were washed with ethanol (20 mL) in the same way as described for washing with DMF. Afterwards, the solids were dried in an oven at 120 °C for 2 h. Zr-abdc (as-synt.) refers to products that were produced in this way. Further purification of the PCPs was carried out by Soxhlet extraction with ethanol for 24 h and subsequent drying in an oven at 120 °C for 2 h. Zr-abdc (Sox.) refers to products that were purified in this way.

Supporting Information (see footnote on the first page of this article): Additional PXRD patterns, tables with atomic coordinates of the structural model, UV/Vis spectra of H₂abdc and Zr-abdc and the NLDFT fitting plot for the sorption data.

Acknowledgments

This work was supported by the Deutsche Forschungsgemeinschaft as a part of the priority program 1362 (Porous metal–organic frameworks).

- [1] S. Kitagawa, R. Kitaura, S. Noro, *Angew. Chem.* **2004**, *116*, 2388; *Angew. Chem. Int. Ed.* **2004**, *43*, 2334–2375.
- [2] O. M. Yaghi, M. O’Keeffe, N. W. Ockwig, H. K. Chae, M. Eddaoudi, J. Kim, *Nature* **2003**, *423*, 705–714.
- [3] M. Eddaoudi, J. Kim, N. Rosi, D. Vodak, J. Wachter, M. O’Keeffe, O. M. Yaghi, *Science* **2002**, *295*, 469–472.
- [4] L. Ma, J. M. Falkowski, C. Abney, W. Lin, *Nat. Chem.* **2010**, *2*, 838–846.
- [5] a) J. H. Cavka, S. Jakobsen, U. Olsbye, N. Guillou, C. Lamberti, S. Bordiga, K. P. Lillerud, *J. Am. Chem. Soc.* **2008**, *130*, 13850–13851; b) L. Valenzano, B. Civalieri, S. Chavan, S. Bordiga, M. H. Nilsen, S. Jakobsen, K. P. Lillerud, C. Lamberti, *Chem. Mater.* **2011**, *23*, 1700–1718.
- [6] S. Surblé, C. Serre, C. Mellot-Draznieks, F. Millange, G. Férey, *Chem. Commun.* **2006**, 284–286.
- [7] A. Schaate, P. Roy, T. Preuße, S. J. Lohmeier, A. Godt, P. Behrens, *Chem. Eur. J.* **2011**, *17*, 9320–9325.
- [8] A. Schaate, P. Roy, A. Godt, J. Lippke, F. Waltz, M. Wiebcke, P. Behrens, *Chem. Eur. J.* **2011**, *17*, 6643–6651.
- [9] a) S. J. Garibay, S. M. Cohen, *Chem. Commun.* **2010**, *46*, 7700–7702; b) M. Kim, S. J. Garibay, S. M. Cohen, *Inorg. Chem.* **2011**, *50*, 729–731; c) M. Kandiah, S. Usseglio, S. Svelle, U. Olsbye, K. P. Lillerud, M. Tilset, *J. Mater. Chem.* **2010**, *20*, 9848–9851.
- [10] M. Kandiah, M. H. Nilsen, S. Usseglio, S. Jakobsen, U. Olsbye, M. Tilset, C. Larabi, E. A. Quadrelli, F. Bonino, K. P. Lillerud, *Chem. Mater.* **2010**, *22*, 6632–6640.
- [11] V. Guillermin, S. Gross, C. Serre, T. Devic, M. Bauer, G. Férey, *Chem. Commun.* **2010**, *46*, 767–769.
- [12] a) S. Diring, S. Furukawa, Y. Takashima, T. Tsuruoka, S. Kitagawa, *Chem. Mater.* **2010**, *22*, 4531–4538; b) T. Tsuruoka, S. Furukawa, Y. Takashima, K. Yoshida, S. Isoda, S. Kitagawa, *Angew. Chem.* **2009**, *121*, 4833; *Angew. Chem. Int. Ed.* **2009**, *48*, 4739–4743.
- [13] F. Rakotonradany, M. A. Whitehead, A.-M. Lebus, H. F. Sleiman, *Chem. Eur. J.* **2003**, *9*, 4471–4780.
- [14] a) X. Lin, T. Liu, J. Lin, H. Yang, J. Lü, B. Xu, R. Cao, *Inorg. Chem. Commun.* **2010**, *13*, 388–391; b) B. Liu, Q. Xu, *Acta Crystallogr., Sect. E* **2009**, *65*, m509; c) C. Volkringer, T.

FULL PAPER

P. Behrens et al.

- Loiseau, T. Devic, G. Férey, D. Popov, M. Burghammer, C. Riekkel, *CrystEngComm* **2010**, *12*, 3225–3228; d) H. Furukawa, J. Kim, N. W. Ockwig, M. O’Keeffe, O. M. Yaghi, *J. Am. Chem. Soc.* **2008**, *130*, 11650–11661; e) B. Chen, S. Ma, E. J. Hurtado, E. B. Lobkovsky, H.-C. Zhou, *Inorg. Chem.* **2007**, *46*, 8490–8492; f) Z.-F. Chen, R.-G. Xiong, B. F. Abrahams, X.-Z. You, C.-M. Che, *J. Chem. Soc., Dalton Trans.* **2001**, *17*, 2453–2455; g) C.-M. Jin, Z. Zhu, Z.-F. Chen, Y.-J. Hu, X.-G. Meng, *Cryst. Growth Des.* **2010**, *10*, 2054–2056.
- [15] a) Z.-F. Chen, Z.-L. Zhang, Y.-H. Tan, Y.-Z. Tang, H.-K. Fun, Z.-Y. Zhou, B. F. Abrahams, H. Liang, *CrystEngComm* **2008**, *10*, 217–231; b) Y. Liu, J. F. Eubank, A. J. Cairns, J. Eckert, V. C. Kravtsov, R. Luebke, M. Eddaoudi, *Angew. Chem.* **2007**, *119*, 3342; *Angew. Chem. Int. Ed.* **2007**, *46*, 3278–3283; c) T. M. Reineke, M. Eddaoudi, D. Moler, M. O’Keeffe, O. M. Yaghi, *J. Am. Chem. Soc.* **2000**, *122*, 4843–4844; d) V. Zelenák, Z. Vargová, M. Al máši, A. Zelenáková, J. Kuchár, *Microporous Mesoporous Mater.* **2010**, *129*, 354–359.
- [16] G. Abellán, H. García, C. J. Gómez-García, A. Ribera, *J. Photochem. Photobiol. A: Chem.* **2011**, *217*, 157–163.
- [17] A. Modrow, D. Zargani, R. Herges, N. Stock, *Dalton Trans.* **2011**, *40*, 4217–4222.
- [18] G. Wißmann, A. Schaate, S. Lilienthal, I. Bremer, A. M. Schneider, P. Behrens, *Microporous Mesoporous Mater.* **2012**, *152*, 64–70.
- [19] *SAINT Integration Engine*, version 7.68A, Bruker AXS, Inc., **2009**.
- [20] G. M. Sheldrick, *SADABS – Area Detector Adsorption and Other Corrections*, version 2.03, Bruker AXS, Inc., **2008**.
- [21] G. M. Sheldrick, *SHELXTL – Program for Solution and Refinement of Crystal Structures*, version 5.1, University of Göttingen, **1997**.
- [22] P. S. Mukherjee, N. Das, Y. K. Kryschenko, A. M. Arif, P. J. Stang, *J. Am. Chem. Soc.* **2004**, *126*, 2464–2473.

Received: October 20, 2011
Published Online: January 9, 2012

5 Porous interpenetrated zirconium-organic frameworks (PIZOFs), a chemically versatile family of MOFs

Preface

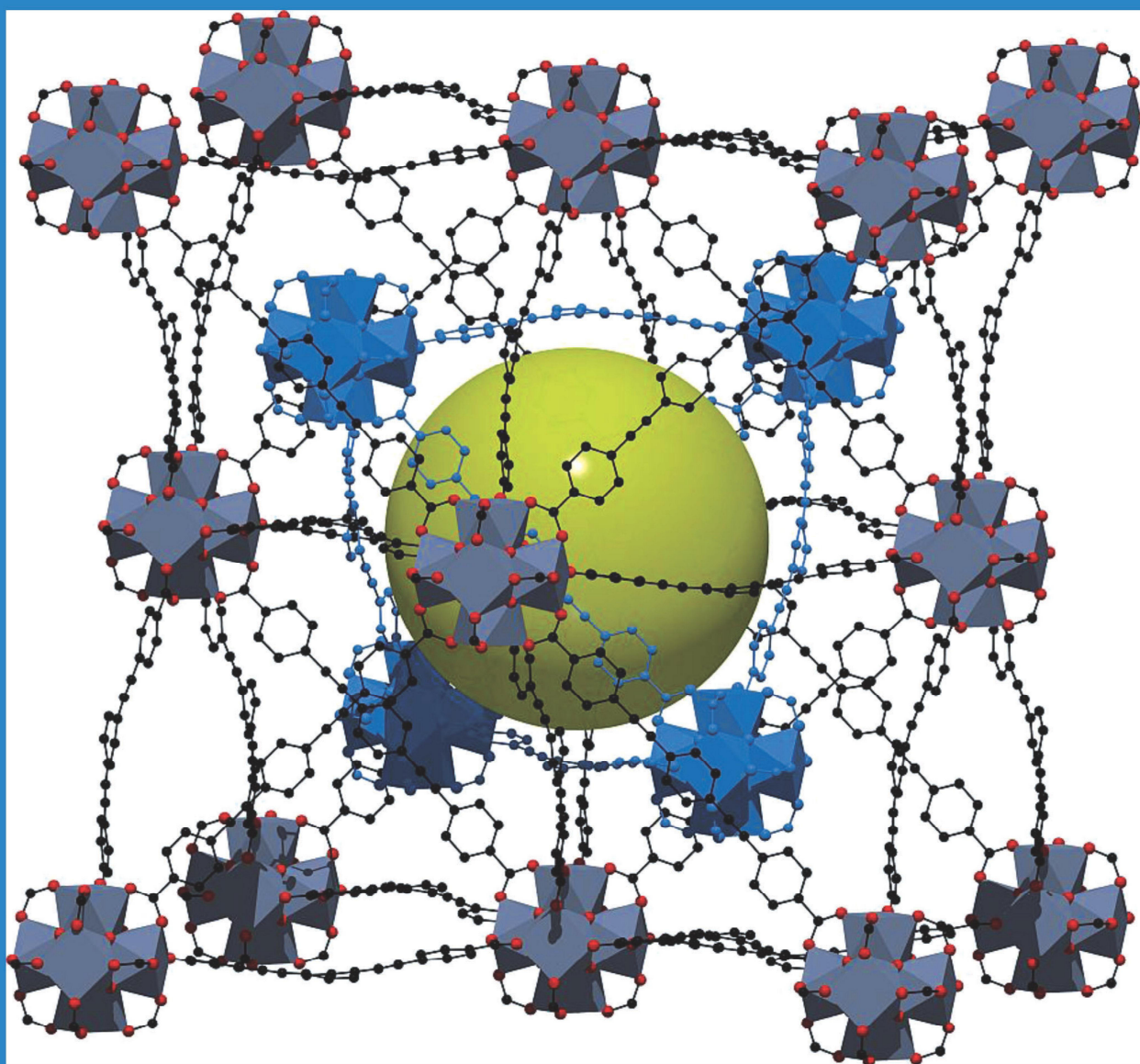
This work has been published as a full paper in "Chemistry – A European Journal" and resulted from the cooperation within the priority program 1362 (Porous Metal-Organic Frameworks) with the Godt group at the Bielefeld University. The paper presents the novel series of PIZOFs which are composed of the same SBU as present in Zr-MOFs of the UiO-66 type and long dicarboxylic acids which share the same length but are very variable concerning their functional groups.

The previously developed modulation approach presented in chapters 2.2.4 and 3 is essential for the successful synthesis of PIZOFs and was the key to obtain single crystals of three different PIZOFs. PXRD measurements revealed that the PIZOFs share a common framework structure indicating that this structural motive is very convenient for this length of dicarboxylic acid and uninfluenced by a variety of functional groups.

The linkers for this work were synthesized and characterized by or under supervision of Pascal Roy and Thomas Preuße from the Godt group at the Bielefeld University. The syntheses of the PIZOFs were carried out by the author or under supervision of the author. Their characterization (PXRD, SXRD, determination of crystal structure, TGA/DTA) was carried out by the author. The Ar sorption isotherms were measured by Sven Jare Lohmeier and evaluated by the author and him.

Porous Interpenetrated Zirconium–Organic Frameworks (PIZOFs): A Chemically Versatile Family of Metal–Organic Frameworks

Andreas Schaate,^[a] Pascal Roy,^[b] Thomas Preuße,^[b] Sven Jare Lohmeier,^[a]
Adelheid Gott,*^[b] and Peter Behrens*^[a, c]



Abstract: We present the synthesis and characterization of porous interpenetrated zirconium-organic frameworks (PIZOFs), a new family of metal-organic frameworks obtained from $ZrCl_4$ and the rodlike dicarboxylic acids $HO_2C[PE-P(R^1,R^2)-EP]CO_2H$ that consist of alternating phenylene (P) and ethynylene (E) units. The substituents R^1, R^2 were broadly varied (alkyl, O-alkyl, oligo(ethylene glycol)), including postsynthetically addressable substituents (amino, alkyne, furan).

The PIZOF structure is highly tolerant towards the variation of R^1 and R^2 . This together with the modular synthesis of the diacids offers a facile tuning of the chemical environment within the pores. The PIZOF structure was solved from single-crystal X-ray diffraction analysis. The PIZOFs are stable under

ambient conditions. PIZOF-2, the PIZOF prepared from $HO_2C[PE-P(OMe,OMe)-EP]CO_2H$, served as a prototype to determine thermal stability and porosity. It is stable up to $325^\circ C$ in air as determined by using thermogravimetry and powder X-ray diffraction. Argon sorption isotherms on PIZOF-2 revealed a Brunauer-Emmett-Teller (BET) surface area of $1250\text{ m}^2\text{ g}^{-1}$ and a total pore volume of $0.68\text{ cm}^3\text{ g}^{-1}$.

Keywords: adsorption • coordination polymers • metal-organic frameworks • porosity • zirconium

Introduction

Metal-organic frameworks or porous coordination polymers are porous materials that are constructed from metal-containing secondary building units (SBUs), typically metal-oxo clusters and organic linkers, most often dicarboxylates. They find interest as materials in heterogeneous catalysis,^[1] gas storage,^[2] separation,^[3] electrodes,^[4] and drug delivery.^[5] MOFs with short linkers are numerous but the synthesis of MOFs with long linkers remains a challenge. Examples of very long linkers are the rodlike diacids $HO_2C[PE-P(R^1,R^2)-EP]CO_2H$ (P stands for phenylene, E for ethynylene, and R^1 and R^2 denote the substituents at the central phenylene unit; Figure 1a). With $R^1, R^2 = \text{Hex}$, OMe, and crown ether, they have served for the preparation of coordination polymers with Zn-based SBUs.^[6] In general, Zn-based MOFs are sensitive to moisture,^[7] and often the framework collapses upon guest removal.^[2,8]

More stable MOFs are described for the highly charged and highly oxygen-affine cation Zr^{4+} . UiO-66 with the linker terephthalate is stable in water,^[9] and UiO-67 and UiO-68-NH₂ with biphenyl dicarboxylate and amino-substituted terphenyldicarboxylate as the linkers can be handled

at atmospheric moisture.^[10] Furthermore, Zr MOFs of the UiO type are highly temperature resistant and exhibit large surface areas.^[9,10] Postsynthetic modifications of UiO-66-NH₂, a MOF isostructural to UiO-66 but with the 2-amino-terephthalate as the linker,^[11] prove good accessibility of the pores and point out the potentials of Zr MOFs.

Here we report on an extension of the class of Zr-based MOFs. The novel MOFs were constructed by using the very long linkers $HO_2C[PE-P(R^1,R^2)-EP]CO_2H$. These MOFs

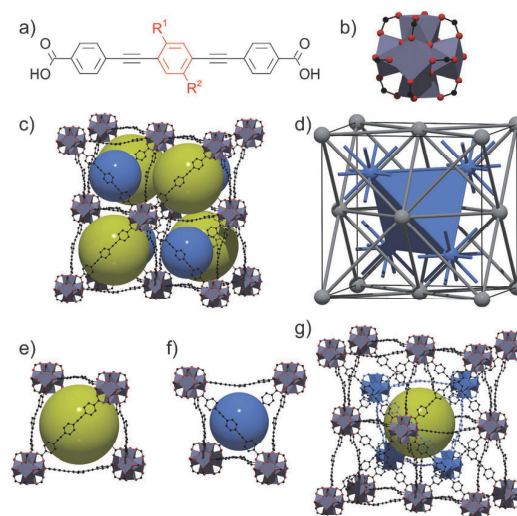


Figure 1. a) Structural formula of the dicarboxylic diacids $HO_2C[PE-P(R^1,R^2)-EP]CO_2H$; the substituents R^1 and R^2 are defined in Scheme 1. b) $Zr_6O_4(OH)_4(O_2C)_{12}$ secondary building unit of the PIZOFs (black: C, red: O, gray: polyhedra around Zr). c) One of the two frameworks of PIZOF-2 showing the arrangement of concave and convex tetrahedral cavities. d) Topological representation of the interpenetrated structure of the PIZOFs. e) Convex cavity. f) Concave cavity. g) Crystal structure of the PIZOFs; the interpenetrating framework is depicted in blue. Due to the fact that linkers from the second framework pass through the “octahedral” voids of the first framework, these “octahedral” voids are effectively reduced to “tetrahedral” voids. In c and e–g, the spheres represent the largest spheres that fit into the cavities (diameters: yellow $\approx 19\text{ \AA}$, blue $\approx 14\text{ \AA}$).

[a] A. Schaate, Dr. S. J. Lohmeier, Prof. Dr. P. Behrens
Institute of Inorganic Chemistry
Leibniz University Hannover
Callinstrasse 9, 30167 Hannover (Germany)
Fax: (+49) 511-762-3006
E-mail: peter.behrens@acb.uni-hannover.de

[b] P. Roy, T. Preuß, Prof. Dr. A. Godt
Department of Chemistry
Bielefeld University
Universitätsstrasse 25, 33615 Bielefeld (Germany)
Fax: (+49) 521-1006-6417
E-mail: godt@uni-bielefeld.de

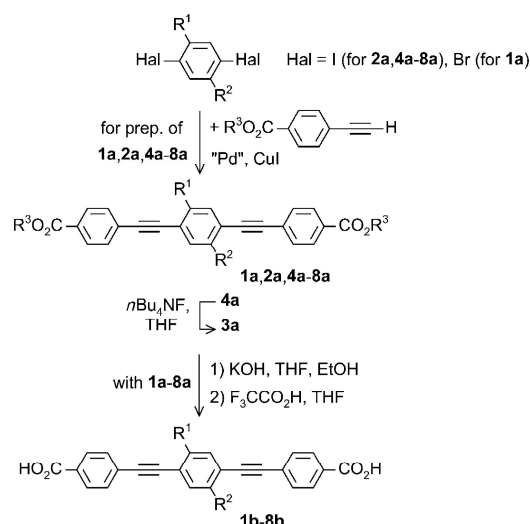
[c] Prof. Dr. P. Behrens
ZFM: Center for Solid-State Chemistry
and New Materials, Leibniz University Hannover
Callinstrasse 9, 30167 Hannover (Germany)

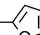
Supporting information for this article is available on the WWW under <http://dx.doi.org/10.1002/chem.201101015>.

constitute a novel series of isostructural porous interpenetrated Zr-organic frameworks (PIZOFs; Figures 1 and 2) with broadly variable substituents R^1 and R^2 . The modulator approach, introduced by Kitagawa and co-workers,^[12] is an essential prerequisite for the synthesis of the PIZOFs. Recently, we have published that with such a modulator approach, the crystal size and the morphology of the Zr MOFs UiO-66, UiO-67, and UiO-68-NH₂ can be controlled.^[10] Additionally, the syntheses of these MOFs became highly reproducible.

Results and Discussion

The PIZOFs were obtained from $ZrCl_4$ and diacids $HO_2C[PE-P(R^1,R^2)-EP]CO_2H$ **1b-8b** (Scheme 1) in DMF in the presence of benzoic acid as the modulating agent.^[10,12] PIZOF-1, PIZOF-2, and PIZOF-8 were obtained as single crystals with octahedral shape; PIZOF-3 to -7 were obtained as powders. The framework structure was determined from single crystals. PIZOF-2 serves as the example here.



a,b	R^1	R^2	R^3	yield (%) of a	yield (%) of b
1	H	NH ₂	Et	37	92
2	OMe	OMe	Et	96	92
3	OMe	OCH ₂ CCH	Et	75	79
4	OMe	OCH ₂ CCTIPS	Et	87	77
5	OPent	OPent	Et	78	73
6	dodec	dodec	Et	83	89
7	O(CH ₂ CH ₂ O) ₂ Me	O(CH ₂ CH ₂ O) ₂ Me	Et	80	86
8	OMe	O(CH ₂) ₃ - 	Me	96	96

Scheme 1. Syntheses of the rodlike dicarboxylic acids $HO_2C[PE-P(R^1,R^2)-EP]CO_2H$ **1b-8b** from the diesters $AlkO_2C[PE-P(R^1,R^2)-EP]CO_2Alk$ **1a-8a**. The diesters were obtained through Pd/Cu-catalyzed C-C cross coupling. The different substituents R^1 and R^2 are introduced with the 1,4-dihalobenzene.

PIZOF-2 crystallizes in space group $Fd\bar{3}m$ with $a = 39.81 \text{ \AA}$. The structure and connectivity of the SBUs are the same as in UiO MOFs.^[9] However, the PIZOFs show two independent interpenetrating networks, whereas the UiO MOFs are not interpenetrated. The SBUs consist of six Zr^{4+} ions with square-antiprismatic coordination by eight oxygen atoms in the form of μ^3-O , μ^3-OH , and carboxylate groups. Each SBU is connected to twelve other SBUs by dicarboxylates (Figure 1b), thereby resulting in an expanded cubic close packing of SBUs with four octahedral and eight tetrahedral voids (Figure 1c). Four of the latter are occupied by the SBUs of a second, structurally identical framework that interpenetrates the first one (Figure 1d). The arrangement of the SBUs of the two frameworks resembles the positions of Zn and S in zincblende. Since the linkers are bent,^[13] there are convex (Figure 1e) and concave tetrahedral cavities (Figure 1f) of substantially different free internal diameters of 19 and 14 Å (excluding van der Waals radii). The convex tetrahedral voids are free of SBUs; the concave ones contain the SBUs of the second framework (Figure 1g). The twelve linkers of these SBUs penetrate the four trigonal windows in groups of three, thereby extending into octahedral cavities. Because each octahedral cavity shares its eight trigonal faces with eight tetrahedral cavities, four of which contain SBUs, each octahedral cavity is penetrated by six linkers that form an additional SBU-free concave tetrahedral cavity (Figure 1g). To the best of our knowledge, this is the first description of an interpenetrated framework with a twelfold connected SBU. Interpenetration is possible due to the length of the linkers, which form triangular windows of sufficient size to let three other linkers pass.

Based on the single-crystal data, the powder X-ray diffraction (PXRD) pattern of PIZOF-2 was simulated. The excellent agreement of simulated and experimental PXRD patterns (Figure S1 in the Supporting Information) together with the close similarity of the PXRDs of PIZOF-1 to -8 (Figure 2) indicates a common framework structure even though substituents R vary significantly; they range from simple alkyl, alkoxy, and oligo(ethyleneglycol) chains of different lengths to the chemically addressable groups amino, alkyne, and furan. Expectedly, all PIZOFs with their common structure have similar cell dimensions (Table S1 in the Supporting Information).

For further characterization, PIZOF-2 also serves as an example. Thermogravimetry of PIZOF-2 in flowing air reveals two distinct steps (Figure 3a; data of other PIZOFs can be found in Table S2). The residue is monoclinic ZrO_2 . We assume that guests are released up to a temperature of 300 °C. The mass loss above 380 °C is ascribed to oxidation of the linkers. PXRD patterns reveal that the framework is stable up to 325 °C in air and that only minor structural changes occur up to this temperature (Figure 3b). PIZOF-2 decomposes upon heating to 350 °C in air.

Despite interpenetration, the framework of PIZOF-2 appears to be accessible for guests. Only one half of the tetrahedral cavities of one framework is occupied with the SBUs of the other, interpenetrating framework. The other half,

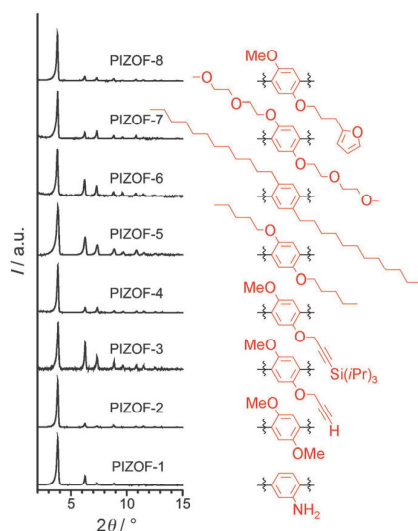


Figure 2. PXRD patterns of PIZOF-1 to PIZOF-8. The structure of the central benzene ring of the corresponding dicarboxylic acid is depicted on the right.

the convex ones (Figure 1e), is free of SBUs. As described above, the octahedral voids of one framework obtain the shape of tetrahedral voids by passage of linkers from the other framework. All voids thus have a similar shape that is described by the yellow spheres in Figure 1c,e,g and Figure 4. As can be seen in Figure 4, these yellow spheres overlap. Therefore, they form a continuous three-dimensional pore system with a topology related to the diamond structure (Figure 4). Each accessible void is surrounded by four other voids in a tetrahedral manner (Figure 4b).

Argon sorption experiments proved the porosity of PIZOF-2. The sorption isotherm (Figure 3c) shows a continuous adsorption up to a pressure of around $p/p_0 = 0.06$ and a steep increase at this pressure. The sharp increase corresponds to the filling of the tetrahedral voids as proven by fitting the curve using nonlinear density functional theory. It corresponds to the presence of pores with a diameter of around 20 Å, which is in very good agreement with the value of 19 Å derived from the crystal structure. The adsorption at low pressure is assigned to the filling of smaller cavities between the SBUs and the linkers and between the linkers of the two networks. PIZOF-2 has a Brunauer–Emmett–Teller (BET) surface area of $1250 \text{ m}^2 \text{ g}^{-1}$ and a total pore volume of $0.68 \text{ cm}^3 \text{ g}^{-1}$.

PIZOFs constitute a family of MOFs with a surprisingly high tolerance in their formation towards changes of the substituents at the linkers. This is probably caused by the strong Zr–O bond, the large driving force for the formation of the SBUs, and the high connectivity of the SBUs. The persistence of the framework structure together with a linker synthesis (Scheme 1) that is modular and itself highly compatible with a large variety of substituents R^1, R^2 allows for deliberate choice of functional groups. The synthesis of the linkers $\text{HO}_2\text{C}[\text{PE-P}(R^1, R^2)\text{-EP}]\text{CO}_2\text{H}$ (**1b–8b**) makes

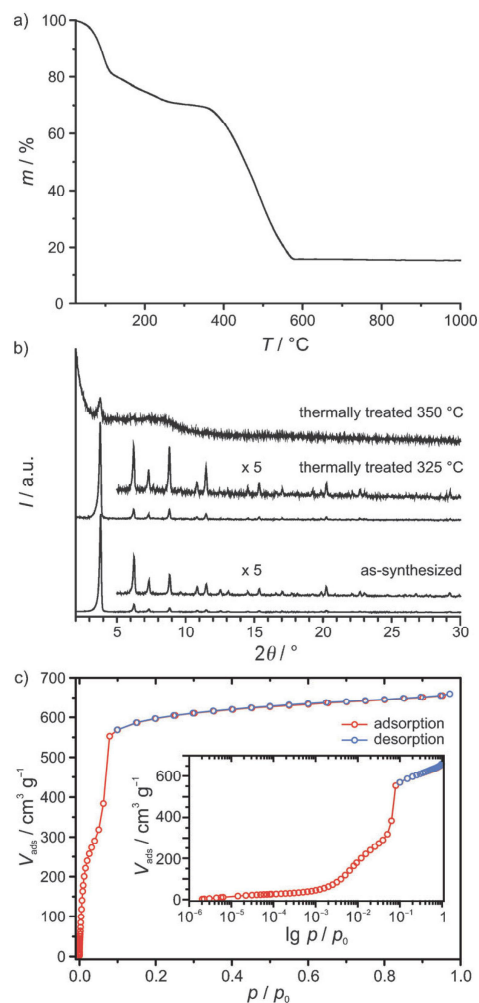


Figure 3. a) Thermogravimetric measurement of PIZOF-2 in flowing air. b) PXRD patterns of as-synthesized PIZOF-2 after being heated to 325 and 350 °C in air for 1 h (from bottom to top). c) Argon-gas sorption isotherms for PIZOF-2 (heated to 300 °C in air prior to sorption experiment) at 87 K as linear scale plot; inset: logarithmic scale plot. Red symbols: adsorption, blue symbols: desorption.

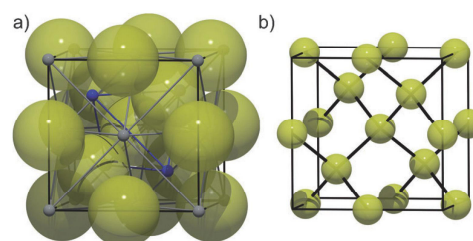


Figure 4. a) Topological representation of the PIZOF structure with yellow spheres representing accessible pore spaces of convex tetrahedral shape as depicted in Figure 1e. b) Connecting the centers of the yellow spheres reveals the relation of the three-dimensional pore system to the topology of cubic diamond.

use of Pd/Cu-catalyzed C–C cross coupling, a reaction that very often gives high yields and is compatible with a variety of functional groups. The coupling partners are 2,5-disubstituted 1,4-dihalobenzenes and alkyl 4-ethynylbenzoate. The resulting diesters **1a–8a** were saponified to obtain the diacids **1b–8b** (Scheme 1). The variation of the substituents R¹ and R² was achieved through use of different 2,5-disubstituted 1,4-dihalobenzenes. The same route has been described for the preparation of diacid HO₂C[PE-P(crown ether)-EP]CO₂H.^[14] The ester as an intermediate makes purification—that is, the removal of metals, metal salts, catalyst ligands, and 1,4-di[(4-alkyloxycarbonyl)phenyl]butadiyne, the product that results from oxidative dimerization (Glaser coupling) of alkyl 4-ethynylbenzoate—easy. This procedure is much shorter than our previously reported synthesis that starts from alkyl 4-iodobenzoate and 2,5-disubstituted 1-ethynyl-4-(2-triisopropylsilylethynyl)benzene.^[15] Furthermore, the second alternative, the coupling of 2,5-disubstituted 1,4-diethynylbenzene with alkyl 4-iodobenzoate,^[14] appears much less attractive to us for several reasons: 1) more consecutive steps, therefore less efficient synthesis, 2) a larger number of consecutive steps with the moiety that is varied to tune the interior of the PIZOFs, and 3) variation of the substituents of 1,4-diethynylbenzene results in different Glaser coupling products during coupling with alkyl 4-iodobenzoate. Therefore, individual protocols for their removal would have to be devised and separation may not always be possible.^[15] Additionally, 1,4-diethynylbenzenes tend to be instable, whereas alkyl 4-ethynylbenzoate can be stored for months.

Conclusion

In conclusion, the use of diacids HO₂C[PE-P(R¹,R²)-EP]CO₂H **1b–8b** as linkers led to PIZOF-1 to PIZOF-8, a new family of Zr MOFs with the characteristics of very long linkers, stability towards atmospheric moisture, high heat resistance, large voids, and a broad variability of substituents at the linkers, including functional groups ready for postsynthetic modification. Thus, PIZOFs with different chemical functionalities and environments within the pores can be obtained in a straightforward manner.

Experimental Section

Synthesis of linkers 1b–8b: For a detailed description of the syntheses, please refer to the Supporting Information.

Synthesis of PIZOF-*n*: The syntheses of the PIZOFs were performed in 100 mL Teflon-capped glass flasks. For a typical synthesis, ZrCl₄ (0.080 g, 0.343 mmol) and benzoic acid (1.256 g, 10.287 mmol) were dissolved in DMF (20 mL) by using ultrasound to give a clear solution. One of the diacids HO₂C[PE-P(R¹,R²)-EP]CO₂H **1b–8b** (0.343 mmol) was added and dissolved by the application of ultrasound. The tightly capped flask was kept in an oven at 120 °C under static conditions for 24 h. The suspension was cooled to room temperature and the precipitate was isolated by centrifugation. The solid was suspended in DMF (10 mL). After standing at

room temperature for 1–4 h, the suspension was centrifuged and the solvent was decanted off. The obtained particles were washed with ethanol (10 mL) in the same way as described for DMF. Finally, the solid was dried under reduced pressure.

Characterization: Powder X-ray diffraction was carried out using a Stoe Stadi P diffractometer operated with Ge(111)-monochromatized Cu_{Kα1} radiation (λ = 1.54060 Å) in transmission mode. TGA measurements were performed using a Netzsch STA 429 thermoanalyzer. For this purpose, the samples were filled into alumina crucibles and heated under a flow of air at a heating rate of 5 °C min⁻¹ up to 1000 °C. Argon sorption isotherms were measured at 87 K using a Quantachrome Autosorb-1 instrument. Initially, the sample was heated to 300 °C in air for 1 h to remove all guests. The sample was further outgassed in vacuum at 150 °C for 24 h directly before the measurement to remove gases taken up from the atmosphere during storage under ambient conditions. The pore-size distribution was determined using the calculation model Ar at 87 K zeolites/silica (cylinder pores, non-local DFT (adsorption branch model)) of the ASiWin software for Autosorb-1 instruments (version 2.11) from Quantachrome.

Single-crystal X-ray diffraction studies for PIZOF-1, PIZOF-2, and PIZOF-8 were carried out using a Bruker KAPPA APEX II CCD diffractometer equipped with a graphite crystal monochromator situated in the incident beam for data collection at 173 K for PIZOF-1, at 123 K for PIZOF-2, and at 103 K for PIZOF-8. The determination of unit-cell parameters and data collections were performed with Cu_{Kα} radiation (λ = 1.54178 Å). The program SAINT was used for integration of the diffraction profiles. Adsorption corrections were applied using the SADABS routine. The structures were solved by direct methods and refined by full-matrix least-squares on F² with anisotropic displacement using the SHELXTL software package.^[16] The hydrogen atoms were added theoretically, riding on the concerned atoms. Free solvent molecules were highly disordered and attempts to locate and refine solvent molecules were unsuccessful. The diffuse electron densities that resulted from these solvent molecules were removed from the data set using the SQUEEZE routine of PLATON^[17] and refined further using the data generated.

Crystal data for PIZOF-1: C₇₂H₂₄O₁₆Zr₃, M_r = 1418.57; space group *Fd3m*, cubic; *a* = 39.845(12) Å; *V* = 63257(34) Å³; *T* = 173 K; *Z* = 16; μ(Cu_{Kα}) = 1.828 mm⁻¹; 40440 reflections measured, 2642 independent reflections (*R*_{int} = 0.1601); *R*₁ (*I* > 2σ(*I*)) = 0.0485, *wR*₂ = 0.1078; GOF = 0.960.

Crystal data for PIZOF-2: C₇₈H₂₄O₂₂Zr₃, M_r = 1586.63; space group *Fd3m*, cubic; *a* = 39.8144(11) Å; *V* = 62113(3) Å³; *T* = 123 K; *Z* = 16; μ(Cu_{Kα}) = 1.892 mm⁻¹; 71558 reflections measured, 2545 independent reflections (*R*_{int} = 0.0769); *R*₁ (*I* > 2σ(*I*)) = 0.0488, *wR*₂ = 0.1056; GOF = 1.084.

Crystal data for PIZOF-8: C₇₂H₂₄O₂₂Zr₃, M_r = 1514.57; space group *Fd3m*, cubic; *a* = 39.8015(8) Å; *V* = 63052(2) Å³; *T* = 103 K; *Z* = 16; μ(Cu_{Kα}) = 1.880 mm⁻¹; 38000 reflections measured, 2613 independent reflections (*R*_{int} = 0.0854); *R*₁ (*I* > 2σ(*I*)) = 0.0936, *wR*₂ = 0.2468; GOF = 1.046.

CCDC-803459 (PIZOF-1), 803460 (PIZOF-2), and 803461 (PIZOF-8) contain the supplementary crystallographic data for this paper. These data can be obtained free of charge from The Cambridge Crystallographic Data Centre via www.ccdc.cam.ac.uk/data_request/cif.

Acknowledgements

This work was supported as a part of the priority program 1362 (Porous Metal–Organic Frameworks) by the Deutsche Forschungsgemeinschaft. We thank Ms. Hülsmann, Ms. Senger, Mr. Heinrich, and Ms. Brosent for their contributions to the linker syntheses and Mr. Lippke for his contribution to the syntheses of the PIZOFs.

[1] a) M. Tonigold, Y. Lu, B. Bredenkötter, B. Rieger, S. Bahn Müller, J. Hitzbleck, G. Langstein, D. Volkmer, *Angew. Chem.* **2009**, *121*,

- 7682–7687; *Angew. Chem. Int. Ed.* **2009**, *48*, 7546–7550; b) K. P. Lillerud, U. Olsbye, M. Tilset, *Top. Catal.* **2010**, *53*, 859–868.
- [2] J. L. C. Rowsell, O. M. Yaghi, *J. Am. Chem. Soc.* **2006**, *128*, 1304–1315.
- [3] a) B. Chen, C. Liang, J. Yang, D. S. Contreras, Y. L. Clancy, E. B. Lobkovsky, O. M. Yaghi, S. Dai, *Angew. Chem.* **2006**, *118*, 1418–1421; *Angew. Chem. Int. Ed.* **2006**, *45*, 1390–1393; b) R. Ahmad, A. G. Wong-Foy, A. J. Matzger, *Langmuir* **2009**, *25*, 11977–11979.
- [4] C. Combelles, M. B. Yahia, L. Pedesseau, M. Doublet, *J. Phys. Chem. C* **2010**, *114*, 9518–9527.
- [5] a) P. Horcajada, T. Chalati, C. Serre, B. Gillet, C. Sebrie, T. Baati, J. F. Eubank, D. Heurtaux, P. Clayette, C. Kreuz, J. Chang, Y. K. Hwang, V. Marsaud, P. Bories, L. Cynober, S. Gil, G. Férey, P. Couvreur, R. Gref, *Nat. Mater.* **2010**, *9*, 172–178; b) N. J. Hinks, A. C. McKinlay, B. Xiao, P. S. Wheatley, R. E. Morris, *Microporous Mesoporous Mater.* **2010**, *129*, 330–334; c) S. R. Miller, D. Heurtaux, T. Baati, P. Horcajada, J. Grenèche, C. Serre, *Chem. Commun.* **2010**, *46*, 4526–4528.
- [6] a) A. Schaate, M. Schulte, M. Wiebcke, A. Godt, P. Behrens, *Inorg. Chim. Acta* **2009**, *362*, 3600–3606; b) Q. Li, W. Zhang, O. S. Miljanić, C. Sue, Y. Zhao, L. Liu, C. B. Knobler, J. F. Stoddart, O. M. Yaghi, *Science* **2009**, *325*, 855–859.
- [7] a) S. S. Kaye, A. Dailly, O. M. Yaghi, J. R. Long, *J. Am. Chem. Soc.* **2007**, *129*, 14176–14177; b) P. L. Feng, J. J. Perry IV, S. Nikodemski, B. W. Jacobs, S. T. Meek, M. D. Allendorf, *J. Am. Chem. Soc.* **2010**, *132*, 15487–15489.
- [8] a) C. A. Bauer, T. V. Timofeeva, T. B. Settersten, B. D. Patterson, V. H. Liu, B. A. Simmons, M. D. Allendorf, *J. Am. Chem. Soc.* **2007**, *129*, 7136–7144; b) Y.-S. Bae, D. Dubbeldam, A. Nelson, K. S. Walton, J. T. Hupp, R. Q. Snurr, *Chem. Mater.* **2009**, *21*, 4768–4777.
- [9] a) J. H. Cavka, S. Jakobsen, U. Olsbye, N. Guillou, C. Lamberti, S. Bordiga, K. P. Lillerud, *J. Am. Chem. Soc.* **2008**, *130*, 13850–13851; b) L. Valenzano, B. Civalieri, S. Chavan, S. Bordiga, M. H. Nilsen, S. Jakobsen, K. P. Lillerud, C. Lamberti, *Chem. Mater.* **2011**, *23*, 1700–1718.
- [10] A. Schaate, P. Roy, A. Godt, J. Lippke, F. Waltz, P. Behrens, *Chem. Eur. J.* **2011**, *17*, 6643–6651.
- [11] a) S. J. Garibay, S. M. Cohen, *Chem. Commun.* **2010**, *46*, 7700–7702; b) M. Kandiah, S. Usseglio, S. Svelle, U. Olsbye, K. P. Lillerud, M. Tilset, *J. Mater. Chem.* **2010**, *20*, 9848–9851.
- [12] a) T. Tsuruoka, S. Furukawa, Y. Takashima, K. Yoshida, S. Isoda, S. Kitagawa, *Angew. Chem.* **2009**, *121*, 4833–4837; *Angew. Chem. Int. Ed.* **2009**, *48*, 4739–4743; b) S. Diring, S. Furukawa, Y. Takashima, T. Tsuruoka, S. Kitagawa, *Chem. Mater.* **2010**, *22*, 4531–4538.
- [13] Oligo(*para*-phenyleneethynylene)s possess substantial backbone bendability: a) A. Godt, M. Schulte, H. Zimmermann, G. Jeschke, *Angew. Chem.* **2006**, *118*, 7722–7726; *Angew. Chem. Int. Ed.* **2006**, *45*, 7560–7564; b) G. Jeschke, M. Sajid, M. Schulte, N. Ramezani, A. Volkov, H. Zimmermann, A. Godt, *J. Am. Chem. Soc.* **2010**, *132*, 10107–10117.
- [14] Y.-L. Zhao, L. Liu, W. Zhang, C.-H. Sue, Q. Li, O. Š. Miljanić, O. M. Yaghi, J. F. Stoddart, *Chem. Eur. J.* **2009**, *15*, 13356–13380.
- [15] V. Hensel, A. Godt, R. Popovitz-Biro, H. Cohen, T. R. Jensen, K. Kjaer, I. Weissbuch, E. Lifshitz, M. Lahav, *Chem. Eur. J.* **2002**, *8*, 1413–1423.
- [16] ShelXTL, Version 5.1, G. M. Sheldrick, Program for Solution and Refinement of Crystal Structures, University of Göttingen (Germany), **1997**.
- [17] A. L. Spek, *J. Appl. Crystallogr.* **2003**, *36*, 7–13.

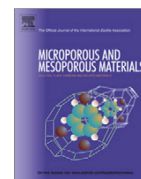
Received: April 3, 2011
Published online: July 27, 2011

6 Modulated Synthesis of Zr-fumarate MOF

Preface

This work has been published as a full paper in "Microporous and Mesoporous Materials". It focuses on the effect of modulators on the synthesis of a novel Zr-fumarate MOF. The compound consists in principle of non-toxic zirconia and the naturally occurring fumaric acid; as modulator, formic acid was chosen. These circumstances may make this compound interesting for biological applications.

The author of this thesis has been involved in generating the concept of this research work. The author initially investigated the powder obtained with PXRD and indexed the reflections in a cubic symmetry which is different to the UiO-MOFs known at that time. Gesa Wißmann carried out all following syntheses, examining the influences of different concentrations of the modulator formic acid. She characterized the products by PXRD and DLS, carried out the stability tests in different media, and purified the Zr-fum MOF via Soxhlet extraction. Thermogravimetric analyses were carried out by the author of this thesis. Georg Platz measured and evaluated the sorption isotherms and Imke Bremer took the SEM images presented in this paper. The structural modeling of Zr-fum MOF were performed by Sebastian Lilienthal under the guidance of Dr. Andreas M. Schneider.



Modulated synthesis of Zr-fumarate MOF

Gesa Wißmann¹, Andreas Schaate¹, Sebastian Lilienthal¹, Imke Bremer¹, Andreas M. Schneider¹, Peter Behrens^{*,1}

Leibniz Universität Hannover, Institut für Anorganische Chemie, Callinstr. 9, 30167 Hannover, Germany

ARTICLE INFO

Article history:

Received 8 April 2011

Received in revised form 2 December 2011

Accepted 5 December 2011

Available online 11 December 2011

Keywords:

Metal–organic frameworks

Microporous materials

Modulator approach

Zr compounds

Zr-fumarate

ABSTRACT

We present the synthesis and characterization of a novel Zr-based metal–organic framework (MOF) which contains fumarate (*fum*) dianions as linkers: OOC-CH=CH-COO^- . The synthesis of this MOF is possible only via modulation, i.e. by the addition of a monocarboxylic acid to the synthesis mixture. We have used formic acid as a modulator and have investigated its influence on the synthesis of the Zr-fumarate MOF in detail. The modulator improves the crystallinity of the material; varying its amounts, the crystal size and the degree of aggregation can be influenced. The novel MOF probably has a topology which is similar to that of UiO-66, but has a primitive cubic lattice instead of a face-centered one. A structural model in line with the experimental data is proposed. The Zr-*fum* MOF is further characterized by thermogravimetric analysis (TGA) and Ar sorption, showing that it can be activated and exhibits microporosity. The linker fumarate as well as the modulator formic acid used in the synthesis of Zr-*fum* MOF are both naturally occurring molecules; possible applications of the MOF may thus lie in the field of biomaterials. Therefore, the stability of Zr-*fum* MOF was tested in water-based salt solutions commonly used in biomedical research.

© 2011 Elsevier Inc. All rights reserved.

1. Introduction

Metal–organic frameworks (MOFs) or porous coordination polymers have emerged as a new class of crystalline porous materials [1]. These compounds are constructed from metal ions or metal ion clusters and bridging organic linkers and often have very high surface areas [2,3]. The pore size can be engineered via the length of the linkers [4,5] and the chemistry of the pore interior can be designed by the functionalities these linkers carry [6]. Potential applications of porous MOFs cover a broad range from adsorption and catalysis to biomaterials [7–10]. A major disadvantage of many MOFs is their limited stability with regard to water, oxygen, other chemicals and temperature. For example, some Zn^{2+} -based MOFs, including the archetype MOF-5, are prone to hydrolysis when stored in air at ambient temperature [11–16].

More stable MOFs have been described with the Zr^{4+} cation [17]. The first members of this class consisted of the series UiO-66 (with terephthalate as linker) [17,18], UiO-67 (with biphenyl dicarboxylate) and UiO-68 (with terphenyl dicarboxylate) [17]. These compounds are isostructural and feature an arrangement of secondary building units (SBUs) which is topologically equivalent to a cubic close-packing. Correspondingly, the SBUs are twelvefold connected with each other by the dicarboxylic acids.

An SBU itself is constructed of six zirconium cations forming an octahedron. Each Zr ion is coordinated in a square–antiprismatic geometry by bridging $\mu_3\text{-O}$, $\mu_3\text{-OH}$ and carboxylate groups. Such Zr-oxo-hydroxo clusters, saturated by monocarboxylate ligands in their periphery, had been described before as isolated molecules [19,20]. In fact, Guillerme et al. used the methacrylate-terminated cluster $\text{Zr}_6\text{O}_4(\text{OH})_4(\text{maa})_{12}$ (maa : $\text{CH}_2=\text{CH}(\text{CH}_3)\text{COO}^-$) as a reagent for the synthesis of UiO-66 and an isostructural MOF possessing the muconic acid dianion as linker [21]. Recently, we have described a novel family of Zr-based MOFs containing very long linkers [22]. The structure of this family corresponds to a twofold interpenetrated version of the UiO-type topology. This can be understood with respect to the very long linkers used in their construction. In spite of the interpenetration, these compounds possess high surface areas and large pore volumes, and have therefore been named “porous interpenetrated Zr-organic frameworks” (PIZOFs) [22].

UiO-66 and the PIZOFs are highly temperature resistant and can be handled at atmospheric moisture [17,18]. The enhanced stability of Zr-based MOFs can be traced back to strong Zr–O bonds within the characteristic SBU which is present in all the described Zr-MOFs and to the high degree of interlinking of these SBUs. Further research in this class of MOFs thus appears worthwhile, and reports on the utility of some Zr-MOFs with the UiO-66 topology have recently appeared [23–26].

We have experienced difficulties in the synthesis of some of these MOFs. However, the modulation approach, originally

* Corresponding author. Tel.: +49 511 762 3660; fax: +49 511 762 3006.

E-mail address: Peter.Behrens@acb.uni-hannover.de (P. Behrens).

¹ ZFM, Center for Solid-State Chemistry and New Materials.

introduced by the group of Kitagawa [27,28], helped us tremendously. This approach consists in the addition of monovalent modulator molecules, in this case monocarboxylic acids, to the reaction mixture. It enhances the reproducibility of the synthesis procedures, allows to increase the crystallinity of the product and in certain cases to control the crystal size and morphology as well as the degree of agglomeration/aggregation of the crystals [27–29]. In case of the synthesis of UiO-66, we were able to vary the size of individual nanocrystals by the addition of benzoic acid as a modulator [29]. In the case of UiO-67, we were not able to reproduce the original synthesis procedure [17]; with the addition of a modulator, the synthesis proved to be highly reproducible and individual micrometer-sized crystals were obtained [29]. Whereas we have never been able to synthesize UiO-68 due to the persistent insolubility of terphenylene dicarboxylic acid in common solvents, we were able to produce an analogous compound, UiO-68-NH₂, with an amino-substituted terphenylene dicarboxylic acid as linker. In fact, in this case the modulator approach even led to the first single crystals of a Zr-based MOF [29]. All members of the PIZOF family could only be obtained using the modulation approach [22]. It is also worth noting that in the low-temperature synthesis of the Zr-muconic acid MOF, where the Zr₆O₄(OH)₄(*maa*)₁₂ complex was used as a precursor, the methacrylic acid anions of the starting complex can act as modulators [21].

It is assumed that the molecules of the modulating agent strongly influence crystal nucleation and growth by competing with the linker molecules for the coordination sites at the Zr atoms or Zr clusters, which become the SBUs of the framework [27–29]. However, there have only been few systematic studies on the application of the modulator approach. Here, we present such a study on a Zr-based MOF with fumarate dianions as linkers. Fumaric acid (*trans*-butene-1,4-dicarboxylic acid; HO₂C–CH=CH–CO₂H; H₂-*fum*) is an unbranched unsaturated dicarboxylic acid. This linker was chosen for its simple constitution and due to the fact that it is a biologically occurring molecule and used as a food additive (E297) so that MOFs constructed from it might find applications in medicine [10,30]. As a modulating agent we used the – also naturally occurring – formic acid, the simplest monocarboxylic acid. Steric effects of the modulating agent, which is presumed to coordinate to Zr atoms or Zr-based clusters during the synthesis reaction, are thus minimized.

2. Experimental

2.1. Zr-fumarate MOF

All chemicals were obtained commercially (Sigma Aldrich) and used without further purification.

The standard synthesis of the Zr-*fum* MOF was performed by dissolving ZrCl₄ (0.517 mmol, 1 eq) and fumaric acid (1.550 mmol, 3 eq) in 20 mL *N,N*-dimethylformamide (DMF) in a 100 mL glass flask at room temperature. To investigate the influence of the modulator, 0–100 eq of formic acid were added. The glass flasks were Teflon-capped and heated in an oven at 120 °C for 24 h. Furthermore, the influence of the modulator concentration on the yield at different reaction times was examined for 5 and 30 eq of modulator by sampling the reaction after 2, 4, 8, 24, and 48 h. After cooling, the white precipitate was washed with 10 mL DMF and 10 mL ethanol, respectively. The washing process was carried out by centrifugation and redispersion of the white powder, which was then dried at room temperature over night.

Further purification of the samples was carried out by Soxhlet extraction in ethanol for 24 h and drying over night at room temperature. Activation before porosity, powder X-ray diffraction and

thermal analysis was performed by heating the sample at 120 °C in vacuum for at least 8 h.

2.2. Characterization

Powder X-ray diffraction (PXRD) patterns were measured using a Stoe StadiP diffractometer operated with Ge(1 1 1)-monochromatized CuK α ₁ radiation with a wavelength of $\lambda = 1.54060$ Å in transmission. The reflections observed were indexed by using the Werner Algorithm implemented in the WinXPow software [31] and were refined by least squares method. The particle size was calculated by applying Scherrer's equation to the first reflection at $8.5^\circ 2\theta$. To determine the reflection broadening caused by the measurement equipment, a silicon standard was measured under the same experimental conditions.

Dynamic light scattering (DLS) measurements were performed on a Zetasizer Nano ZS from Malvern Instruments. The solid materials were redispersed in ethanol by sonification with a Sonorex Digitec ultrasonic bath with 640 W for 5 min. Afterward the suspensions were transferred to a polystyrene cuvette.

Scanning electron microscope (SEM) images were taken on a JEOL JESM-6700F field emission SEM with a semi in-lens detector using a working distance of 3 mm and an acceleration voltage of 2 kV. For the sample preparation the solid material was dispersed in ethanol and dropped onto a polished carbon block which was then dried under reduced pressure.

Thermogravimetric analysis (TGA) measurements were carried out using a Netzsch STA 429 thermoanalyser. The samples were heated with a rate of 5 °C/min in alumina crucibles. Air was used as a flushing gas and the measurements were terminated at 1000 °C.

Ar sorption isotherms were measured on a Quantachrome Autosorb-1 instrument. The samples were outgassed in vacuum at 120 °C for 74 h prior to the sorption measurement. The pore size distribution was calculated using non-linear density-functional theory (NLDFT) fitting of the Quantachrome Kernel "Ar at 87 K_zeolites/silica" to the experimental data.

For solution ¹H NMR spectroscopy, the Zr-*fum* was digested in DMSO-d₆ through the addition of CsF and a drop of aqueous DCl (35 wt%). Then K₂CO₃ was added [32].

2.3. Structural simulations

Simulations of the structure of the Zr-*fum* MOF were performed within Accelrys' modeling environment 'Materials Studio 5.0' [33]. For the simulations, we chose the Universal forcefield [34]. In order to find low energy conformations, a quenched dynamics simulation was performed in the *NpT* ensemble (constant number of particles, pressure and temperature). All simulations were carried out in space group *P1*. The temperature of $T = 900$ K was controlled by scaling the velocities to hold the temperature in the desired region ($\Delta T = \pm 10$ K). The dynamics runs lasted 25 ps with a time step of 0.1 fs. Structures were saved and energy-minimized after every 250th step using the Smart algorithm implemented in the Forcite Module of Materials Studio. The algorithm employs a cascade of minimization algorithms starting with the robust steepest descent [35] method, after which an Adjusted Basis Set Newton-Raphson (ABNR) [36] minimization follows. The last step is the Quasi-Newton method in the Broyden-Fletcher-Goldfarb-Shanno (BFGS) variant [37]. The simulations were performed on a workstation system (AMD Athlon 64 X2 Dual Core 4800+, 2 × 2.4 GHz, 2 GB RAM). The simulated powder diffraction patterns were calculated using Powder Cell for Windows Version 2.4.

3. Results and discussion

3.1. Modulated synthesis of Zr-fumarate MOF

In the following, we state the amount of modulator added to a synthesis batch in relation to the amount of $ZrCl_4$ used and give this value as equivalents (eq). For example, in a synthesis designated as “5 eq”, the molar ratio between the modulating agent formic acid and $ZrCl_4$ is 5:1. In the investigations presented here, the amount of formic acid was varied between 0 and 100 eq.

In Fig. 1, the PXRD patterns of the products of these syntheses are shown. Without the addition of a modulator (0 eq), an amorphous phase is obtained under the reaction conditions used here. Already with the addition of only 0.5 eq of the modulator, two broadened reflections can be discerned on the amorphous background. The product prepared with 1 eq of formic acid already shows the full set of reflections of a crystalline phase, although amorphous material is still present. When more than 5 eq of the modulator were present during the synthesis, a fully crystalline material was obtained as judged from the PXRD pattern. The characterization of this novel compound, the Zr-fumarate MOF (Zr-*fum* MOF), will further be described in Section 3.2.

The PXRD patterns in Fig. 1 reveal further changes due to the influence of the modulating agent. When smaller amounts of formic acids are used, the reflections are broadened. From Scherrer's equation, crystallite sizes can be calculated and are given in Table 1. In those cases where this method can be reasonably applied, the crystallite size increases with the amount of modulator present during the synthesis.

The samples were further investigated by SEM in order to ascertain the particle size and morphology as well as the state of agglomeration. Fig. 2 shows a selection of characteristic images, Table 1 summarizes characteristic findings (size ranges of particles and particle aggregates, morphological characteristics). Products obtained at small modulator concentrations (from 0 to 10 eq) show strongly intergrown small crystallites. No specific shape of the individual crystals can be discerned. When more than 30 eq of

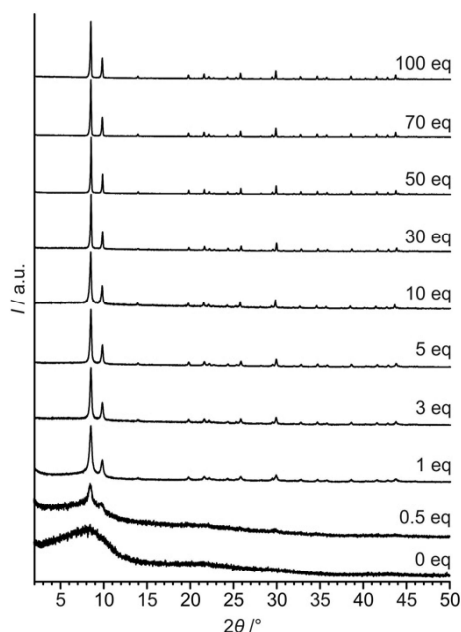


Fig. 1. PXRD patterns of the products of syntheses of Zr-*fum* MOFs performed in the presence of different equivalents (with respect to $ZrCl_4$) of formic acid as modulator.

modulator were used, the crystals attain an octahedral shape. The degree of agglomeration decreases on increasing the amount of formic acid from 30 to 100 eq. At the highest modulator concentration investigated, individual crystals were obtained. For the samples prepared at 5 and 10 eq, the sizes of the particles are around the values determined by evaluating the X-ray line broadening, as far as can be recognized. For modulator concentrations higher than 30 eq, the crystal sizes are outside the range of the application of Scherrer's equation.

Below 10 eq of modulator the SEM images show strongly aggregated particles. This results in broad size distributions in the DLS measurements. Larger aggregates observed in the SEM images cannot be detected by DLS, because they cannot be stabilized in suspensions and sediment during the measurement. Correspondingly, only smaller aggregates are measured. Samples prepared with high modulator concentrations (30–100 eq) show comparable values with regard to the size determination from SEM images and by DLS. This good agreement can be explained by the low agglomeration of octahedral crystals which remain suspended in aqueous media. The size distribution is rather broad, the sizes are in the range of 150–200 nm.

According to these observations the application of formic acid as a modulator on the synthesis of Zr-*fum* MOF has several effects which have in part already been discussed in preceding publications of our group [22,29]. At low concentrations of modulator, its presence inhibits the formation of an amorphous precipitate (which we observe when the concentration of the modulator is too small) and slows down the growth rate, yielding more crystalline products. This can possibly be ascribed to the formation of intermediate complexes between formate ions and Zr cations. With increasing concentration of formic acid, the competition between deprotonated linker molecules and formate ions for the coordination of the Zr cations reduces the number of nuclei of the crystalline Zr-*fum* framework; fewer nuclei then grow to larger crystals. Furthermore, with increasing amount of modulator, the aggregation of the product particles is reduced and more and more isolated MOF particles are obtained. This effect is only observed at modulator amounts higher than 10 eq, i.e. when a large excess of modulator is deployed.

Similar effects had been observed in the synthesis of UiO-66 and UiO-67 when benzoic acid or acetic acid were used as modulators [29]. However, in those cases we observed that precipitation of the product took longer and longer times as the concentration of modulating agent was increased, a behavior which is in accord with a coordination modulation mechanism as described above. When formic acid is used as a modulator, the situation is different: The higher the amount of modulator, the earlier the formation of a white precipitate starts. XRD measurements showed that in all cases, even after a reaction time of only 2 h, a crystalline product was obtained. So, formic acid obviously accelerates the formation of the crystalline Zr-*fum* MOF and thus appears to play a special role as a modulator. A possible reason for this could be that formic acid is a direct product of the decomposition of the solvent DMF with water:



The presence of formic acid added as a modulator could displace this equilibrium to the left side so that more water is available in the reaction system. Water is essential for the hydrolysis of the Zr precursor and for the supply of oxygen atoms for the

Table 1

Characterization of the products of syntheses performed in the presence of different equivalents of formic acid (with respect to $ZrCl_4$) as modulator. Crystallite size d_{XRD} from X-ray diffraction line broadening, size range of agglomerates d_{SEM} and characterization of sample morphology from SEM images, hydrodynamic diameters d_{DLS} from dynamic light scattering measurements.

Eq of formic acid	d_{XRD} (nm)	d_{SEM} (nm)	Sample morphology	d_{DLS} (nm) ^a
0	– ^b	1600–6000	Strong agglomeration	360–740 (535)
0.5	– ^c	1000–4000	Strong agglomeration	410–860 (594)
1	39	1000–5000	Strong agglomeration	270–550 (386)
3	73	400–6000	Strong agglomeration, ill-defined crystal shape	170–480 (276)
5	86	700–6000	Strong agglomeration, ill-defined crystal shape	410–860 (627)
10	102	1000–4000	Strong agglomeration, ill-defined crystal shape	480–1150 (753)
30	– ^d	80–260	Medium agglomeration, indication of octahedral shape	130–310 (208)
50	– ^d	100–200	Weak agglomeration, octahedral shape with rounded edges	50–230 (166)
70	– ^d	80–280	Weak agglomeration, octahedral shape with rounded edges	100–200 (141)
100	– ^d	110–290	Individual octahedral	110–230 (156)

^a Data for particle sizes from DLS measurements (the maximum of the distribution by using the Gauss fit is given in parentheses).

^b Product is amorphous.

^c Due to high background, no reasonable value for the peak width can be determined.

^d Crystallite sizes were out of scope for determination by Scherrer's equation.

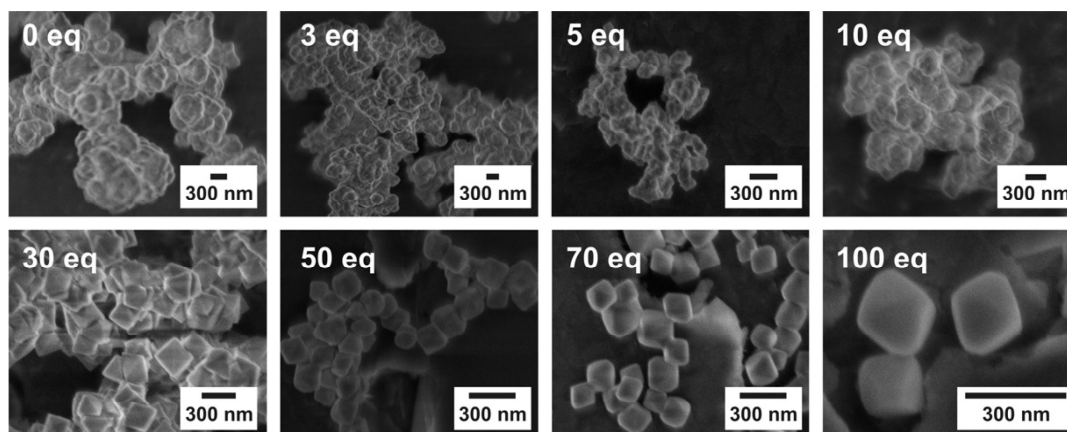


Fig. 2. SEM images of the products of *Zr-fum* MOF syntheses carried out in the presence of different amounts of modulator (from 0 to 100 eq, as given in the images).

formation of the $Zr_6O_4(OH)_4(O_2C)_{12}$ SBU. Thus, formic acid could indirectly enhance the formation of the SBU and thus accelerate the formation of the *Zr-fum* MOF.

3.2. Characterization of *Zr-fumarate* MOF

All products synthesized in the presence of more than 30 eq of formic acid gave similar diffraction patterns which correspond to a fully crystalline material. An example is shown for the product obtained in the presence of 30 eq in Fig. 3, in comparison to a diffraction pattern of UiO-66.

The pattern of the novel *Zr-fum* MOF resembles that of UiO-66, taking into account that the reflections of the former are shifted to larger diffraction angles corresponding to a smaller lattice constant. For the new material we determined a cubic lattice constant of 17.9090 Å (the indexing of the PXRD pattern of *Zr-fum* MOF is given in the Supplementary material as Table A1). The lattice constant of UiO-66 has been given as 20.755 Å [17]. As the fumarate linker is shorter than the terephthalate linker in UiO-66, the smaller lattice constant for the *Zr-fumarate* MOF can be easily rationalized. On this basis it can be assumed that the novel material has a framework topology which is generally similar to that of UiO-66, i.e. similar SBUs are arranged in a packing similar to a cubic close-packing and are twelvefold connected by the linkers. However, a close inspection of the indexed diffraction pattern shows that, although an indexing based on a cubic lattice is possible,

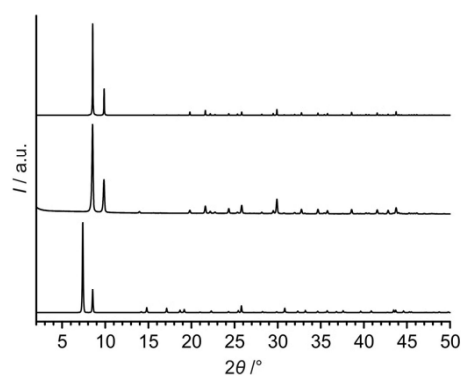


Fig. 3. Comparison of powder X-ray diffraction patterns. Top: simulated pattern based on the proposed structural model for the *Zr-fum* MOF (see text); middle: experimental pattern from a *Zr-fum* MOF synthesized with 30 eq of modulator; bottom: experimental pattern of UiO-66.

reflections are present in the PXRD of the *Zr-fum* MOF which break the face-centered symmetry of the *Fm-3m* space group of UiO-66. We ascribe this circumstance to the lower symmetry of the fumarate linker as compared to the terephthalate unit, as it is not strictly linear due to the *trans* configuration around the double bond (Fig. 4a). Any ordered distribution of the fumarate linkers

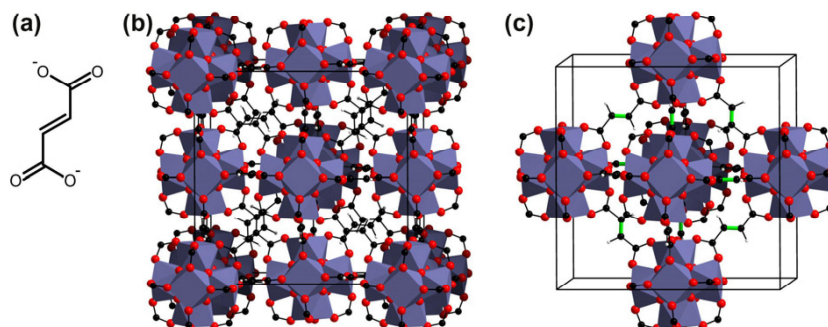


Fig. 4. (a) Structure of the non-linear linker fumarate; (b) and (c): structural model for the *Zr-fum* MOF as described in the text. In (b), the cubic unit cell is outlined. (c) Shows the central octahedron of a unit cell with the double bonds of the fumarate linkers depicted in green.

in the *Zr-fum* MOF should then lead to a lowering of the space group symmetry. Various models of a possible order of the orientation of the fumarate linkers were tested in order to derive a structure for the *Zr-fum* MOF. The best result was obtained by a symmetry reduction from space group *Fm-3m* (of UiO-66) to *P-3n*. This space group is in accordance with the indexing of the powder pattern. A PXRD pattern simulated on the basis of this model is compared to the experimentally obtained one in Fig. 3. There is a strong similarity between the two patterns so that we assume that the structural model as presented in Fig. 4b and c, which only contains the framework atoms, is correct (a list of the positional parameters for this structural model is given as Table A2 in the Supplementary material). In this model, the topology of the structure of UiO-66 is retained, i.e. $Zr_6O_4(OH)_4(O_2C)_{12}$ clusters are positioned at the corners and the faces of a cube and are interconnected to other SBUs by 12 linkers. However, due to the kinked geometry of the fumarate linkers, the Zr–O clusters are tilted into different directions; this destroys the face-centered symmetry present in UiO-66. Half of the SBUs (those at the corners and those in the front/back faces in Fig. 4b) are tilted in one direction, the other half (those at the left/right and bottom/top faces) in the other direction. When the structure of UiO-66 is seen as being related to the cubic close-packing of Cu metal, then the different tilting of the SBUs in the *Zr-fum* MOF leads to an analogy with the superstructure of the intermetallic phase CuAu.

The minor differences observed between the experimental PXRD pattern and the one simulated on the basis of this structural model can possibly be traced back to occluded guest molecules (see Supplementary material, Fig. A1). The low-resolution PXRD data do not allow for a full refinement of the structure including such guest species. We think that the structural model presented in Fig. 4b and c is basically correct, but as the focus of this publication lies on the modulated synthesis of the *Zr-fum* MOF, we refrain from further structural investigations.

The composition of the novel *Zr-fum* MOF material was investigated using thermogravimetric analysis (TGA, Fig. 5 and Table 2). The as-synthesized sample shows a nearly continuous mass loss up to 400 °C with no specific steps. This mass loss probably corresponds to the removal of all organic material, including the evaporation of guest molecules from the pores (like the solvents DMF and ethanol) and the combustion of the linker. A combined extraction-activation procedure was therefore applied to the material. The sample was Soxhlet-extracted for 24 h in ethanol, and after drying at room temperature, was heated to 140 °C for 8 h to remove the guest molecules. In fact, several investigations show that such a sample is essentially pure: IR spectra reveal, apart from the presence of carboxylate groups (symmetric and asymmetric stretching vibrations at $\nu_{\text{sym}}(\text{C-O})$: 1410 cm^{-1} and at $\nu_{\text{sym}}(\text{C-O})$: 1590 cm^{-1} , respectively), that a sample so treated does

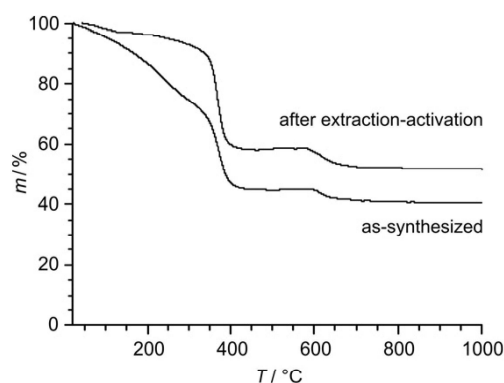


Fig. 5. Thermogravimetric analyses of *Zr-fum* MOFs (synthesized in the presence of 30 eq formic acid) in the as-synthesized state and after the Soxhlet extraction-activation procedure described in the text.

Table 2

Evaluation of thermogravimetric analyses. Mass losses measured in the given temperature ranges on a *Zr-fum* MOF synthesized in the presence of 30 eq of modulator after Soxhlet extraction and activation as described in the text.

Mass loss (%)	<i>T</i> (°C)	Calculated	Measured	Guest-free ^a
Guests	25–140	–	2.9	–
Linker	140–660	45.8	45.7	47.0
Residue	1000	54.2	51.5	53.0

^a Experimental mass loss after correction for the removal of guest molecules.

not contain any DMF anymore, because the amide stretching vibration $\nu(\text{C-O})$ at about 1660 cm^{-1} is lacking. Correspondingly, a CHN analysis also showed the absence of nitrogen. In addition, after dissolving such a sample, a ^1H NMR spectrum of the solution gives no signals for DMF or for formic acid [32]. The TG curve of a Soxhlet-extracted sample is much clearer and reveals two plateaus. The mass loss up to 140 °C is ascribed to the evaporation of residual guest molecules. The TGA then shows a plateau until at about 260 °C the decomposition of the linkers starts. This obviously occurs in two steps, one which is finished at 400 °C and another one which takes place at around 600 °C. The decomposition thus starts at a relatively low temperature as compared, for example, to UiO-66 which is stable in air up to a temperature of about 400 °C [29]. This is in line with the enhanced reactivity of an unsaturated linker as compared to an aromatic one. The decomposition of a sample of pure fumaric acid occurs between 200 and 400 °C. IR-spectroscopic investigation of a sample heated to 440 °C shows

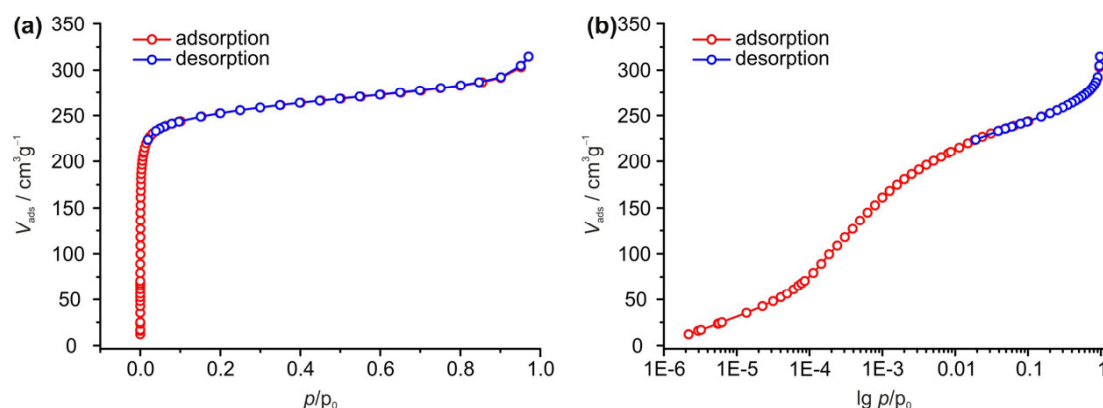


Fig. 6. Ar sorption isotherms of Zr-fum MOF synthesized with 30 eq of modulator.

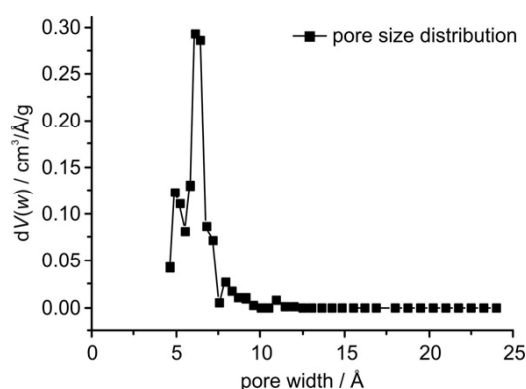


Fig. 7. Pore size distribution of Zr-fum MOF synthesized with 30 eq of modulator, calculated from the data given in Fig. 5.

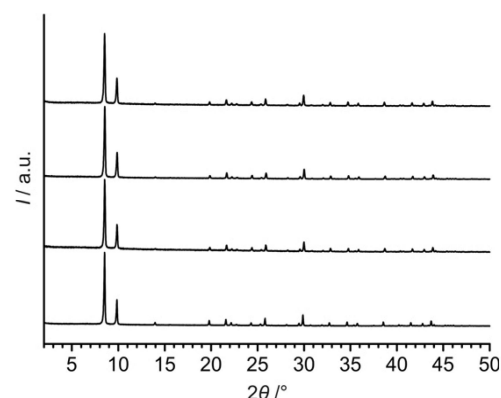


Fig. 8. Stability of Zr-fum MOFs in aqueous media: PXRD patterns measured after stirring for 1 week in comparison to the as-synthesized sample. From bottom to top: as-synthesized sample (synthesized with 50 eq of modulator); after stirring in water; after stirring in physiological NaCl solution; after stirring in PBS solution.

that any signs of the presence of C–H bonds have disappeared, but bands at 1410 cm^{-1} and at 1550 cm^{-1} still persist. We ascribe these signals to carbonate ions coordinated to Zr^{4+} ions, possibly to still intact Zr-oxo clusters. The last step in the TG curve at about $650\text{ }^{\circ}\text{C}$ can then be assigned to the final decomposition where the carboxylate groups are released as CO_2 . The residual sample was identified as monoclinic ZrO_2 using PXRD. When the mass loss between 260 and $700\text{ }^{\circ}\text{C}$ is assumed to be due to release of the linker, and when this mass loss is compared to the residual mass, the ratio is near to the value expected for a Zr-fum MOF with a composition similar to that of UiO-66, i.e. $\text{Zr}_6\text{O}_4(\text{OH})_4(\text{O}_2\text{C}-(\text{CH}_2)_2-\text{CO}_2)_6$ (Table 2). This finding further corroborates the assignment of the UiO-66 topology to the Zr-fum MOF.

To characterize the porosity of Zr-fum MOFs, Ar sorption measurements were performed on a sample of Zr-fum MOF prepared with 30 eq of modulator which was Soxhlet-extracted and activated. The linear and logarithmic depictions of the isotherms are shown in Fig. 6. They correspond to type I adsorption isotherms, as classified by IUPAC. When we calculate the pore size distribution (Fig. 7) using NLDFT fitting (see Fig. A2 in the Supplementary material for the fit). The corresponding plot shows the presence of micropores in the diameter range between 5 and $7\text{ }\text{\AA}$, peaking at $6\text{ }\text{\AA}$; the diameters of the cavities of UiO-66 were given as 8 – $11\text{ }\text{\AA}$ [25]. The BET surface area determined from the sorption isotherm for the Zr-fum MOF is $856\text{ m}^2\text{ g}^{-1}$. Due to the shorter linker it is not surprising that this value is smaller than that of UiO-66 for which a surface area of $1069\text{ m}^2\text{ g}^{-1}$ was given [18,25]. We note that the re-

sults from the sorption measurements agree with the assignment of a UiO-66-type topology to the Zr-fum MOF.

For several Zr-MOFs, a remarkably high stability versus high temperatures and various chemical agents has been reported [17,18,22,29]. From the thermogravimetric analyses described above, we estimate that Zr-fum MOF is stable up to a temperature of ca. $260\text{ }^{\circ}\text{C}$ in air. In addition, we have investigated the stability of this novel Zr-MOF in water and in aqueous solutions. As we see possible applications of this MOF in the biomedical field we chose phosphate buffered saline (PBS) solution or physiological NaCl solution. For testing the stability, the solid material was dispersed in water or in one of the solutions and stirred at room temperature for 1 week. PXRD patterns of the re-isolated materials do not show any sign of destruction or disorder in comparison to the as-synthesized powder (Fig. 8).

4. Conclusions

This paper describes the modulated synthesis of a novel Zr-based metal-organic framework, namely the Zr-fumarate MOF. It is most interesting to note that whereas we have not been able to obtain this compound in the absence of a modulator, even very small amounts of the modulating agent formic acid induced the formation of this MOF. This gives rise to two speculations: (i) many MOFs which have been missed so far could possibly be synthesized

in the presence of a minor amount of a suitable “foreign” substance acting as a modulator; (ii) the fact that some syntheses of MOFs described in the literature are difficult to reproduce in other laboratories could be explained by the circumstance that obviously even small amounts of a “foreign” substance which acts as a modulator can decide about the success of a synthesis.

As in the case of the modulated synthesis of UiO-66 and UiO-67 [29], varying the concentration of the modulating agent allows for the preparation of samples with very different morphologies. However, formic acid is differentiated from other modulating agents by the fact that it accelerates the formation of a crystalline MOF, whereas usually the crystallization rate is decreased in the presence of a modulator.

Further characterization of the Zr-*fum* MOF using a variety of techniques gives results which all agree with the assumption that the structure of this novel MOF can be derived from the basic topology of the UiO-66 to -68 MOFs. A structural model which takes into account the kinked geometry of the linker molecule as well as the absence of face centering (deduced from the PXRD pattern) is proposed. Zr-*fum* MOF is porous, thermally stable up to a temperature of 260 °C in air and chemically stable in various aqueous media. As the organic components used in the synthesis of this MOF occur naturally, possible applications in the biomedical field are envisaged.

Acknowledgements

This work was performed within the DFG priority program 1362 (Porous Metal-organic Frameworks). We thank Georg Platz for the measurement of the Ar sorption isotherm as well as Britta Hering and Florian Waltz for performing scanning electron microscopy. Adelheid Godt and Thomas Preuße are kindly acknowledged for performing the ¹H NMR analysis.

Appendix A. Supplementary data

Supplementary data associated with this article can be found, in the online version, at doi:10.1016/j.micromeso.2011.12.010.

References

- [1] J.R. Long, O.M. Yaghi, *Chem. Soc. Rev.* 38 (2009) 1213–1214.
- [2] S. Kitagawa, R. Kitaura, S. Noro, *Angew. Chem.* 116 (2004) 2388–2430. *Angew. Chem. Int. Ed.* 43 (2004) 2334–2375.
- [3] G. Férey, *Chem. Soc. Rev.* 37 (2008) 191–214.
- [4] O.M. Yaghi, M. O’Keeffe, N.W. Ockwig, H.K. Chae, M. Eddaoudi, J. Kim, *Nature* 423 (2003) 705–714.
- [5] A. Robson, *Dalton Trans.* (2008) 5113–5131.
- [6] Z. Wang, S.M. Cohen, *Chem. Soc. Rev.* 38 (2009) 1315–1329.
- [7] S.T. Meek, J.A. Greathouse, M.D. Allendorf, *Adv. Mater.* 23 (2011) 249–267.
- [8] H.-L. Jiang, Q. Xu, *Chem. Commun.* 47 (2011) 3351–3370.
- [9] A.U. Czaja, N. Trukhan, U. Müller, *Chem. Soc. Rev.* 38 (2009) 1284–1293.
- [10] S. Keskin, S. Kizilel, *Ind. Eng. Chem. Res.* 50 (2011) 1799–1812.
- [11] J.L.C. Rowsell, O.M. Yaghi, *J. Am. Chem. Soc.* 128 (2006) 1304–1315.
- [12] J. Hafizovic, M. Bjorgen, U. Olsbye, P.D.C. Dietzel, S. Bordiga, C. Prestipino, C. Lamberti, K.P. Lillerud, *J. Am. Chem. Soc.* 129 (2007) 3612–3620.
- [13] S.S. Kaye, A. Dailly, O.M. Yaghi, J.R. Long, *J. Am. Chem. Soc.* 129 (2007) 14176–14177.
- [14] C.A. Bauer, T.V. Timofeeva, T.B. Settersten, B.D. Patterson, V.H. Liu, B.A. Simmons, M.D. Allendorf, *J. Am. Chem. Soc.* 129 (2007) 7136–7144.
- [15] Y.-S. Bae, D. Dubbeldam, A. Nelson, K.S. Walton, J.T. Hupp, R.Q. Snurr, *Chem. Mater.* 21 (2009) 4768–4777.
- [16] P.L. Feng, J.J. Perry IV, S. Nikodemski, B.W. Jacobs, S.T. Meek, M.D. Allendorf, *J. Am. Chem. Soc.* 132 (2010) 15487–15489.
- [17] J.H. Cavka, S. Jakobsen, U. Olsbye, N. Guillou, C. Lamberti, S. Bordiga, K.P. Lillerud, *J. Am. Chem. Soc.* 130 (2008) 13850–13851.
- [18] L. Valenzano, B. Cavalleri, S. Chavan, S. Bordiga, M.H. Nilsen, S. Jakobsen, K.P. Lillerud, C. Lamberti, *Chem. Mater.* 23 (2011) 1700–1718.
- [19] G. Kicelbick, U. Schubert, *Chem. Ber.* 130 (1997) 473–477.
- [20] P. Piszczek, A. Radtke, A. Grodzicki, A. Wojtczak, J. Chojnacki, *Polyhedron* 26 (2007) 679–685.
- [21] V. Guillermin, S. Gross, C. Serre, T. Devic, M. Bauer, G. Férey, *Chem. Commun.* 46 (2010) 767–769.
- [22] A. Schaate, P. Roy, T. Preuße, S.J. Lohmeier, A. Godt, P. Behrens, *Chem. Eur. J.* 17 (2011) 9320–9325.
- [23] S.J. Garibay, S.M. Cohen, *Chem. Commun.* (2010) 7700–7702.
- [24] M. Kandiah, S. Usseglio, S. Svelle, U. Olsbye, K.P. Lillerud, M. Tilset, *J. Mater. Chem.* 20 (2010) 9848–9851.
- [25] P.S. Bácia, D. Guimarães, P.A.P. Mendes, J.A.C. Silva, V. Guillermin, H. Chevreau, C. Serre, A.E. Rodrigues, *Micropor. Mesopor. Mater.* 139 (2011) 67–73.
- [26] F. Vermoortele, R. Ameloot, A. Vimont, C. Serre, D. De Vos, *Chem. Commun.* 47 (2011) 1521–1523.
- [27] T. Tsuruoka, S. Furukawa, Y. Takashima, K. Yoshida, S. Isoda, S. Kitagawa, *Angew. Chem.* 121 (2009) 4833–4837. *Angew. Chem. Int. Ed.* 48 (2009) 4739–4743.
- [28] S. Diring, S. Furukawa, Y. Takashima, T. Tsuruoka, S. Kitagawa, *Chem. Mater.* 22 (2010) 4531–4538.
- [29] A. Schaate, P. Roy, A. Godt, J. Lippke, F. Waltz, M. Wiebcke, P. Behrens, *Chem. Eur. J.* 17 (2011) 6643–6651.
- [30] A.C. McKinlay, R.E. Morris, P. Horcajada, G. Férey, R. Gref, P. Couvreur, C. Serre, *Angew. Chem. Int. Ed.* 49 (2010) 6260–6266.
- [31] WinXPow, Version 1.08, STOE & Cie GmbH, Darmstadt, Germany, 2000.
- [32] P. Roy, A. Schaate, P. Behrens, A. Godt, *Chem. Eur. J.* submitted for publication.
- [33] Materials Studio, Version 5.0, Accelrys Software Inc., San Diego, CA, 2009.
- [34] A.K. Rappe, C.J. Casewit, K.S. Colwell, W.A. Goddard, W.M. Skiff, *J. Am. Chem. Soc.* 114 (1992) 10024.
- [35] K.B. Wiberg, *J. Am. Chem. Soc.* 87 (1965) 1070.
- [36] B.R. Brooks, R.E. Bruccoleri, B.D. Olafson, D.J. States, S. Swaminathan, M. Karplus, *J. Comput. Chem.* 4 (1983) 187.
- [37] D.F. Shanno, *Math. Comput.* 24 (1970) 647.

7 Conclusions and Outlook

The first part of this work was devoted to the development of a synthesis concept for the reliable preparation of Zr-MOFs. This new synthesis method was inspired by the work of Kitagawa and co-workers and was designated by them as coordination modulation method.^[1] Monocarboxylic acids are added to the synthesis to compete with the linkers for the coordination sites of Zr cations, thus affecting the nucleation and the growth of the Zr-MOFs.

Zr-bdc-MOF prepared without modulators precipitated as intergrown nanocrystals.^[2] In the case of Zr-bdc-MOF the use of a certain amount of modulator (benzoic or acetic acid) leads to isolated nanocrystals the sizes of which can be adjusted by choosing the concentration of modulator. It is assumed that the more modulator is present in the synthesis, the more metal cations are complexed. This decreases the supersaturation of the metal precursor and slows down the nucleation of framework material. Isolated nanocrystals prepared in this way could be useful for drug delivery systems,^[3] nanoporous membranes,^[4] or thin film devices.^[5]

Furthermore, the coordination modulation method proved to be essential for the successful preparation of some known and several novel MOFs presented in this thesis. The knowledge about the mechanisms behind this new concept of synthesis is sparse and could be expanded with the following ideas.

The synthesis of Zr complexes with monocarboxylic acids in DMF could facilitate the discussion about the processes involved in the modulated synthesis as was commenced in chapter 2.2.4. The Zr complexes introduced there were not synthesized in DMF and so single crystals of such potentially existent complexes would affirm the current comprehension of the effects of modulators and/or uncover additional hints. This information could then be used to get even more control over the synthesis by the choice of modulator and to further explain the role of modulators.

Another possibility to get a deeper understanding of the crystallization of these MOFs would be *in-situ* analyses of unmodulated and modulated syntheses. For this purpose it would be recommended to use time-resolved *in-situ* energy dispersive X-ray diffraction (EDXRD) with synchrotron irradiation. This method has already been

-
- [1] a) T. Tsuruoka, S. Furukawa, Y. Takashima, K. Yoshida, S. Isoda, S. Kitagawa, *Angew. Chem., Int. Ed.* **2009**, *48*, 4739–4743; b) S. Diring, S. Furukawa, Y. Takashima, T. Tsuruoka, S. Kitagawa, *Chem. Mater.* **2010**, *22*, 4531–4538.
- [2] J. H. Cavka, S. Jakobsen, U. Olsbye, N. Guillou, C. Lamberti, S. Bordiga, K. P. Lillerud, *J. Am. Chem. Soc.* **2008**, *130*, 13850–13851.
- [3] P. Horcajada, T. Chalati, C. Serre, B. Gillet, C. Sebrie, T. Baati, J. F. Eubank, D. Heurtaux, P. Clayette, C. Kreuz, J.-S. Chang, Y. K. Hwang, V. Marsaud, P.-N. Bories, L. Cynober, S. Gil, G. Férey, P. Couvreur, R. Gref, *Nat. Mater.* **2009**, *9*, 172–178.
- [4] Y. Li, F. Liang, H. Bux, W. Yang, J. Caro, *J. Membrane Sci.* **2010**, *354*, 48–54.
- [5] A. Demessence, P. Horcajada, C. Serre, C. Boissière, D. Grosso, C. Sanchez, G. Férey, *Chem. Commun.* **2009**, 7149–7151.

applied to investigate the crystallization of some prototypical MOFs and provided insight into parameters of the reaction like induction and reaction time, rate constants, and the type of reaction control (phase-boundary- or diffusion-controlled).^[6] By applying this method to modulated syntheses it would be possible to get a more precise idea of the mechanism of the crystallization of Zr-MOFs and how modulator molecules affect it. The synthesis of Zr-bdc-MOF is suitable as a model system for such investigations, because this MOF crystallizes reliably with and without the application of modulators. Zr-bpdc-MOF is an example of a problematic MOF synthesis which does not yield crystalline products without a modulator and could serve as comparison to Zr-bdc-MOF. Indeed, a preliminary EDXRD study carried out by the author of this thesis together with co-workers from the group showed that with increasing modulator/metal ratio the induction time for the crystallization of Zr-bpdc-MOF is extended. This is a first substantiation by an *in-situ* analysis method for the here described modulation approach.

Another, hitherto not further investigated, element of the synthesis of Zr-MOFs is the role of water. On the one hand, it is conceivable that the concentration of water influences the hydrolysis of the Zr species in solution and supplies the oxygen atoms for the construction of the $[\text{Zr}_6\text{O}_4(\text{OH})_4]^{12+}$ clusters and that it thus should affect the nucleation rate of the forming MOF. All MOF syntheses described in this work were performed in DMF that contained $\leq 0.15\%$ water. This small amount of water in the solvent is sufficient for the hydrolysis of the zirconium tetrachloride and for the assembly of the Zr-SBU. On the other hand, some of the Zr-MOFs investigated in this thesis (Zr-bdc-NH₂, Zr-tpdc-NH₂, Zr-abdc) can only be obtained with high crystallinity if a certain amount of water is added to the synthesis. Some of the PIZOFs currently investigated in our laboratory are also affected by this phenomenon, which there appears to be more pronounced when alkyl chains are attached to the central benzene unit of the linker. Possible starting points for explanations could be that the water influences the solubility of certain linker molecules or that the amount of water in the synthesis mixture controls the decomposition of DMF to reactive species which are necessary for a successful synthesis. Taken together, these findings would justify a closer examination of the role of water during the synthesis of Zr-MOFs, which could also be carried out by systematic EDXRD measurements. If DMF is decomposed to gaseous species during the synthesis, these can be examined by observing the gas phase from the head space of the reaction vial by mass spectrometry and/or infrared measurements as was done for the synthesis of MOF-5 by the Mertens group.^[7]

The preparation of the first single crystals of Zr-MOFs was the second benefit of the

[6] F. Millange, M. I. Medina, N. Guillou, G. Férey, K. M. Golden, R. I. Walton, *Angew. Chem., Int. Ed.* **2010**, 763–766; b) T. Ahnfeldt, J. Moellmer, V. Guillerm, R. Staudt, C. Serre, N. Stock, *Chem. Eur. J.* **2011**, 17, 6462–6468; c) J. Cravillon, C. A. Schröder, R. Nayuk, J. Gummel, K. Huber, M. Wiebcke, *Angew. Chem., Int. Ed.* **2011**, 50, 8067–8071.

[7] S. Hausdorf, F. Baitalow, J. Seidel, F. O. R. L. Mertens, *J. Phys. Chem. A* **2007**, 111, 4259–4266.

modulation coordination approach. In this way it was possible to elucidate the structure of the Zr-tpdc-NH₂ MOF, a Zr-MOF isorecticular to Zr-bdc and Zr-bpdc but with larger cavities suitable for post-synthetic modifications with larger molecules. Additionally, the modulation approach yielded single crystals of a novel Zr-MOF composed of the same SBU and H₂abdc. The kink in H₂abdc caused by the azo group made it difficult to determine the complete structure of Zr-abdc-MOF solely by SXRD but indicated that its structure is isorecticular to the other mentioned Zr-MOFs. Computer-aided modeling techniques were used to compare different models of linker arrangement. This investigation indicates that the structure is best described with statistically disordered linkers. The sorption measurements and thermogravimetric analysis further verified the assignment of this MOF as an UiO analogue compound. The synthesis of H₂abdc is modular with regard to the introduction of different organic functionalities and so Zr-abdc-MOF could be the first Zr azo-MOF of an isostructural series. However, recent results of Simon Dühren^[8] and Sebastian Lilienthal from our group give reason to believe that functionalities, attached to the benzene units of H₂abdc, have a stronger impact on the resulting structure than expected.

Finally, the new synthetic approach was used to synthesize a new isostructural series of porous interpenetrated zirconium-organic frameworks (PIZOFs). All PIZOFs are composed of the already known Zr-SBU linked together by long dicarboxylic acids with different functional groups attached to their backbone. PXRD revealed that all PIZOFs share a common framework structure which was determined from single crystal analyses of three different PIZOFs.

In total, eight different PIZOFs are presented in this thesis. At the time where this thesis is submitted, the number of known PIZOFs has increased further to 14 by the recent work carried out by Jann Lippke^[9] and Philip Zerner of our group. PIZOFs are porous and their backbone show a high thermal stability. Dependent on the functionalities attached on its linker, the thermal stability of a PIZOF (including the functionalities) varies, because some of the functional groups are more reactive than others and can be released at lower temperatures before the framework is decomposed upon heating. Current investigations of Jann Lippke of our group show that the resistivity to water of a PIZOF also depends on its attached functionalities.

Some of these functionalities are so spacious that they should nearly fill the available pore space. Such MOFs could be designated as immobilized liquids since the alkyl, alkoxy, or oligo(ethyleneglycol) chains should be flexible like in a liquid but at the same time are covalently attached to the framework and thus immobilized. Solid-state NMR spectroscopic studies and differential scanning calorimetry should be suitable methods to confirm this idea experimentally.

In this context it is interesting that poly(ethylene oxide) (PEO) is discussed as polymer electrolyte material for lithium conduction in batteries. It was disclosed that the

[8] S. Dühren, Master Thesis, Universität Hannover, 2011.

[9] J. Lippke, Master Thesis, Universität Hannover, 2011.

confinement of PEO in nanopores of diameters from 30 to 400 nm can increase the ionic conduction of Li salts compared to that in pure PEO films; the highest conductivities were observed in channels of 30 nm diameter.^[10] The maximal pore diameter of the PIZOFs is 2 nm (the conductivity in the referred study increases reciprocally to the diameter of the channels) and as was mentioned above, the interior of the individual PIZOFs can be adjusted over a broad range by deploying linkers with functionalities like oligo(ethylene glycol) chains with the desired length. This should make it possible to carefully tune its properties. Thus, PIZOFs could be interesting materials for ionic conduction. Indeed, first investigations on MOFs as Li conductors show that they could serve as battery separator materials.^[11]

For this purpose it is crucial to find ways to grow dense PIZOF membranes or layers on different kind of materials. The current work of Imke Bremer of our group is focused on this topic and first results show that certain modulators (*e.g.* benzoic acid, 3-chloropropionic acid) have beneficial influence on the growth of Zr-MOFs to reach this goal.

Due to their common framework structure, PIZOFs should be excellent candidates to create hybrid PIZOFs with more than one linker, based on the example of the 'multivariate' MOF-5 crystals^[12] or on core-shell crystals, as inspired by the work of Kitagawa.^[13] The latter approach would be of particular interest because using this route it could be possible for example to encapsulate PIZOFs that are less resistant to water with a PIZOF shell with good water resistivity as protection, or to protect PIZOF layers or membranes from destructive molecules.

In conclusion, a novel modulation method for the recently described, important class of Zr-MOFs has been developed. This method turned out to be a powerful instrument not only to influence crystal sizes and aggregation of known Zr-MOFs but furthermore to obtain the novel family of PIZOFs. Due to their high stability and the enormous number of possibilities to tune their properties PIZOFs offer a great potential to fulfill a huge variety of different tasks in the future.

[10] S. Vorrey, D. Teeters, *Electrochim. Acta* **2003**, *48*, 2137–2141.

[11] N. Yanai, T. Uemura, S. Horike, S. Shimomura, S. Kitagawa, *Chem. Commun.* **2011**, *47*, 1722–1724;
b) B. M. Wiers, M.-L. Foo, N. P. Balsara, J. R. Long, *J. Am. Chem. Soc.* **2011**, *133*, 14522–14525.

[12] H. Deng, C. J. Doonan, H. Furukawa, R. B. Ferreira, J. Towne, C. B. Knobler, B. Wang, O. M. Yaghi, *Science* **2010**, *327*, 846–850.

[13] K. Hirai, S. Furukawa, M. Kondo, H. Uehara, O. Sakata, S. Kitagawa, *Angew. Chem., Int. Ed.* **2011**, *50*, 8057–8061.

8 List of publications

8.1 Articles presented in this work

Modulated Synthesis of Zr-Based Metal-Organic Frameworks: From Nano to Single Crystals

A. Schaate, P. Roy, A. Godt, J. Lippke, F. Waltz, M. Wiebcke, P. Behrens

Chemistry - A European Journal **2011**, *17*, 6643–6651

A novel Zr-based porous coordination polymer containing azobenzene dicarboxylate as linker

A. Schaate, S. Dühren, G. Platz, S. Lilienthal, A. M. Schneider, P. Behrens

European Journal of Inorganic Chemistry **2012**, 790–796

Porous Interpenetrated Zirconium–Organic Frameworks (PIZOFs): A Chemically Versatile Family of Metal–Organic Frameworks

A. Schaate, P. Roy, T. Preuße, S. J. Lohmeier, A. Godt, P. Behrens

Chemistry - A European Journal **2011**, *17*, 9320–9325

Modulated synthesis of Zr-fumarate MOF

G. Wißmann, A. Schaate, S. Lilienthal, I. Bremer, A. M. Schneider, P. Behrens

Microporous and Mesoporous Materials **2012**, *152*, 64–70

8.2 Further Articles

Photoisomerisation for a molecular switch in contact with a surface

J. Henzl, P. Puschnig, C. Ambrosch-Draxl, A. Schaate, B. Ufer, P. Behrens, K. Morgenstern

Physical Review B **2012**, *85*, 035410

Postsynthetic modification of Zr-MOFs through cycloaddition reactions

P. Roy, A. Schaate, P. Behrens, A. Godt

Under revision, Chemistry - A European Journal **2011**

Highly Oriented Surface-Growth and Covalent Dye Labeling of Mesoporous Metal-Organic Frameworks

F. M. Hinterholzinger, S. Wuttke, P. Roy, T. Preuße, A. Schaate, P. Behrens, A. Godt, T. Bein

Dalton Transactions **2012**, *41*, 3899–3901

One-dimensional Zn(II) oligo(phenyleneethynylene)dicarboxylate coordination polymers: Synthesis, crystal structure, thermal and photoluminescent properties

A. Schaate, M. Schulte, M. Wiebcke, A. Godt, P. Behrens

Inorganica Chimica Acta **2009**, *362*, 3600–3606

Two Zinc(II) Coordination Polymers Constructed with Rigid 1,4-Benzenedicarboxylate and Flexible 1,4-Bis(imidazol-1-ylmethyl)-2,3,5,6-tetramethylbenzene Linkers: From Interpenetrating Layers to Templated 3D Frameworks

A. Schaate, S. Klingelhöfer, P. Behrens, M. Wiebcke
Crystal Growth & Design **2008**, 8, 3200–3205

8.3 Oral presentations

Zr-based metal-organic frameworks: From nano to single crystals via a modulation approach

A. Schaate, P. Behrens, J. Lippke, P. Roy, F. Waltz, A. Godt

2nd International Conference on Metal-Organic Frameworks and Open Framework Compounds, September 5–8, **2010**, Marseille, France

8.4 Poster presentations

Porous interpenetrated zirconium-organic frameworks (PIZOFs): Sorption Properties of a chemically versatile family

A. Schaate, G. Platz, P. Roy, T. Preuß, A. Godt, P. Behrens

23. Deutsche Zeolith Tagung, March 2–4, **2011**, Erlangen, Germany

Synthesis and luminescence of Zn-based MOFs built up from rod-shaped Secondary Building Units and long oligo(phenyleneethynylene)dicarboxylate linker

A. Schaate, P. Roy, J. Panke, M. Wark, A. Godt, P. Behrens

2nd International Conference on Metal-Organic Frameworks and Open Framework Compounds, September 5–8, **2010**, Marseille, France

Porous interpenetrated zirconium-organic frameworks (PIZOFs) containing a variety of functionalized long linkers

A. Schaate, P. Roy, J. Lippke, A. Godt, P. Behrens

2nd International Conference on Metal-Organic Frameworks and Open Framework Compounds, September 5–8, **2010**, Marseille, France

Control over Size and Morphology of Zirconium-based Metal-organic Frameworks via a Modulator Approach: Nanocrystals and Single Crystals

A. Schaate, J. Lippke, P. Roy, F. Waltz, A. Godt, P. Behrens

16th International Zeolite Conference, July 4–9, **2010**, Sorrento, Italy

Combination of Zn-based Rod-Shaped Secondary Building Units with Long Oligo(phenyleneethynylene)-dicarboxylate Linkers: Synthesis and Luminescent Properties

A. Schaate, P. Roy, J. Panke, M. Wark, A. Godt, P. Behrens

22. Deutsche Zeolith Tagung, March 3–5, **2010**, München, Germany

Modulated Synthesis to Obtain Control over Size and Morphology

A. Schaate, J. Lippke, P. Roy, A. Godt, P. Behrens

22. Deutsche Zeolith Tagung, March 3–5, **2010**, München, Germany

Optical Properties of Zn(II) Oligo(phenyleneethynylene)dicyrboxylate Coordination Polymers

A. Schaate, P. Roy, J. Panke, M. Wiebcke, M. Wark, A. Godt, P. Behrens

Functional Metal Organic Frameworks as Heterogeneous Catalysts, June 17–19, **2009**, Oslo, Norway

Zirconium-based Metal-organic Framework Materials

A. Schaate, P. Roy, S. J. Lohmeier, M. Wiebcke, A. Godt, P. Behrens

21. Deutsche Zeolith Tagung, March 4–6, **2009**, Kiel, Germany

Zn(II) Oligo(phenyleneethynylene)dicarboxylate Coordination Polymers

A. Schaate, P. Roy, M. Schulte, M. Wiebcke, A. Godt, P. Behrens

1st International Conference on Metal-Organic Frameworks and Open Framework Compounds, October 8–10, **2008**, Augsburg, Germany

Porous Zirconium-Organic Framework Materials

B. Papendorf, A. Schaate, P. Behrens, M. Wiebcke

1st International Conference on Metal-Organic Frameworks and Open Framework Compounds, October 8–10, **2008**, Augsburg, Germany

Zn(II) Oligo(phenyleneethynylene)dicarboxylate Coordination Polymers: Synthesis and Characterization

A. Schaate, M. Schulte, M. Wiebcke, A. Godt, P. Behrens

20. Deutsche Zeolith Tagung, March 5–7, **2008**, Halle, Germany

Mixed-ligand Zn(II) Coordination Polymers: From Interpenetrating Layers to Templated 3D Frameworks

A. Schaate, S. Klingelhöfer, P. Behrens, M. Wiebcke

20. Deutsche Zeolith Tagung, March 5–7, **2008**, Halle, Germany

9 Curriculum Vitae

Name	Andreas Schaate
geboren am	20. April 1982
geboren in	Uelzen
12/2007–02/2012	Beginn der Promotion zum Dr. rer nat. in Chemie in der Arbeitsgruppe Prof. Dr. P. Behrens Institut für Anorganische Chemie Gottfried Wilhelm Leibniz Universität Hannover Thema: Synthesis and Characterization of Zirconium- based Metal-Organic Frameworks using a Modulation Approach
05/2007–11/2007	Diplomarbeit in der Arbeitsgruppe Prof. Dr. P. Behrens Institut für Anorganische Chemie Gottfried Wilhelm Leibniz Universität Hannover Thema: Metall-organische Gerüstverbindungen mit neuartigen Linker-Molekülen
10/2002–04/2007	Studium im Fach Chemie (Diplom) Gottfried Wilhelm Leibniz Universität Hannover
2001–2002	Zivildienst beim DRK Kreisverband Uelzen e.V.
2001	Abitur
1994–2001	Herzog-Ernst-Gymnasium Uelzen
1992–1994	Orientierungsstufe Lucas-Backmeister-Schule, Uelzen
1989–1992	Grundschule Lucas-Backmeister-Schule, Uelzen
1988–1989	Grundschule Sternschule, Uelzen

